Title
Viral-induced global mRNA degradation influences viral mRNA abundance and host transcription rates

Author
Abernathy, Emma

Publication Date
2015

Peer reviewed|Thesis/dissertation

Viral-induced global mRNA degradation influences viral mRNA abundance and host transcription rates

By

Emma Abernathy

A dissertation submitted in partial satisfaction of the

Requirements for the degree of

Doctor of Philosophy

In

Microbiology

In the

Graduate Division

Of the

University of California, Berkeley

Committee in charge:

Professor Britt A. Glaunsinger
Professor Laurent Coscoy
Professor David Raulet

Spring 2015

Abstract

Viral-induced global mRNA degradation influences viral mRNA abundance and host transcription rates

by

Emma Abernathy

Doctor of Philosophy in Microbiology

University of California, Berkeley

Professor Britt A. Glaunsinger, Chair

Lytic gammaherpesvirus infection restricts host gene expression by promoting widespread degradation of cytoplasmic mRNA through the activity of the viral endonuclease SOX. Though generally assumed to be selective for cellular transcripts, the extent to which SOX impacts viral mRNA stability has remained unknown. We addressed this issue using the model murine gammaherpesvirus MHV68 and, unexpectedly, found that all stages of viral gene expression are controlled through mRNA degradation. Using both comprehensive RNA expression profiling and half-life studies we reveal that the levels of the majority of viral mRNAs but not noncoding RNAs are tempered by MHV68 SOX (muSOX) activity. The targeting of viral mRNA by muSOX is functionally significant, as it impacts intracellular viral protein abundance and progeny virion composition. In the absence of muSOX-imposed gene expression control the viral particles display increased cell surface binding and entry as well as enhanced immediate early gene expression. These phenotypes culminate in a viral replication defect in multiple cell types as well as *in vivo*, highlighting the importance of maintaining the appropriate balance of viral RNA during gammaherpesviral infection. This is the first example of a virus that fails to broadly discriminate between cellular and viral transcripts during host shutoff and instead uses the targeting of viral messages to fine-tune overall gene expression.

We also address some downstream consequences of viral-mediated mRNA decay for the host. We reveal that mammalian cells respond to this widespread cytoplasmic mRNA decay by altering levels of RNA polymerase II (RNAPII) transcription in the nucleus. Measurements of both RNAPII recruitment to promoters and nascent mRNA synthesis revealed that the majority of affected genes are transcriptionally repressed in SOX-expressing cells. The transcriptional feedback does not occur in response to the initial endonuclease-induced cleavage, but instead to degradation of the cleaved fragments by cellular exonucleases. In particular, Xrn1 catalytic activity is required for transcriptional repression. Notably, viral mRNA transcription escapes decay-induced repression, and this escape requires Xrn1. Collectively, these results indicate that mRNA decay rates impact transcription in mammalian cells, and that gamma-herpesviruses have incorporated this feedback mechanism into their own gene expression strategy.

Table of Contents

Chapter 1: Introduction

Introduction I: Viral nucleases accelerate mRNA degradation……1
Introduction II: The gammaherpesvirus lifecycle……..……10
Figures……..……..16

Chapter 2: Gammaherpesviral gene expression and virion composition are broadly controlled by accelerated mRNA degradation

Introduction…….……20
Results…….……21
Discussion…….……..……26
Materials and Methods……28
Figures…….……32

Chapter 3: Viral nucleases reveal an mRNA degradation-transcription feedback loop in mammalian cells

Introduction…….……41
Results…….……42
Discussion……..……47
Materials and Methods……49
Figures…….……53

Chapter 4: Discussion and Conclusions……63

References……68

Acknowledgements

First and foremost I want to thank my mentor, Britt Glaunsinger. I could not have asked for a more competent and enthusiastic mentor to guide me through the challenges of grad school. I also would like to thank everyone in the Glaunsinger lab, who not only make sure work is exciting and fun every day, but also are invaluable resources of knowledge and ideas. I would like to thank Zoe Davis for having so much enthusiasm she literally could not contain it within her bay, John Karijolich for teaching me that RNase treatment is unnecessary, and Sarah Gilbertson and Ella Hartenian for extremely helpful discussions and carrying on the project with exceptionally capable hands. I would also like to thank my undergrads, Mansee Desai and Aprilgate Wang, who bravely listened to me even when I had no idea what I was talking about. I have enjoyed living and working in Berkeley and could not image a better place to have completed my graduate studies.

Chapter 1: Introduction

Introduction I: Viral nucleases accelerate mRNA degradation

A recurring theme in many virus-host interactions is the attempt to restrict gene expression. For the cell, such restriction is used as an antiviral mechanism. For the virus, dampening gene expression can be used to liberate cellular resources, escape immune detection, and regulate viral transcript abundance. For many viruses, the virus-host battle plays out at a terminal stage of the gene expression cascade—that of messenger RNA (mRNA) degradation. Research over the last several years has revealed how regulating mRNA demise plays important and unexpected roles in the lifecycles of diverse viruses. Unrelated viruses have evolved remarkably similar strategies to promote mRNA degradation, even though the degree and nature of selectivity often differ. Studying different aspects of how virus manipulate mRNA degradation can lead to a better understand of the host machinery and fundamental cellular processes.

Overview of basal and specialized mRNA degradation

Rates of individual mRNA degradation in a cell vary widely, and are regulated by a large cohort of RNA binding proteins that control translation, localization, and access to the decay machinery. However, nearly all mRNAs are protected by a 5' 7-methyl-guanosine (7mG) cap and a 3' poly(A) tail, features that physically protect the mRNA ends from exonucleolytic decay, and also serve to recruit translation initiation machinery. Circularization of mRNA during translation through interactions between cap-binding and poly(A) tail binding proteins adds additional protection from cellular decay enzymes.

Degradation of mRNAs at the end of their translational life, termed basal decay, occurs in several stages but initiates with gradual shortening of the poly(A) tail, termed deadenylation, by cellular decay factors including the Ccr4-Not complex and poly(A)-specific ribonuclease (PARN). Poly(A) tail length is a determinate of mRNA stability and translational competence, and thus is tightly controlled (Eckmann et al., 2011). Deadenylation triggers removal of the 7mG cap by the decapping complex Dcp1/2 and its activators. These events expose the mRNA to rapid exonucleolytic degradation, primarily from the 5' end by Xrn1, but also from the 3' end by the exosome and Dis3L2 (Figure 1) (Gallouzi and Wilusz, 2013).

The fact that basal decay proceeds from the mRNA ends allows for tight control of mRNA degradation, as removal of the poly(A) tail and cap is regulated, rate-limiting, and in some cases may even be reversible (Schoenberg and Maquat, 2009; Weill et al., 2012) . However, the subsequent exonucleolytic decay of the message body is rapid and irreversible. To maintain transcriptome fidelity cells also need to immediately destroy cytoplasmic mRNAs recognized as aberrant. In such cases, the strategy for degradation differs fundamentally from that of basal decay, in that mRNAs are usually cleaved internally by an endonuclease rather than gradually trimmed from either end.

The best-characterized cellular mRNA quality control (QC) pathway is nonsense-mediated decay (NMD), which identifies mRNAs with premature termination codons (PTC) (Figure 1) (Popp and Maquat, 2013). Numerous cellular factors comprise the NMD machinery, but the central NMD regulator is UPF1, whose activation leads to

translational repression and accelerated degradation of the PTC-containing mRNA. During NMD in mammals, this rapid mRNA degradation is triggered by endonucleolytic cleavage of the mRNA by the Smg6 endonuclease at the site of the PTC, followed by degradation of the cleaved fragments by components of the basal mRNA decay machinery such as Xrn1 (Lykke-Andersen et al., 2014; Schweingruber et al., 2013). Other RNA QC pathways similarly recognize aberrant translation events such as stalled or non-terminating ribosomes indicative of RNA errors and lead to inactivation of the mRNA in question through endonucleolytic cleavage (Inada, 2013).

Viral endonucleases and decapping enzymes bypass regulatory steps of mRNA decay

All viruses known to drive widespread mRNA degradation do so by causing internal endonucleolytic cleavages or by directly removing the mRNA 5' cap structure (Figure 1). Regardless of the precise mechanisms used, these strategies have in common one salient feature: they bypass the rate-limiting and regulated steps of deadenylation and cellular decapping, much like the cellular RNA QC pathways. This ensures both immediate translational inactivation and exposure of the mRNA ends to the processive cellular exonucleases. However, unlike the tightly regulated cellular QC endonucleases, during infection a large proportion of the cytoplasmic mRNA population is targeted for cleavage. This allows the viruses to broadly restrict gene expression, as mRNAs they target are degraded much more rapidly than they would be if they entered the basal decay pathway. Furthermore, akin to cellular pathways like NMD, viruses that cleave mRNAs often usurp Xrn1 to complete the degradation process (Gaglia et al., 2012).

Four classes of viruses have been shown to cause endonucleolytic cleavage of mRNAs for the purpose of restricting gene expression (Table 1). The alpha-herpesviruses, gamma-herpesviruses, and influenza A viruses encode non-homologous endonucleases that cleave mRNAs directly. SARS coronavirus (SARS CoV) does not encode an RNA cleaving enzyme, but nonetheless activates an as yet unknown cellular endonuclease to cleave mRNAs. In each examined case, viral specificity for mRNAs (as opposed to other types of RNA) is conferred by the act of translation or recognition of mRNA features associated with translational competence, similar to cellular RNA QC pathways (Covarrubias et al., 2011; Kamitani et al., 2009; Read, 2013).

DNA virus-encoded endonucleases

Alpha-herpesviruses such as herpes simplex-1 (HSV-1) express a FEN1-like nuclease termed virion host shutoff protein (vhs) that is directed to mRNAs through interactions with the translation initiation factors eIF4H and eIF4AI/II (Feng et al., 2005; Page and Read, 2010). If this interaction is disrupted but the catalytic endonuclease activity remains intact, no host shutoff occurs, indicating that recruitment of vhs to the pool of translating mRNAs is crucial to its ability to dampen gene expression (Feng et al., 2005; Sarma et al., 2008; Shiflett and Read, 2013). *In vitro*, vhs lacks specificity, cleaving mRNAs and non-mRNAs indiscriminately, as well as anywhere along the RNA (Read, 2013). However, in cells or in the presence of cell extracts, vhs preferentially cuts mRNAs at unstructured sites within the 5' UTR or near the start codon of capped

mRNAs (Karr and Read, 1999; Shiflett and Read, 2013). Cut sites also cluster downstream the encephalomyocarditis virus (EMCV) internal ribosome entry site (IRES), which recruits the vhs-targeting translation factors eIF4AI/II, but not near the more minimal Cricket Paralysis virus (CrPV) IRES that recruits the ribosome in the absence of eIF4F (Shiflett and Read, 2013). Further support for the hypothesis that vhs accesses its cleavage sites during translation initiation comes from experiments showing that specific cleavage sites can be repressed or enhanced by mutating the target mRNA start codon or enhancing its Kozak consensus context, respectively (Read, 2013; Shiflett and Read, 2013). However, the observation that an mRNA with a cap-proximal hairpin structure that prevents 40S recruitment remains fully susceptible to vhs cleavage argues against an absolute requirement for ribosomal scanning (Gaglia et al., 2012). One possibility is that assembly of the eIF4F complex on the mRNA cap induces local RNA structure remodeling that creates vhs accessible sites, but that more directed cleavages occur near the start codon during the process of 40S scanning. After vhs-induced cleavage, the resulting 3' mRNA fragments are degraded by the cellular Xrn1 exonuclease (Gaglia et al., 2012).

Gamma-herpesviruses encode a viral endonuclease that, although not homologous to alpha-herpesvirus vhs, also broadly targets cytoplasmic mRNAs for cleavage and subsequent degradation. This protein, termed SOX in Kaposi's sarcoma-associated herpesvirus (KSHV), muSOX in murine gamma-herpesvirus 68 (MHV68), and BGLF5 in Epstein-Barr virus (EBV), is a member of the PD(D/E)XK restriction endonuclease superfamily. The SOX ortholog in HSV-1 was originally shown to have DNase activity involved in viral DNA genome replication (Wilkinson and Weller, 2003), a function it presumably retains in all herpesviruses in addition to the gamma-herpesvirus-specific mRNA degradation activity. Both the DNA and RNA cleavage activities of the protein require the same catalytic core region (Bagneris et al., 2011; Glaunsinger et al., 2005). Although SOX specifically targets translationally competent mRNAs, active translation is not a requirement for target recognition and the molecular features that direct SOX to mRNAs remain unknown. SOX-induced mRNA cleavage occurs at one or more specific, but as-yet poorly sequence defined RNA elements ($\geq$50 nt) that can be present anywhere along the length of a target (Covarrubias et al., 2011; Gaglia et al., 2012). Although a SOX targeting element can confer a new cleavage event if moved to a different location on an mRNA, it is incapable of directing cleavage by SOX if introduced into noncoding RNAs transcribed by RNA polymerase I or III (Gaglia et al., 2012). Similar to vhs, recombinant SOX and BGLF5 display relaxed RNA targeting specificity *in vitro* (Bagneris et al., 2011; Buisson et al., 2009), indicating that additional mRNA-specific features must be required for SOX recruitment in cells. Single function mutants of SOX and muSOX that are defective for mRNA cleavage but retain their DNase activity have mutations that map to regions outside the catalytic core on the protein surface (Bagneris et al., 2011; Covarrubias et al., 2009; Glaunsinger et al., 2005). Furthermore, the crystal structure of BGLF5 revealed the presence of a flexible "bridge" domain that crosses the active site and contains residues involved in host shutoff (Buisson et al., 2009; Horst et al., 2012). These non-catalytic regions may therefore function in targeting the gamma-herpesvirus SOX orthologs to translationally competent mRNAs, perhaps through interactions with specific mRNA binding proteins. Similar to vhs, SOX-cleaved mRNAs

subsequently enter the cellular mRNA decay pathway and are degraded by Xrn1 (Covarrubias et al., 2011; Gaglia et al., 2012).

RNA virus-encoded endonucleases

The PA-X protein of influenza A virus (IAV) is a recently discovered mRNA endonuclease involved in restricting host gene expression (Jagger et al., 2012). It is expressed by a ribosome frameshifting event during translation of the PA subunit of the viral RNA-dependent RNA polymerase (RdRp), itself an endonuclease that is responsible for cap snatching in the nucleus. Like the gamma-herpesvirus SOX orthologs (and many endonucleases involved in cap snatching), PA-X is a member of the PD(D/E)XK nuclease family. PA-X retains the N-terminal PA endonuclease domain but contains a distinct C-terminus that augments the cellular mRNA degradation activity of the protein via unknown mechanisms (Desmet et al., 2013; Jagger et al., 2012). One possibility is that C-terminal sequences are involved in directing PA-X to its mRNA targets. In this regard, it would be interesting to determine whether PA-X targeting is linked to translation and feeds into the cellular Xrn1 decay pathway, as has been shown for other viral mRNA restriction factors.

SARS CoV expresses a host shutoff factor, nsp1, that binds the 40s ribosome, simultaneously inducing cleavage of mRNAs and inactivating the ribosome (Huang et al., 2011; Kamitani et al., 2009). By binding the 40s ribosome, nsp1 is recruited to all translationally competent mRNAs, allowing for broad targeting of cellular transcripts. Nsp1 itself does not possess detectable intrinsic nuclease activity, suggesting that nsp1-induced mRNA cleavage may instead occur through activation of a cellular RNA surveillance pathway (Almeida et al., 2007; Huang et al., 2011). Candidate pathways include those involved in monitoring translational efficiency, given that the nsp1-40S interaction leads to ribosome inactivation in addition to mRNA cleavage (Narayanan and Makino, 2013). For example, the no-go decay pathway degrades mRNAs with stalled ribosomes, albeit using a currently unknown endonuclease (Harigaya and Parker, 2010). As has been observed for cellular QC pathways like NMD as well as the herpesviral endonucleases, degradation of the cleaved mRNAs in nsp1-expressing cells is executed by Xrn1 (Gaglia et al., 2012).

Viral decapping enzymes

Poxviruses and African Swine Fever Virus (ASFV) are the only viruses known to encode decapping enzymes. Similar to cellular decappers, the vaccinia virus (VACV) D9 and D10 decapping proteins contain a Nudix hydrolase domain that is essential for cleaving the 7mGpppN cap between the alpha- and beta-phosphates (Parrish and Moss, 2007; Shors et al., 1999; Souliere et al., 2009). The ASFV decapping enzyme g5R also contains a Nudix domain essential for decapping. Both the VACV and ASFV decapping enzymes are inhibited in the presence of excess uncapped RNAs, but only the VACV D10 enzyme is also inhibited by cap analogs (Parrish et al., 2009). This suggests that g5R recognizes its substrates by binding the RNA body rather than the cap, whereas VACV D10 binds both the methylated cap and the RNA body (Parrish et al., 2009). Extensive site-directed mutagenesis of VACV D10 identified eight amino acids in the catalytic core

of D10 important for decapping activity and showed that D10 recognizes the cap in a manner distinct from other characterized cap binding proteins (Souliere et al., 2010).

It is unknown why poxviruses expresses two functional decapping enzymes, although the reason may be linked to the fact that D9 is expressed early during infection while D10 is expressed later, after DNA replication. Additionally, there are some differences between the two enzymes, including the observations that D9 requires longer RNA substrates than D10, and D9 mutants have less pronounced phenotypes than D10 mutants (Parrish and Moss, 2006, 2007). Therefore, the kinetic and functional requirements for decapping may vary as VACV infection progresses. As decapping renders the 5' end of an mRNA unprotected, it is likely that D9 and D10 cleaved mRNAs are digested by Xrn1, similar to the cleavage products induced by vhs, SOX, and nsp1. Interestingly, a recent RNAi screen suggested a positive role for Xrn1 in VACV replication (Sivan et al., 2013), perhaps indicating that Xrn1-mediated RNA degradation plays an important role in the viral lifecycle.

Viral mRNAs do not broadly escape inactivation

It is often presumed that restriction of cellular gene expression during infection serves in part to divert resources for the selective enhancement of viral gene expression. However, in each of the above documented examples there is not a clear escape mechanism to broadly protect viral mRNAs from inactivation. Instead, these viruses may benefit from reduced transcript levels during infection, either because mRNA inactivation helps them regulate their gene expression kinetics or other aspects of the viral lifecycle. During VACV infection, the decapping enzymes D9 and D10 fail to discriminate between viral and cellular mRNA. Targeting viral transcripts is proposed to help facilitate transitions between the classes of gene expression, as D10 mutants exhibit delayed onset of early and late viral gene expression (Liu et al., 2014; Parrish and Moss, 2006). Similarly, alpha- and gamma-herpesviral mRNAs are inherently susceptible to endonucleolytic cleavage. During HSV-1 infection, vhs plays an important role in mediating the effective transition between the expression of immediate-early (α), early (β), and late (γ) genes (Read, 2013). There are some discrepancies in the field as to exactly which viral mRNAs are susceptible to vhs-mediated degradation during infection. Some data suggest that only α mRNAs are targeted (Shu et al., 2013b; Taddeo et al., 2013), while data from other groups indicate that α, β, and even some γ mRNAs are susceptible to degradation by vhs (Kwong and Frenkel, 1987; Oroskar and Read, 1987, 1989). Regardless of the extent of viral mRNA degradation, targeting of viral mRNAs by vhs helps facilitate the transition between viral gene classes as infection progresses. Furthermore, during infection with a vhs null virus, γ mRNAs are excluded from polysomes due to 'translational overload', whereby the capacity of the translation machinery becomes overwhelmed due to an excess of mRNAs produced earlier in infection (Dauber et al., 2014). This confirms the long-held hypothesis that host shutoff is a means of liberating translational machinery for viral use—with the twist that both host and viral transcripts must be degraded to ensure efficient translation of γ mRNAs.

Further contributing to the robust accumulation of γ proteins is the inactivation of vhs later during infection by the virion proteins VP16, VP22, and UL47 (Read, 2013; Shu et al., 2013a). All three are packaged into the viral particle along with vhs, and it has been

suggested that sequestering vhs in this complex represents an early stage in virion assembly and protects mRNAs from cleavage late in infection. Thus, despite widespread viral mRNA susceptibility, vhs targeting of mRNAs appears temporally controlled.

The SOX homologs in EBV (BGLF5) has also been shown to target viral mRNAs for cleavage (Horst et al., 2012). Unlike vhs, however, there is no indication that SOX or its orthologs are inactivated as infection progresses. Thus, unlike HSV-1 infection, the targeting of viral mRNAs during gamma-herpesvirus infection is not a mechanism to redirect the translation machinery towards viral genes. Deletion of BGLF5 during EBV infection also results in accumulation of several viral proteins, as well as causes nuclear egress defects (Feederle et al., 2009). However, because BGLF5 has dual roles in viral genome maturation and mRNA degradation and the BGLF5 mutant virus lacks both functions, it is not possible to ascribe the above phenotypes solely to a defect in host shutoff. Nonetheless, these data support the hypothesis that degradation of viral mRNA during gamma-herpesvirus infection plays important roles in regulating gene expression and subsequent viral particle composition.

Unlike herpesviral and poxviral mRNAs, SARS CoV transcripts are categorically resistant to nsp1-induced cleavage and degradation. This protection is due to the presence of a protective 5' leader sequence present on all viral mRNAs, although the mechanism of protection remains unclear (Huang et al., 2011). However, while CoV mRNAs escape endonucleolytic cleavage, they do not escape nsp1-induced ribosome inactivation, raising the issue of what advantage is conferred by the protective sequence (Huang et al., 2011; Lokugamage et al., 2012). One likely possibility is that ribosome inactivation is not complete, and consequently viral gene expression is not as severely impacted as cellular gene expression. Whether this represents a mechanism to fine tune viral protein synthesis in a manner important for the viral lifecycle *in vivo* remains an interesting question for future investigation.

Downstream consequences of virus-induced cytoplasmic mRNA degradation

Degradation of mRNA has recently been shown to be highly interconnected with many other cellular processes including transcription, mRNA export, and translation (Braun and Young, 2014; Huch and Nissan, 2014). It is thus likely that the broad virus-induced mRNA decay described above will result in changes to other RNA processes as well. One example of this is altered mRNA 3' end processing in the nucleus that occurs as a consequence of enhanced mRNA decay in the cytoplasm (Figure 2). Poly(A) binding protein (PABPC) normally binds to poly(A) tails of mRNAs in the cytoplasm, where it contributes to the regulation of mRNA stability and enhances translation. However, PABPC becomes strongly relocalized to the nucleus in cells expressing SOX, muSOX, BGLF5, vhs, or nsp1 (Arias et al., 2009; Kumar and Glaunsinger, 2010; Lee and Glaunsinger, 2009; Park et al., 2014). Nuclear import occurs because within its RNA binding domains, PABPC harbors noncanonical nuclear localization signals (NLS) that are masked when it is bound to poly(A) tails in the cytoplasm. However, during accelerated mRNA degradation by these viral proteins, PABPC is released from poly(A) tails, exposing its NLS for interaction with the nuclear import machinery (Kumar et al., 2011). Such aberrant accumulation of PABPC in the nucleus causes hyperadenylation of nascent transcripts by cellular poly(A) polymerase II (Kumar and Glaunsinger, 2010; Lee

and Glaunsinger, 2009). These hyperadenylated mRNAs are retained in the nucleus, presumably because they are recognized as aberrant by the nuclear RNA QC machinery. This process thus contributes to the overall magnitude of host shutoff, as the cytoplasm cannot be efficiently repopulated with newly transcribed mRNAs.

Accelerated cytoplasmic decay and consequent PABPC nuclear localization may also lead to inhibition of stress granules (SGs). SGs form in response to translational arrest that often occurs during viral infection, but many viruses have evolved mechanisms to block their formation to ensure proper translation of viral proteins. Along with several other viral proteins from IAV, endonuclease PA-X was identified as a potent inhibitor of SGs (Khaperskyy et al., 2014). PA-X mediated SG inhibition coincided with PABPC relocalization, hinting at a link between host shutoff and SG dynamics. Similarly, it was found that vhs from HSV-2 was capable of inhibiting SGs, perhaps by bulk reduction of mRNAs needed to nucleate SG formation (Finnen et al., 2014). Future studies may elucidate the connection between mRNA decay and inhibition of SGs.

Contributions of virus-induced mRNA degradation towards immune evasion

Widespread dampening of gene expression during infection is presumed to contribute to viral immune evasion, both by inhibiting expression of cellular immune regulatory genes and by reducing the abundance of viral antigens available for detection. Indeed, viruses containing mutations in HSV-1 vhs, MHV68 muSOX, coronavirus nsp1, and VACV D10 exhibit more severe phenotypes in a mouse model of infection than in cultured cells (Liu et al., 2014; Richner et al., 2011; Smiley, 2004; Zust et al., 2007), suggesting mRNA degradation contributes to virulence. Activation of the innate immune response leads to expression of hundreds of genes involved in establishing an antiviral state. Vhs suppresses the expression of several of these genes including tetherin and viperin, which would normally act to restrict HSV-1 infection (Shen et al., 2014; Zenner et al., 2013), as well as many pro-inflammatory cytokines (Suzutani et al., 2000). Some of the differences in the *in* vivo infectivity of WT versus the vhs mutant HSV-1 are alleviated in interferon receptor defective (IFNAR KO) mice, suggesting that vhs-induced suppression of the innate immune response contributes to viral fitness (Leib et al., 1999; Smiley, 2004).

Selective inactivation of the muSOX mRNA degradation activity leads to a severe attenuation of MHV68 in B cells during the phase of peak latency establishment (Richner et al., 2011). This could be due to improper immune evasion and/or cell-type specific replication defects, as the muSOX mutant virus replicates to WT titers in the mouse lung but traffics inefficiently to B cells (Richner et al., 2011). Similar to the ability of vhs to degrade immune modulatory mRNAs, EBV BGLF5 also reduces expression of immune molecules, in particular HLA I and II (Rowe et al., 2007; Zuo et al., 2008). However, this activity is redundant with other EBV proteins that specifically combat HLA processing and transport and thus appears to have only a small effect on CD8+ T cell recognition (Quinn et al., 2014). Whether CD8+ T cell recognition or innate immune signaling are influenced by mRNA degradation during *in vivo* infection with other gamma-herpesviruses remains to be determined.

Both VACV decapping mutants and CoV nsp1 mutants also display altered virulence phenotypes, although further research is needed to determine the extent to

which these are directly linked to mRNA degradation. Mice infected with VACV D10 stop and catalytic mutants show less weight loss and mortality compared to a WT infection, and these mutant viruses replicate to lower titers in all organs (Liu et al., 2014). Although there is not *in vivo* data for nsp1 of SARS CoV, the nsp1 protein of the coronavirus mouse hepatitis virus (MHV) retains the mRNA degradation function, as well as several additional roles in inhibiting immune signaling pathways. These activities align well with the observation that an MHV nsp1 deletion virus is severely attenuated in WT mice, but is completely rescued in IFNAR KO mice (Zust et al., 2007). Determining the extent to which nsp1-induced virulence links to its host shutoff activity will require the use of single function nsp1 mutants selectively defective for mRNA cleavage or immune pathway impairment. In this regard, the recent characterization of a panel of SARS CoV nsp1 mutants that exhibit selective functional defects should help determine the contribution of mRNA degradation to the nsp1 virulence phenotypes (Jauregui et al., 2013).

The future of viral nuclease research

While many viral nucleases and host shutoff factors have been discovered, there is still much to learn not only about mechanisms of targeting, but also the myriad of downstream consequences that likely result from the global degradation of mRNAs from many different subsets.

The expanding number of viruses shown to exert control over the cytoplasmic mRNA population through the activity of virally encoded endonucleases or by activating cellular nucleases highlights the importance of this process in diverse viral lifecycles. Although we have highlighted select examples of viral endonucleases that promote mRNA decay, many other viruses impact RNA fate by inactivating mRNA degradation enzymes, hijacking or competing with the cellular decay machinery, and relocalizing cellular proteins that control mRNA stability (Moon and Wilusz, 2013).

Furthermore, as is frequently the case in virology, the study of this virus-host interplay is sure to offer new insights into the regulation of cellular RNA decay pathways. The field is now beginning to uncover how cellular RNA degradation enzymes with central roles in basal and QC-associated RNA decay are also key contributors to the antiviral response. Yet, in some cases the precise players or their regulation may differ from their previously characterized roles in the context of uninfected cells. In this regard, revealing how viral RNAs are recognized and marked for degradation by pathways such as NMD remains an important endeavor. This should simultaneously provide insight into cellular RNA features that impact QC surveillance, especially given the numerous parallels between mRNA degradation by viruses and cellular QC pathways.

Much remains to be discovered about the mechanisms underlying mRNA targeting by viral endonucleases as well. Questions surrounding the precise roles of translation factors in recruiting or activating nucleases, what sequence elements and context confer cleavage, as well as how active translation impacts targeting all remain active areas of research. Finally, although the data all point to important roles for virus-induced mRNA degradation in replication and immune evasion *in vivo*, very little is known about the relative importance of regulating host versus viral mRNA abundance in these processes. Ongoing and future research should provide answers to these questions,

as well as reveal the impact of virus-induced mRNA degradation on a diversity of other cellular processes.

Introduction II: The gammaherpesvirus lifecycle

Herpesviridae

Herpesviruses are large, double-stranded DNA viruses that are ubiquitously found through the animal kingdom. Their genomes typically encode for 80-100 proteins and are 120-200 kilobases long. The virion structure includes an icosahedral capsid containing the DNA that is surrounded by viral proteins and RNA that are collectively called the tegument. The host cell-derived lipid membrane surrounds the tegument and is studded with viral glycoproteins.

The herpesvirus family is subdivided into 3 subfamilies: alpha-, beta-, and gammaherpesviruses. The human alphaherpesviruses include herpes simplex viruses (HSV-1 and 2) and varicella zoster (VSV; chicken pox). These viruses are characterized by their ability to establish latency in life long neuronal cells. The human betaherpesviruses include HHV-6 and 7, common childhood diseases, and cytomegalovirus (HCMV). These viruses are characterized by B and T cell tropisms. The human gammaherpesviruses include Kaposi's sarcoma-associated herpesvirus (KSHV) and Epstein-Barr virus (EBV), which are characterized by establishing latency in B cells. KSHV and EBV infections can lead to various B-cell lymphomas in immunocompromised patients, including multicentric Castleman's disease and primary effusion lymphoma. These malignancies are typically seen in people with HIV-AIDS. Kaposi's sarcoma is common in Sub-Saharan Africa as well as regions of the Mediterranean (Bhutani et al., 2015).

Herpesviruses are highly species-specific, meaning the human gammaherpesviruses cannot generally be used to infect models in vivo. Therefore, in order to study the gammaherpesvirus lifecycle, a murine gammaherpesvirus is utilized, called MHV68, which was originally isolated from bank voles (Blaskovic et al., 1980). This model has proven to be extremely useful in determining virulence factors and host immune responses to gammaherpesviruses (Barton et al., 2011).

Herpesvirus lifecycle

All herpesviruses establish lifelong latent infections, but periodically reactivate to seed new populations of infected cells. This biphasic lifecycle is essential for successful host colonization, but very little is known about how viruses switch between the two lifecycles (Figure 3). Cellular tropism switches are known to be important for HSV-1, as the virus lytically infects epithelial cells but latently infects neuronal cells (Knipe and Cliffe, 2008; Penkert and Kalejta, 2011). The proteins found in the tegument are thought to play an important role in modulating the host environment immediately upon infection and could potentially facilitate the entry into either the lytic or latent pathway.

Lytic infection consists of a cascade of gene expression that results in expression of all viral genes. The immediate-early genes (IE) are expressed immediately upon viral entry into the nucleus and include RTA in KSHV. RTA is considered the lytic transactivator and orchestrates the cascade of lytic gene expression. RTA alone is sufficient to induce lytic reactivation (Hair et al., 2007; Liu et al., 2000). The IE genes coordinate the expression of the delayed-early genes (E), many of which are important

for viral replication. Only after viral replication are the late genes (L) expressed, which are structural proteins like capsid and glycoproteins (Ebrahimi et al., 2003).

The gammaherpesvirus genome, while simpler and more spatially constricted than the host genome, contains some ambiguous transcription. At the left end of the MHV68 genome, 8 viral tRNAs are clustered which have tRNA-like secondary structure, but lack amino-acylation capabilities (Bowden et al., 1997). These tRNA transcripts are expressed during both lytic and latent cycles and are transcribed by RNA Polymerase III (Simas et al., 1999). Furthermore, it was discovered that at least 12 microRNAs are processed from these tRNA transcripts (Reese et al., 2010). Recently a role for these RNA Pol III transcripts was found using an MHV68 mutant virus that lacks all 8 vtRNAs and all miRNAs. Acute infection in an immunodeficient mouse model showed the mutant virus resulted in a higher number of infected cells overall, but showed lower virulence as compared to a WT infection (Diebel et al., 2015). A different but similar MHV68 mutant with separate mutations in all 12 miRNAs was shown to have a latency establishment defect, but was dispensable for acute replication in vivo (Feldman et al., 2014). These viral noncoding RNAs likely temper key host cellular pathways important for viral colonization.

Another class of viral putative noncoding transcripts are the expressed genomic regions (EGRs) found scattered throughout the genome. These are 30 RNA Pol II transcripts that are polyadenylated yet contain no obvious protein coding region (Johnson et al., 2010). These transcripts are expressed with kinetics from all 3 viral classes and range in size from 700 to 10,000 nucleotides. Recently, several of these EGRs were found to be functionally relevant to the viral lifecycle. Strand-specific targeting of 6 EGRs reduced viral replication and the expression of other viral genes, indicating a functional role for these noncoding transcripts previously thought to be “noise” (Canny et al., 2014). These findings highlight the complexity of the gammaherpesvirus genome and caution the interpretation of mutations spanning both strands of the genome, as a functional noncoding EGR could be inadvertently affected.

After viral transcription and late gene production, capsid packaging occurs in the nucleus followed by nuclear envelopment through the first nuclear membrane layer and de-envelopment through the second nuclear membrane. The naked capsid then acquires the tegument layer and associates with Golgi-derived membrane structures (Peng et al., 2010). The complete virion buds into an exocytic vesicle, creating a temporary double membrane-bound virion, which traffics to the outer cellular membrane and buds out, releasing a single membrane-bound virion.

While the lytic cycle is necessary for viral spread, latency is the default pathway for many herpesviruses. Latency is characterized by the almost complete shutdown of viral transcription, except for a handful of latency-specific genes. Latency-associated nuclear antigen (LANA) is the best studied of these genes. During latency, the viral genome circularizes to form an episome that attaches to host chromosomes through LANA binding. LANA has binding domains for the episome found within the terminal repeat (TR) region of the genome and also binds host histone H2B (Tempera and Lieberman, 2010), essentially tethering the mostly silenced viral genome to the host. The viral genome is replicated along with host chromosomes and partitioned to daughter cells, ensuring that each new cell retains a copy of the viral genome.

Viral entry and the lytic/latent decision

Herpesvirus binding and entry is a complex topic due to the fact that there are many different glycoproteins, host cell receptors, and tropism switches that occur. There are 3 core viral glycoproteins that are conserved across all herpesviruses: gB, gH and gL. The gammaherpesviruses have several additional glycoproteins, although it is unclear which ones are needed to enter which cell types. Glycoprotein B (gB) is the fusion protein and essential for entry into any cell type. gH/gL form a heterodimer that binds integrins on epithelial cells and triggers conformational changes in gB, allowing fusion to proceed (Connolly et al., 2011).

Events that occur immediately after viral entry are thought to play an important role in the lytic/latent decision. Whether or not the viral genome gets chromatinized and silenced or lytic expression dominates and pushes the virus to enter the lytic cycle is likely determined by a complex series of events as well as cell type specific factors. In HSV-1 infection, the cell type determines the route of infection. When HSV-1 infects epithelial cells, viral proteins promote open chromatin marks such as acetylation on the newly chomatinized viral genome, allowing expression of lytic genes (Knipe and Cliffe, 2008). However, when HSV-1 infects neuronal cells, closed chromatin marks are favored, leading to silenced viral lytic genes and ensuring a latent infection is established. These cell type specific chromatin changes are though to be at least partially due to the localization of viral protein VP16, a transcriptional activator protein. In epithelial cells, VP16 is brought to the nucleus by cellular protein HCF, while in neuronal cells VP16 is trapped in the cytoplasm, unable to enact transcriptional activation, ultimately leading to closed chromatin and latency (Knipe and Cliffe, 2008; Penkert and Kalejta, 2011).

While the cell type differences in the route of infection are relatively straightforward for HSV-1, how gammaherpesviruses determine lytic versus latent infection remains unknown. KSHV has been shown to express bursts of lytic genes immediately following infection that is overcome and silenced in order for the virus to enter latency (Krishnan et al., 2004). RTA expression and a handful of RTA-responsive viral genes showed bursts of expression at 2 hours post infection (hpi) but declined by 24 hpi, while LANA and other latency gene expression increased substantially over 24 hpi. Lytic genes associated with immune modulation were expressed, while genes involved in viral replication and virion packaging were not. This concurrent expression of latent and lytic genes immediately following infection could be indicative of a viral strategy to modulate the immune response as latency is established, or could be a byproduct of the time it takes for a lytic/latent decision to be made.

In contrast to KSHV, MHV68 enters the lytic cycle upon de novo infection of cells in tissue culture. The basis of this difference is unknown. Several tegument proteins associated with MHV68 have been shown to influence RTA expression, which can correspond to increased chance of lytic cycle entry. ORF49 was found to disrupt the interaction between RTA and its negative regulator, PARP-1, which suppresses RTA activity by poly(ADP-ribosyl)ating RTA (Gwack et al., 2003; Lee et al., 2007; Noh et al., 2012). The presence of ORF49 in the tegument led to increased RTA expression and activity. ORF75c, another tegument protein, was found to induce the degradation of PMLs, antiviral factors known to suppress viral lytic gene expression. ORF75c presence

in the nucleus corresponds to PML reduction by directly ubiquitinating PML proteins via its E3 ligase activity (Ling et al., 2008; Sewatanon and Ling, 2013).

While tegument proteins are thought to play important roles in regulating the lytic/latent decision immediately upon infection, how the tegument is formed and what constitutes it is relatively complex. The architecture of the herpesvirus virions has been shown to be dynamic and complex (Bohannon et al., 2013). Many of the known tegument proteins interact with each other, capsid proteins, or glycoproteins to create an interaction network, specifically recruiting viral proteins that serve functions upon the next round of infection (Sathish et al., 2012). However, cellular proteins are also found in herpesvirus virions, although no specific role has been determined. It is thought that tegument packaging may incorporate some proteins in relation to their abundance in the infected cell (del Rio et al., 2005; Michael et al., 2006). This suggests that if abundance of virion proteins was altered, virion composition could be altered as well. Whether or not an altered virion composition would result in functional differences in early events has yet to be determined.

How the viral genome acquires and modulates chromatin structure also plays an important role in determining how and when viral gene expression and thus lytic replication occur. Herpesvirus DNA packaged in the virion is devoid of histones, but rapidly associates with core histones upon infection (Knipe and Cliffe, 2008). It was also found with HSV-1 and MHV68 that a lower MOI resulted in a greater number of histone associations with the viral genome, with decreasing histone association occurring as viral DNA replication proceeded (Mounce et al., 2011). It is thought that histones subsequently get removed from the template DNA by an early viral gene, thus promoting DNA replication and unrestrained viral transcription. KSHV LANA is known to interact with several different cellular histone acetyltransferases (HATs), presumably to maintain appropriate chromatin structure (Tempera and Lieberman, 2010). Adding histone deacetylase (HDAC) inhibitors induces reactivation of latent genomes, due to the chromatin reorganization that occurs around RTA, allowing the expression of the lytic cycle cascade that is normally subjected to a closed chromatin state (Gunther and Grundhoff, 2010). Therefore, host recruited chromatin structure is essential for viral maintenance of latency and the switch from latent to lytic lifecycle.

Mouse model of infection

Tissue culture experiments are helpful for deducing roles of viral proteins in entry, replication and assembly, but pathogenesis and virulence can only be determined by in vivo models of infection. Many viral genes have been found to be dispensable for replication in tissue culture, but result in attenuation during infection of mice. During the intranasal route of infection, lung epithelial cells are lytically infected with MHV68, with viral loads peaking at 5 days post infection (Hwang et al., 2008). This acute infection is typically cleared by the immune system, but some virus traffics to the lymph nodes in dendritic cells (DCs) and macrophages. It is thought that the virus infects DCs early after host entry, as most of the virus that ends up in B cells passes through DCs first (Gaspar et al., 2011). Viruses attenuated for replication in DCs are impaired in B cell colonization and WT MHV68 disrupts DC cytoskeletal structure, suggesting the virus can manipulate DC migration, possibly influencing DC to B cell viral spread (Gaspar et al., 2011). B

cells, the preferred latency reservoir of MHV68, carry the virus to the spleen, where peak latency is established at 2 weeks post infection, with about 1 in 200 spleen cells carrying the latent genome. Many of the infected B cells are cleared, leaving a persistent population of 1 in 10,000 spleen cells infected with latent MHV68 (Collins et al., 2009). The virus maintains a latent infection in memory B cells for the lifetime of the host, undergoing low levels of reactivation in order to seed new populations of infected cells and contribute to host-to-host spread (Stevenson and Efstathiou, 2005).

An in vivo mouse model of infection opens doors for exploring the lytic/latent switch in a more relevant context. Viral mutants that are attenuated in latency establishment include an MHV68 that overexpresses RTA (May et al., 2004; Rickabaugh et al., 2004). This virus may be defective for latency establishment because high levels of RTA favor a lytic infection at inappropriate times, either blocking latency in the right cell type at the right time, or promoting clearance of infected cells by triggering an immune response that latently infected cells would normally evade. A similar phenotype is seen with a muSOX MHV68 mutant (Richner et al., 2011). It is difficult to tease apart what roles RNA degradation play in viral pathogenesis, whether it is due primarily to host driven immune evasion or viral transcript abundance dictating downstream events in the lytic cycle, or some combination.

Outline

The following work focuses on the various downstream consequences of viral-mediated host shutoff using infection with MHV68. First, the fate of viral transcripts are shown to be subjected to muSOX-mediated cleavage and degradation. This is shown to be specific to viral mRNAs, while viral noncoding transcripts escape cleavage, consistent with the proposed mechanism of muSOX. Viral protein abundance is altered in the ΔHS virus, which contains a point mutation in the muSOX gene rendering it defective in shutoff of both host and viral mRNAs. It is further shown that the ΔHS virus has altered virion composition, likely due to altered protein levels during the tegumentation and virion assembly stage of infection. These changes contribute to early events upon subsequent rounds of infection, as viral binding and entry are more efficient with the ΔHS virus. We hypothesize that changes in early events of viral infection must be due to changes in virion composition because muSOX is not expressed until later in infection, and that these changes in early events could influence the ratio of lytic to latent infected cells. Indeed, we see a higher percentage of infected cells that have progressed through the lytic cycle with the ΔHS virus compared to WT. However, although we see more efficient binding and more lytic replication, total viral titer remains equivalent to WT or even shows attenuation in a murine dendritic cell line. Together, these data show that viruses may have a reason to target their own transcripts for degradation, as a means to keep tight control of downstream processes such as deploying latent infections at appropriate times to evade the immune response and establish a lifelong latent infection.

The next chapter addresses some of the downstream consequences of accelerated RNA decay for the host. The idea that multiple cellular processes are interconnected has been explored in yeast by introducing perturbations in RNA decay, translation, or transcription (Braun and Young, 2014; Huch and Nissan, 2014) and observing subsequent changes in global processes not previously thought to be connected. We find

that accelerating mRNA decay by viral infection, or transfection with host shutoff factors alone, leads to transcriptional repression in a subset of host housekeeping genes. This transcriptional repression is dependent on the presence of catalytically active Xrn1 to degrade the fragments produced by the viral endonucleases. Interestingly, we find that viral transcription largely escapes this transcriptional repression, and indeed the WT virus shows more transcription in the presence of Xrn1. These data suggest there is a feedback mechanism in mammalian cells, connecting mRNA decay in the cytoplasm to transcription in the nucleus, potentially as part of a stress response.

Figures

Table 1: Viral endonucleases that broadly restrict gene expression

Virus	Host shutoff factor	Nuclease superfamily	Targeting mechanism	Cleavage location	viral mRNAs
HSV-1	vhs	FEN-1	Binds translation factors eIF4F	5' UTR, near cap	Susceptible (early)
KSHV, MHV68, EBV	SOX, muSOX, BGLF5	PD(D/E)XK	unknown	At targeting sequence	Susceptible
Influenza A	PA-X	PD(D/E)XK	unknown	unknown	unknown
SARS-CoV	Nsp1	N/A	Binds 40s ribosome	ribosome binding site	Protected by 5' leader sequence
Vaccinia virus	D10, D9	Nudix domain decappers	Cap-binding	5' cap	Susceptible

Figure 1

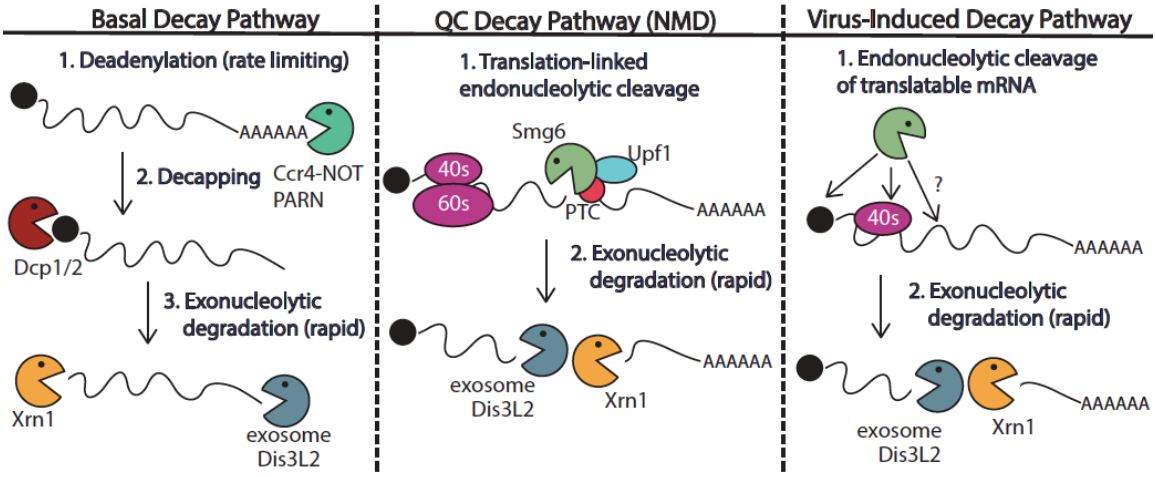

Figure 1: Overview of cellular and viral decay pathways
Basal decay begins with the rate-limiting step of deadenylation, followed by decapping and exonucleolytic degradation of the mRNA body. Quality control decay pathways such as NMD recognize aberrant mRNAs during translation, including the presence of premature termination codons (PTC), and induce endonucleolytic cleavage, whereupon the fragments are degraded by exonucleases. Virus-induced decay also bypass early steps of the basal decay pathway and involves internal cleavage of mRNAs, usually in a translation-linked manner, which is followed by degradation by host exonucleases.

Figure 2

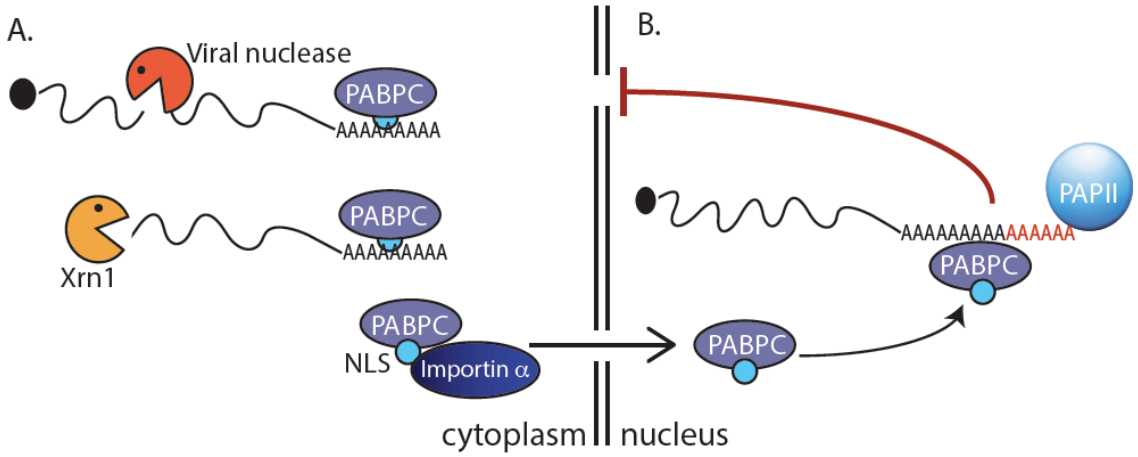

Figure 2: Virus-induced mRNA degradation impacts RNA processing
Widespread mRNA degradation in the cytoplasm leads to release of PABPC from poly(A) tails. This exposes its NLS, which is normally masked during RNA binding, leading to nuclear import via interactions with importin α. Nuclear accumulation of PABPC promotes hyperadenylation of nascent transcripts via PAP II and an mRNA export block.

Figure 3

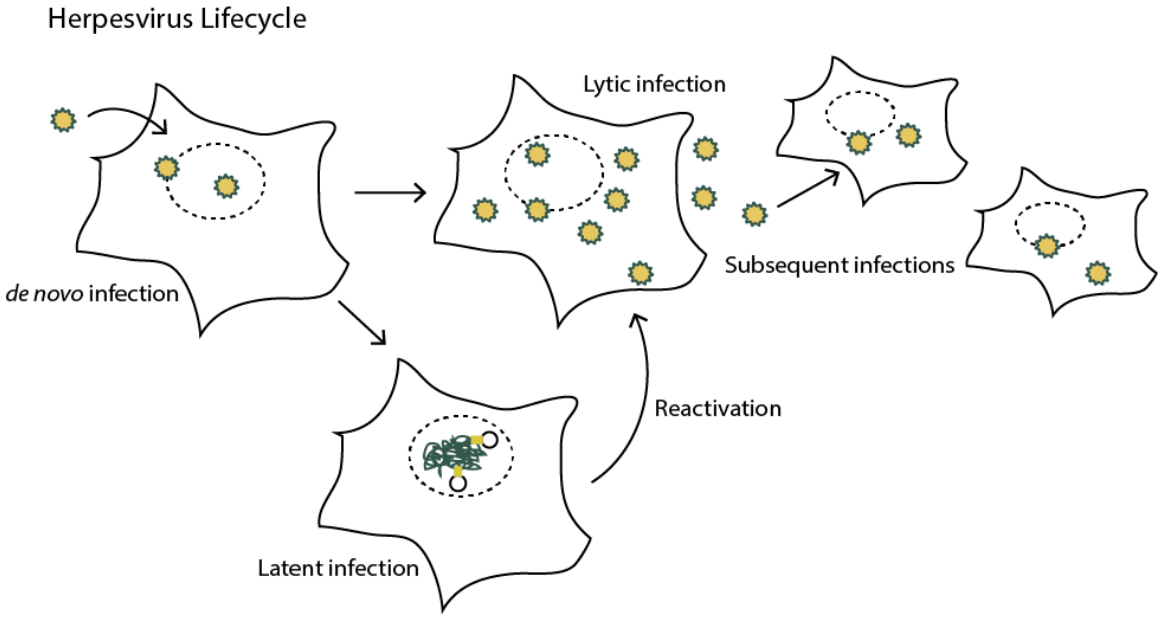

Figure 3: The herpesvirus lifecycle. Upon de novo infection with herpesvirus, either the lytic or latent route of infection progresses. Lytic infection results in complete expression of viral genes and virion production. Virion release leads to subsequent infections of nearby cells. Latency is characterized by episome formation of the viral genome that attaches to the host DNA via viral protein LANA. Very few viral genes are expressed. Reactivation is the process of inducing the lytic cycle cascade from latent genomes.

Chapter 2: Gammaherpesviral gene expression and virion composition are broadly controlled by accelerated mRNA degradation

Introduction

Viruses use a variety of mechanisms to dampen host gene expression, including inhibiting cap-dependent translation, transcription, splicing, and promoting host mRNA degradation. The presumed viral benefits of this 'host shutoff' phenotype include reduced competition for gene expression machinery and resources, as well as impaired immune responses through decreasing host factors involved in sensing infection. The importance of this phenotype *in vivo* has been directly confirmed for both alpha- and gammaherpesviruses, where host shutoff mutants exhibit defects in immune evasion (in the case of the herpes simplex viruses HSV-1 and HSV-2), viral trafficking, and latency establishment (Kwong and Frenkel, 1989; Richner et al., 2011; Strelow and Leib, 1995).

In all cases studied to date, viral transcripts largely escape the effects of host shutoff, thus affording them a competitive expression advantage. For example, poliovirus inhibits cap-dependent translation by cleaving eIF4G, thus enhancing translation of viral mRNAs that contain an internal ribosome entry site (IRES) but not a 5' cap (Krausslich et al., 1987; Kuyumcu-Martinez et al., 2004; Zamora et al., 2002). One mechanism of HSV-induced host shutoff involves altering phosphorylation of SR proteins to inhibit spliceosome assembly and block the biogenesis of nascent host mRNAs, the vast majority of which contain introns (Sciabica et al., 2003). In contrast, HSV mRNAs are largely unspliced, enabling them to circumvent this block and, furthermore, are preferentially exported to the cytoplasm by the ICP27 protein (Chen et al., 2002; Koffa et al., 2001). HSV-1 also promotes endonucleolytic cleavage of host mRNAs through its virally encoded ribonuclease vhs, which is packaged into viral particles and can thus impact host gene expression immediately after viral entry (Kwong and Frenkel, 1989; Kwong et al., 1988). Although HSV-1 mRNAs can be degraded by vhs in the absence of infection, recent data suggest that vhs is regulated by other viral factors in a manner that restricts its activity against viral RNA, particularly during delayed early and late gene expression (Shu et al., 2013b; Taddeo et al., 2013). SARS coronavirus also causes host shutoff by promoting endonucleolytic cleavage of cellular mRNAs, but its viral mRNAs bear a protective 5' leader sequence that prevents their cleavage (Huang et al., 2011).

Similar to alphaherpesviruses and SARS coronavirus, gammaherpesviruses promote host shutoff by inducing widespread cellular mRNA degradation (Covarrubias et al., 2009; Glaunsinger and Ganem, 2004). This viral subfamily includes the oncogenic human pathogens Kaposi's sarcoma-associated herpesvirus (KSHV) and Epstein-Barr virus (EBV), as well as the murine herpesvirus MHV68, a widely used model for understanding gammaherpesviral replication and pathogenesis *in vivo*. Gammaherpesviruses encode a viral nuclease termed SOX in KSHV that endonucleolytically cleaves cytoplasmic mRNAs during lytic infection, leading to their degradation by the host exoribonuclease Xrn1 (Covarrubias et al., 2011). SOX targets the majority of host mRNAs, and the ensuing depletion of cytoplasmic poly(A) mRNA causes nuclear relocalization of cytoplasmic poly(A) binding protein (PABPC), aberrant polyadenylation of RNAs in the nucleus, and an mRNA export defect (Kumar and Glaunsinger, 2010; Kumar et al., 2011; Lee and Glaunsinger, 2009). These downstream phenotypes effectively magnify the gene expression block. Global mRNA destruction is

mechanistically conserved in the SOX homologs in EBV (termed BGLF5) and MHV68 (termed muSOX), as are the PABPC relocalization and RNA processing and export sequelae (Covarrubias et al., 2009; Gaglia et al., 2012; Rowe et al., 2007). This activity likely contributes to viral immune evasion, as it has been shown that the RNA degradation function of EBV BGLF5 impairs CD8+ T cell recognition in cultured cells (Zuo et al., 2008). Additionally, MHV68 bearing a muSOX mutant specifically defective for mRNA cleavage exhibits *in vivo* defects in viral trafficking from the mouse lung to distal sites, as well as a marked reduction in viral loads during peak latency establishment (Richner et al., 2011). Thus, widespread mRNA degradation during lytic replication of gammaherpesviruses contributes measurably to the *in vivo* viral lifecycle, as well as to its interactions with the host immune system.

The prevailing assumption has been that host mRNA degradation is the driver of these phenotypes and, similar to other viruses studied to date, that viral transcripts must possess some mechanism to escape degradation. However, the susceptibility of viral transcripts to SOX-induced cleavage during infection has yet to be directly addressed, although they do not possess any common sequences that might aid in their escape. SOX and muSOX are expressed with early gene kinetics beginning at 8-10 hours post infection (hpi) and continuing through the end of the viral lifecycle (Covarrubias et al., 2009). It has therefore been presumed that, at a minimum, viral gene expression prior to the onset of host shutoff would be unaffected by SOX or muSOX activity. Here, we challenge both of these assumptions by showing that, unexpectedly, all stages of viral gene expression are strongly influenced by muSOX-induced RNA degradation during MHV68 infection. The majority of viral mRNAs are targeted by muSOX during a lytic infection, whereas escapees are enriched for viral noncoding RNAs. The decreased viral mRNA levels in a wild-type MHV68 infection dampens viral protein accumulation and directly influences the composition of progeny viral particles. This, in turn, impacts early events in subsequent rounds of infection prior to the onset of host shutoff. Finally, we demonstrate that inhibiting this global virus and host mRNA degradation restricts MHV68 replication in a cell type specific manner both in cell culture and *in vivo*. Our findings reveal a new layer of complexity underlying gammaherpesvirus gene expression control, and highlight the importance of mRNA degradation in the viral life cycle.

Results

Expression of the majority of viral mRNAs is dampened during host shutoff

The gammaherpesviral SOX protein drives widespread degradation of cellular mRNAs during lytic infection, yet the extent to which viral transcripts escape this fate remains unknown. We addressed this question by comparing an MHV68 mutant that is impaired for host shutoff (ΔHS; host shutoff defective) with its matched mutant rescue (MR) virus in which the mutation was restored to wild type. ΔHS contains an R443I mutation located in the ORF37 gene encoding the SOX homolog (MHV68 muSOX) that renders muSOX selectively defective for mRNA degradation (Richner et al., 2011). Viral transcript abundance was comprehensively evaluated using an MHV68 microarray platform containing 12,000 tiled 60-mer probes that provides 3-fold coverage of each strand of the viral genome. Relative transcript levels were measured in NIH 3T3 cells infected at an MOI of 5 at 24 hours post infection (hpi), a time at which the mRNA

degradation phenotype is well established. Surprisingly, the majority of viral mRNAs from all three kinetic classes (immediate early (IE), early (E), and late (L)) were significantly downregulated during a MR infection as compared to a ΔHS infection, suggesting that viral transcripts do not broadly escape muSOX-induced degradation (Figure 1A, red bars). This trend was confirmed using RT-qPCR as an independent measure of viral mRNA levels during infection for three representative genes (ORFs 8, 49, and 54) after normalization to the host shutoff resistant 18S ribosomal RNA (Covarrubias et al., 2011; Gaglia et al., 2012). Furthermore, RT-qPCR analysis of several genes that appeared unchanged in the array data (ORFs 4, 9, 65, 68, and 73) indicated that these were also decreased during infection with MR relative to ΔHS MHV68, suggesting that the microarray results may be an underestimation of the extent of viral mRNA targeting by muSOX (Figure 1B). RT-qPCR analysis of these transcripts in a murine dendritic cell line (DC2.4) infected with the MR or ΔHS virus yielded similar results, indicating that muSOX targeting of viral transcripts during infection occurs in multiple cell types (Figure 1C).

The reduced viral transcript levels could either be due to cleavage of viral mRNAs by muSOX, or be a secondary consequence of altered levels of cellular proteins (e.g. transcription factors) affected by host shutoff. To distinguish these possibilities, we compared the half-life of representative IE (ORF57), E (ORFs 54 and 55), and L (ORF8) viral transcripts following infection of 3T3 cells with MR or ΔHS virus. The decay rate of each mRNA was calculated following addition of actinomycin D (ActD) to halt transcription at 18 hpi. In all cases, the ΔHS mutation led to a significant increase in transcript stability, indicating they are directly targeted for degradation by muSOX (Figure 1D-G). Thus, host shutoff is not restricted to cellular mRNAs, but also broadly impacts viral mRNA abundance during gammaherpesvirus infection.

Noncoding RNAs are enriched in the escapee population

Although the majority of MHV68 transcripts appear subject to degradation during host shutoff, a subset may escape this fate (Figure 1A, green bars). For example, levels of the M1 and M2 mRNAs are higher in MR infected cells relative to ΔHS infection as measured both by microarray analysis and RT-qPCR (Figure 2A). Interestingly, many of the other putative escapees are candidate or confirmed non-coding RNAs (ncRNAs). Indeed, analysis of the viral mRNA and ncRNA distribution revealed that most of the viral mRNAs fall under the muSOX-susceptible category, whereas the population of muSOX escapees is strongly enriched for ncRNAs (Figure 2B). This observation correlates well with previous data indicating that the gammaherpesviral SOX proteins preferentially target translationally competent cellular mRNAs.

To confirm that noncoding transcripts are not depleted by muSOX, we compared the abundance of seven of the RNA polymerase III (Pol III) transcribed viral tRNAs during infection with MR or ΔHS virus at 24 hpi by RT-qPCR (Figure 2C-D). In contrast to the viral ORF54 mRNA, none of the tRNA levels were decreased during a MR infection relative to infection with the ΔHS virus. We next examined several of the Expressed Genomic Regions (EGRs), which are RNA polymerase II (Pol II) transcripts distributed throughout the MHV68 genome that lack apparent coding capacity (Johnson et al., 2010). Similar to the viral tRNAs and in accordance with the microarray data, qPCR analysis indicated that several of the EGRs escape downregulation by muSOX, a

finding confirmed by half-life analysis for EGRs 9, 15, and 26 (Figure 1A, 2E-H). Some EGRs, such as EGR1, were modestly or markedly upregulated during a MR infection, though this was due to a secondary transcriptional increase rather than enhanced RNA stability (data not shown). We noted that not all of the EGRs escape the effects of host shutoff, as EGRs 24, 27, and 29 were decreased during a MR relative to ΔHS MHV68 infection (Figure 2E). Given that the EGRs have yet to be functionally characterized, it is possible that those that are decreased in the presence of active muSOX are not truly noncoding, or may possess certain mRNA-like features. Collectively, however, these data suggest that muSOX preferentially targets viral mRNAs for degradation, while many viral ncRNAs are unaffected (or upregulated) during host shutoff.

RNA degradation alters intracellular viral protein levels and virion composition

We reasoned that if muSOX-induced depletion of viral mRNAs was important for regulating viral gene expression, then the differences in mRNA levels should lead to corresponding alterations in viral protein abundance. Protein levels were therefore measured for viral factors with available antibodies by Western blotting lysates of NIH 3T3 cells infected with MR or ΔHS MHV68. Indeed, in accordance with the mRNA abundance data, ΔHS infected cells contained higher protein levels of ORF51 (gp150), ORF8 (gB), ORF45, ORF37 (muSOX), ORF49, and ORF72 (v-Cyclin) relative to cells infected with MR virus (Figure 3A). Not all of the mRNA abundance changes resulted in altered protein levels however, as ORF4 (gp70) and ORF65 (M9) proteins accumulated to similar levels during MR and ΔHS infections even though their transcripts were targeted by muSOX. These results indicate that in most cases, muSOX targeting of viral mRNAs regulates protein abundance during MR infection.

How might the broad muSOX-driven reduction in viral gene expression impact the outcome of infection? One possibility is that increased abundance of select viral proteins in the absence of functional muSOX might lead to alterations in viral particle composition, for example through elevated concentrations of envelope or tegument proteins. In particular, it has been shown that tegument composition can be influenced by intracellular protein concentration (Michael et al., 2006). We therefore analyzed the composition of virions purified from MR or ΔHS infected cells by mass spectrometry (MS). Figure 3B shows the relative abundance of proteins detected in both MR and ΔHS virions from two MS runs (several proteins were detected in only 1 sample and thus were excluded from the comparative analysis). To ensure that differences were not due to unequal viral particle numbers between samples, peptide counts were first normalized to the major capsid protein ORF25, as capsid composition is geometrically constrained and thus should not be influenced by intracellular protein abundance. We then performed a secondary normalization against genome number (Table 1). Among the viral proteins available for comparison, there was a 2-3-fold increase in the abundance of select tegument (ORFs 45, 49, and 75c) and envelope (ORF8; gB) proteins in ΔHS virions relative to MR virions (Figure 3B). As expected, the levels of the minor capsid protein ORF65 and minor scaffolding protein ORF17 remained unchanged, validating the normalization strategy. Tegument proteins ORF75b and ORF52 appeared unchanged as well, indicating that not all components of the virion were altered. To confirm these data and compare the abundance of additional virion components not detected in the MS, purified viral particles were resolved by SDS-PAGE and Western blotted with antibodies

against ORFs 4, 8, 45, 49, and 65. Indeed, tegument proteins ORF45 and ORF49 and the glycoprotein ORF8 (gB) accumulated to higher levels in ΔHS virions (Figure 3C). In contrast, we observed no differences in the relative abundance of the ORF65 minor capsid protein or ORF4 (gp70). To confirm that altered virion composition in the absence of host shutoff was not restricted to virions derived from 3T3 cells, we compared the levels of the muSOX-impacted tegument proteins ORF45 and ORF49 by Western blot of virions purified from infected MEFs, and observed a similar increase in their levels in the ΔHS virus (Figure 3D). Thus, in the absence of muSOX-induced mRNA degradation, the abundance of several viral proteins increases, resulting in altered composition of progeny virions.

Altered virion composition leads to enhanced cell surface binding and entry

We next sought to determine whether the differences in MR and ΔHS MHV68 particles resulted in any functional distinctions during a *de novo* infection. Given that viral envelope glycoproteins are involved in cell surface binding and internalization, we hypothesized that increased glycoprotein concentrations such as those we observed for gB might influence these events. We first measured viral attachment to NIH 3T3 cells and to the dendritic cell line DC2.4 by incubating them with MR or ΔHS MHV68 for 90 min at 4°C to allow attachment but prevent uptake, then measuring the relative level of attached virions by qPCR for the viral genome (Figure 4A). Indeed, there was a marked (10-15 fold) increase in ΔHS virus binding relative to MR binding in both cells types (Figure 4A). We observed similar results when we quantified viral entry by incubating at 37°C for 90 min, acid stripping, and measuring intracellular viral particles by qPCR, indicating that the bound particles were successfully internalized (Figure 4B). This increase in binding and entry of ΔHS virions was not a secondary consequence of excess defective particles, as we observed no significant differences in the particle:PFU ratio between the WT, MR and ΔHS viruses (Figure 4C). We conclude that the altered virion composition of ΔHS directly influences the first step of the viral lifecycle.

Failure to degrade viral mRNAs leads to enhanced lytic cycle entry

We next examined whether the altered virion composition influenced progression of the MHV68 lifecyle post entry. In particular, tegument proteins are deposited directly into newly infected cells and thus are poised to have an early impact on the course of infection. A key early outcome of a herpesvirus infection is whether the incoming virus establishes latency or progresses to lytic replication, with latency generally favored upon gammaherpesvirus infection *in vivo* and in cultured cells. Although MHV68 is atypical in that in cell culture (unlike *in vivo*) it defaults to lytic replication, we previously observed that not all infected cells immediately enter the lytic cycle and a larger proportion of NIH 3T3 cells displayed a lytic marker (muSOX) upon infection with the ΔHS virus compared to the MR virus (Richner et al., 2011). To determine whether the enhanced lytic entry phenotype of ΔHS MHV68 was specific to NIH3T3 cells or represented a more general effect, we measured the proportion of infected cells expressing the lytic protein ORF65 (M9) in both NIH 3T3 cells and mouse embryo fibroblasts (MEFs) at 18 hpi (Figure 5A). M9 was used as a lytic marker because its levels are not influenced by muSOX activity (see Figure 3A). Both viruses constitutively express GFP, which serves as a marker of infected cells. Indeed, in both NIH 3T3 and

MEF cells 82.4% and 84.3%, respectively, of the GFP+ infected cells were also M9+ during infection with ΔHS virus. However, only 46.6% and 50.9% of NIH 3T3 and MEF cells infected with the MR virus were double positive (Figure 5A). Thus, RNA degradation by muSOX tempers viral lytic cycle entry during a *de novo* infection.

We hypothesized that the increased number of ΔHS infected cells directly entering the lytic cycle might be a consequence of enhanced activity of RTA, the major lytic transactivator. Although RTA is not a component of MHV68 particles, it is an IE gene whose activity is influenced by tegument proteins (Ling et al., 2008; Noh et al., 2012), some of which are over represented in ΔHS virions (Figure 3B-C). We assessed RTA activity at early times post infection by measuring levels of the RTA-responsive transcripts ORF 50 (RTA), ORF 57, and ORF 6 by RT-qPCR (Figure 5B-D). All three RTA-responsive transcripts were induced to significantly higher levels at 4 hpi (p-value <0.007) after infection with the ΔHS virus as compared to the MR virus. A similar trend was observed at 6 and 8 hpi, although the differences at these time points were not statistically significant. Importantly, the levels of the cellular GAPDH mRNA remained unchanged between 2-8 hpi but, as expected, decreased at 24 hpi during host shutoff (Figure 5E), which generally starts 10-18 hpi (Covarrubias et al., 2009). This confirmed that the effects on viral transcript accumulation manifested prior to the onset of muSOX-induced mRNA degradation, and therefore must derive from differences in the incoming viral particles. Thus, RTA activity is stimulated shortly after infection with the ΔHS virus, likely due to higher levels of RTA activators within the virion itself.

muSOX-induced mRNA degradation is important for viral amplification in a cell type specific manner *in vitro* and *in vivo*

Given the enhanced viral gene expression and lytic cycle entry phenotypes of the ΔHS virus, it might be predicted that this mutant virus would replicate more efficiently, as has been observed for MHV68 engineered to constitutively express RTA (Hair et al., 2007; May et al., 2004). However, ΔHS was shown to have no growth advantage over MR in NIH 3T3 cells and, furthermore, in mice it displayed defects in trafficking from the lung to distal sites, as well as severely decreased abundance in splenocytes at 2 weeks post infection during peak latency establishment (Richner et al., 2011). These observations suggest that there may be cell type specific replication defects associated with impaired muSOX RNA degradation activity that manifest subsequent to the viral entry and gene expression enhancements observed above. We therefore compared the replication rates of the MR and ΔHS viruses in NIH 3T3, MEF, and DC2.4 cells using multi-step growth curves. As reported previously, the MR and ΔHS viruses grew to similar titers in NIH 3T3 cells (Figure 6A). However, ΔHS displayed moderately delayed kinetics in MEF cells, resulting in a 2 log defect at 5 dpi (Figure 6B) and severely delayed kinetics in DC2.4 cells, resulting in a 5 log defect at 5 dpi (Figure 6C). The DC2.4 result is notable given that MHV68 infects and traffics through dendritic cells in mice (Gaspar et al., 2011). Thus, although the ΔHS virus binds and enters these cells more efficiently than MR, its failure to control gene expression through muSOX activity results in a downstream amplification defect.

B cells are key sites of viral replication and latency establishment *in vivo*, however these cells cannot be readily infected in culture. We therefore sought to monitor viral replication in these cells in infected mice. MHV68 infection via the intraperitoneal

route (i.p.) leads to lytic replication in macrophages and B cells in the spleen that peaks at 10 dpi, whereupon the lytically infected cells are largely cleared prior to the onset of peak latency at 18 dpi (Barton et al., 2011; Hwang et al., 2009). We therefore measured viral load in splenocytes of mice infected i.p. with each virus at 10 dpi during the lytic replication phase, and found significantly reduced viral titers with ΔHS compared to MR (Figure 6D). These data indicate that inhibition of muSOX-induced RNA degradation restricts MHV68 amplification in a cell type specific manner both *in vitro* and *in vivo*.

Discussion

Our findings demonstrate that the majority of gammaherpesviral mRNAs are targeted by the muSOX nuclease and thus reveal a novel layer of regulation in viral gene expression. The importance of this activity is highlighted by the alterations in virion composition, as well as in viral entry, early lytic gene induction, and viral amplification that manifest in the absence of functional muSOX. Thus, controlling viral mRNA abundance through enhanced degradation is a regulatory activity that exerts influence throughout the viral lifecycle. This gammaherpesviral strategy is distinct from that of all other host shutoff-inducing viruses characterized to date, each of which has evolved mechanisms to selectively target host gene expression. Even when comparing the gammaherpesviruses to the related alphaherpesviruses such as HSV-1, which also induce mRNA cleavage, several distinctions are apparent in the regulation and function of their host shutoff activities. For example, the HSV-1 host shutoff factor vhs is packaged into the viral particle and therefore promotes RNA degradation immediately after viral entry, before the onset of most viral gene expression (Kwong and Frenkel, 1989; Kwong et al., 1988). It has been proposed that vhs-induced degradation of immediate early HSV-1 mRNAs may facilitate the transition between immediate early and early viral gene expression (Oroskar and Read, 1989). However, at least three other viral proteins, VP16, VP22, and UL47, subsequently interact with vhs and restrict its activity against viral transcripts expressed in the early and late kinetic classes (Lam et al., 1996; Shu et al., 2013a; Smibert et al., 1994; Taddeo et al., 2007). In contrast, the gammaherpesviral SOX protein is not packaged in virions and is expressed with early kinetics beginning at 8-10 hpi (Bechtel et al., 2005b; Bortz et al., 2003; Cheng et al., 2012; Covarrubias et al., 2009; Zhu et al., 2005). Global mRNA degradation occurs following SOX expression and continues for the remainder of the viral lifecycle (Covarrubias et al., 2009; Glaunsinger and Ganem, 2004). Unlike alphaherpesviruses, where there are distinct transitions between each kinetic class of viral genes, during gammaherpesvirus infection the onset of each new phase does not coincide with the downregulation of the prior class of viral genes. Thus, muSOX continues to accumulate even during the final stages of the viral replicative cycle, resulting in degradation of viral transcripts in both early and late kinetic classes.

The targeting of viral and cellular mRNA by muSOX is likely to occur via similar mechanisms. It has been previously shown that SOX and its homologs preferentially cleave RNAs that have been transcribed by Pol II and are translationally competent, but fail to degrade RNAs transcribed by RNA Pol I or III (Covarrubias et al., 2011; Gaglia et al., 2012). In agreement with these data, we observed a similar preference for viral mRNAs over ncRNAs in the muSOX targets. In particular, none of the RNA Pol III transcribed viral tRNAs were depleted by muSOX and there was a clear enrichment for

other putative ncRNAs (EGRs) in the escapee population. The susceptibility of certain EGRs to muSOX may reflect differences in their composition, such as the presence of small ORFs, or in their localization or potential regulatory activities. Our findings may therefore be useful for future studies aimed at probing the function of the EGRs. Though the majority of viral mRNAs appear targeted by muSOX, there are coding transcripts that escape depletion. This has also been observed for a population of cellular mRNAs (Clyde and Glaunsinger, 2011; Glaunsinger and Ganem, 2004), which presumably escape either because they lack a SOX-targeting element(s) or because they contain specific protective features, as has been demonstrated recently for the cellular interleukin 6 transcript (Hutin et al., 2013). The select viral mRNAs refractory to muSOX-induced turnover may exhibit a similar diversity of protective features, and delineation of the precise muSOX-targeting RNA element(s) should shed light on this issue. In addition, whether their selective protection impacts viral replication or pathogenesis remains an important question for future study.

A particularly striking finding was that muSOX-induced degradation of viral mRNAs influenced events that occur during the first 6 hpi, before either its expression or host shutoff initiates. These effects manifested as a consequence of alterations in virion composition imposed during the prior round of replication. There is evidence suggesting that extensive protein-protein interactions dictate tegument composition and deleting certain proteins can alter this balance (Guo et al., 2009; Mettenleiter, 2004; Michael et al., 2006). Furthermore, pseudorabies virions lacking select tegument proteins accumulate actin in the viral particles, suggesting there is a critical mass that is filled in relation to protein abundance in an infected cell (del Rio et al., 2005; Michael et al., 2006). These findings and others, together with our observations, indicate that tegumentation is a highly orchestrated process regulated through specific protein interactions as well as by protein abundance, which can be at least partially controlled at the level of viral mRNA stability. We anticipate that in addition to the protein composition changes examined herein, there are presumably increased levels of viral and perhaps cellular mRNAs packaged into the ΔHS virions that may also impact early events in the viral lifecycle. Indeed, it has been previously observed that RNAs can be packaged into herpesviral particles in a manner largely linked to their intracellular abundance (Bechtel et al., 2005a; Terhune et al., 2004).

In addition to potential structural roles in the virion, tegument proteins can manipulate the cellular environment immediately after their release and thus are thought to play key roles in facilitating infection (Sathish et al., 2012). For example, immune evasion is partly mediated through the activities of KSHV ORF36 and its homologs, which inhibit the type 1 IFN response (Hwang et al., 2009), as well as HSV-1 UL41, which downregulates MHCII on the cell surface (Trgovcich et al., 2002). Other tegument proteins are involved in augmenting early viral gene expression, such as HSV-1 VP16, HCMV pp71, and KSHV RTA, which act as lytic transactivators through coordination with other viral and cellular factors (Bechtel et al., 2005a; Bresnahan and Shenk, 2000; Kelly et al., 2009; Zhu et al., 2005). Unlike in KSHV, RTA is not packaged into the MHV68 virion, although it is expressed with immediate early kinetics and several tegument proteins facilitate lytic infection by boosting its activity. For example, MHV68 ORF49 interacts with PARP-1, a cellular inhibitor of RTA (Noh et al., 2012), while ORF75c degrades PML-NBs, which interfere with lytic cycle progression (Ling et al.,

2008). Our observation that cells infected with the ΔHS virus displayed enhanced RTA activity shortly after infection confirms that failure to moderate viral protein levels through mRNA degradation has marked consequences for subsequent rounds of infection, including preferential or enhanced immediate early lytic gene expression.

MHV68 infects a variety of cell types *in vitro* with varying outcomes, including efficient lytic replication in fibroblasts, delayed lytic entry in dendritic cells, and primarily latent or abortive lytic infection in macrophages (Goodwin et al., 2010; Rochford et al., 2001). *In vivo*, evidence suggests that epithelial cells are lytically infected, while dendritic cells, macrophages, and B cells mainly support latency after an initial burst of lytic infection to amplify the virus and seed a population of infected cells (Barton et al., 2011; Flano et al., 2000; Milho et al., 2009; Sunil-Chandra et al., 1992). Previously, we reported that the MHV68 ΔHS virus exhibits dramatically reduced viral loads at 17 dpi during peak latency (Richner et al., 2011). Here, we found that the ΔHS virus also exhibits cell type specific defects during the lytic amplification stage both *in vivo* and in cultured cells. Thus, despite the enhanced lytic gene expression phenotype of the ΔHS virus, one or more subsequent steps in the replication cycle are impaired in certain cell types. Though the basis for the cell autonomous replication defect remains unknown, the reduced amplification *in vivo* could manifest in part through impaired immune evasion, for example as a consequence of elevated viral antigen levels or abortive infection. One possibility is that the innate immune sensing and response mechanisms are differentially tuned in a cell type specific manner, such that failure to degrade viral and host mRNAs triggers a more robust antiviral response in certain cell types. Additionally, we have noted that the WT MHV68 lifecycle progresses more slowly in dendritic cells relative to 3T3 cells or MEFs (unpublished observations), perhaps making these cells more impacted by the increased accumulation of viral mRNAs in the ΔHS infection.

Our data challenge the assumption that viruses that dampen host gene expression do so categorically to provide a competitive advantage to viral gene expression. Instead, we reveal that degradation of viral transcripts during lytic gammaherpesviral infection is integral to establishing the appropriate balance of viral factors necessary for replication and optimal virion composition. Clearly, degradation of viral mRNAs is not absolute and mechanisms may exist to temper the effects of muSOX to ensure adequate accumulation of viral transcripts. For example, it has been shown that KSHV ORF57 can stabilize viral RNA in the nucleus and cytoplasm (Nekorchuk et al., 2007; Sahin et al., 2010). Additionally, viral mRNAs may contain regulatory sequences that help modulate their stability. Deciphering how the many layers of gene expression regulation are coordinated during infection remains an important future challenge.

Material and Methods

Cells, Viruses, and Infections

NIH 3T3, NIH 3T12, Vero, DC2.4, and MEF cells were maintained in Dulbecco's modified Eagle medium (DMEM; Invitrogen) supplemented with 10% fetal bovine serum (FBS; Invitrogen). The green fluorescent protein (GFP)-expressing MHV68 bacterial artificial chromosome (BAC) has been described elsewhere (Adler et al., 2000), and the R443I host shutoff mutant was previously generated by allelic exchange as previously described (Richner et al., 2011). BAC-derived MHV68 virus was produced by

transfecting BAC DNA into NIH 3T3 cells using SuperFect (Qiagen). Virus was then amplified in NIH 3T12 cells and titered by plaque assay on NIH 3T3 cells. Before infecting mice, the loxP-flanked BAC vector sequence was removed by passaging the virus through Vero cells expressing Cre recombinase (kindly provided by Dr. Samuel Speck, Emory University).

Tiled Microarray Hybridization and Analysis

Array data was derived from two independent biological replicates of each infection condition. Custom MHV68 tiled arrays in the 4 by 44,000 format were designed as described previously (Cheng et al., 2012). 1 μg of RNA was reverse transcribed using an oligo(dT) promoter-primer, subjected to linear amplification and Cy3 or Cy5 labeling using an Agilent Quick Amp labeling kit. Adenovirus spike-in controls were added to each labeling reaction to allow normalization per the two-color spike-in kit instructions (Agilent). The Cy5-labeled reference RNA derived from an independent infection of NIH 3T3 cells at 8 hpi with WT MHV68 was generated, purified, fragmented, and then hybridized in parallel with the Cy3-labeled sample RNA at 65°C for 17 h. Microarrays were scanned with Agilent Scanner Control software (version 7.0), and hybridization signal intensities were quantified using Agilent Feature Extraction software (version 9.5).

Raw data were processed by subtracting the median background signals from the mean signals in the Agilent feature extraction file and then normalized by multiplying the $\log_2$ values of the probe intensities by the spike-in scale factor for each array. The scaling factor was calculated from the linear fit of the spike-ins versus their concentration. The normalized $\log_2$ Cy5-labeled reference RNA signal was subtracted from the normalized $\log_2$ Cy3-labeled experimental sample RNA signal for each probe. The expression value of each viral ORF was calculated as the median of the normalized signal of all tiling probes enclosed inside the ORF. Quality control analyses indicated strong correlation between the biological replicates. Differentially expressed genes were identified after performing empirical Bayes moderated t-statistics using the Bioconductor LIMMA package (version 3.12.1) (Smyth, 2004).

Nucleic acid isolation and measurement

RNA was isolated using the Zymo Mini RNA II Isolation Kit (Zymo Research), treated with Turbo DNase (Ambion) to remove genomic DNA contamination, and reverse transcribed using AMV RT (Promega) with oligo(dT) and 18s specific primers. For ncRNA analysis, transcript specific reverse primers were used instead of oligo(dT) during cDNA synthesis. cDNA levels were then quantified using DyNAmo color flash SYBR green master mix, ROX passive reference dye (Thermo Scientific), and transcript specific primers (listed in Table S2). Transcript levels were normalized to 18s. Viral genomes were quantified by isolating DNA using the DNeasy Blood and Tissue kit (Qiagen), and using 10-fold dilutions of 1 ng BAC DNA to generate a standard curve. For mRNA half-life analyses, at 18 hpi 2 μg of actinomycin D (Sigma) was added to halt transcription, and RNA was isolated at the indicated time points for quantification by RT-qPCR using TaqMan reagents (Applied Biosystems). Primers used to detect ORF54 (probe TCACACCTATATCTGTCCAACCCAGCGAA) and ORF55 (probe CCAACCTTTGGCCACGCCCC) are listed in Table S2. Final primer concentrations of

900 nM and probe concentrations of 250 nM were used. ORF57 and ORF8 primers and probes were used as described previously (Richner et al., 2011; Weinberg et al., 2004). GAPDH levels were measured using the TaqMan Rodent GAPDH Control and Ribosomal RNA Control reagents (Applied Biosystems). The data were plotted relative to the t=0 time point which was set to 1.

Virion Isolation and Mass Spectrometry

Viral supernatants were collected 7 dpi from 6 plates (15 cm) of NIH 3T3 or MEF cells infected at an MOI of 0.5 and centrifuged at 4,000 rpm for 15 min to pellet cellular debris, then subsequently centrifuged over a 20% sucrose cushion at 24,000 rpm for 1 h to pellet the virus. The pellet was resuspended in 200 µl PBS and centrifuged through a 10-60% continuous sucrose gradient at 24,000 rpm for 1 h. Fractions (1 mL) were collected, and DNA was extracted from a portion of each fraction using the DNeasy Blood and Tissue kit (Qiagen) to quantify viral DNA by qPCR using gB-specific primers. Fractions enriched in viral genomes were pooled, pelleted by centrifugation at 24,000 rpm for 1 h, and resuspended in 100 µl of lysis buffer [50 mM Tris-Hcl, pH7.4, 150 mM NaCl, 2 mM EDTA, 1% Nonidet P-40, 0.1% SDS] for Western blots or 50 µl of ammonium bicarbonate (25 mM) for mass spectrometry.

Western blots

Cell lysates were prepared in lysis buffer and quantified by Bradford assay. Equivalent amounts of each sample were resolved by SDS-PAGE and Western blotted with the following anti-MHV68 primary antibodies: hybridoma supernatants T1A1 anti-gp150, MG-2C10 anti-gB, and 9c7 anti-gp70, diluted 1:10 (kindly provided by Phillip Stevenson, University of Cambridge); anti-M9, anti-ORF26, and anti-ORF45, diluted 1:500 (kindly provided by Ren Sun, UCLA); anti-ORF72, diluted 1:500 (kindly provided by Linda van Dyk, University of Colorado, Denver); anti-ORF49, diluted 1:500 (kindly provided by Moon Jung Song, Korea University). Primary antibodies were followed by HRP-conjugated goat anti-mouse or goat anti-rabbit secondary antibodies (Southern Biotechnology, 1:5000).

Viral Binding and Entry Assays

NIH 3T3 or DC2.4 cells were infected at 4°C (to measure binding) or 37°C (to measure entry) for 90 min at an MOI of 5. For the binding assay, cells were then washed 4X with ice-cold PBS, scraped, and DNA isolated by DNeasy Blood and Tissue kit (Qiagen). For the entry assay, cells were washed 2X with PBS, and 0.5 ml of citric acid [135 mM NaCl, 10 mM KCl, 40 mM citric acid, pH 3] was added for 5 minutes at RT to strip off remaining cell surface-bound viral particles. Cells were washed twice more with PBS, scraped, and DNA was isolated. Relative genome levels were quantified by qPCR with gB-specific primers.

Immunofluorescence Assays

NIH 3T3 or MEF cells were grown on coverslips and infected with GFP-BAC MHV68 at MOI of 5. At 24 hpi, coverslips were washed with PBS and cells were fixed in 4% formaldehyde for 30 min at RT. Cells were then permeabilized in 1% Triton-X-100 and 0.1% sodium citrate in PBS for 10 min, and incubated with anti-M9 antibodies at

1:500 in 10% goat serum at 37°C. After 1 hour, coverslips were washed 3X in PBS and incubated with goat anti-rabbit AlexaFluor546 secondary antibody at 1:1500 (Invitrogen). Coverslips were washed 3X in PBS and mounted in DAPI-containing Vectashield mounting medium (VectorLabs) to stain cell nuclei.

Growth Curves and *in vivo* Experiments

For multi-step growth curves, $1.5x10^5$ NIH 3T3, MEF, or DC2.4 cells were infected with MHV68 at MOI of 0.05 and both supernatant and cells were harvested at 0, 1, 2, 3, 4, and 5 dpi and frozen. Samples were freeze-thawed once before titering by plaque assay on NIH 3T3 cells.

For *in vivo* experiments, female C57BL/6J mice were obtained from the Jackson Laboratory (Bar Harbor, ME) and infected when 4-6 weeks old through injection of $1x10^3$ pfu of virus in 0.2 ml PBS into the peritoneal cavity. Spleens were harvested at 10 dpi, and DNA isolated and quantified by qPCR, using gB-specific primers to determine relative levels of viral genomes.

Figure 1

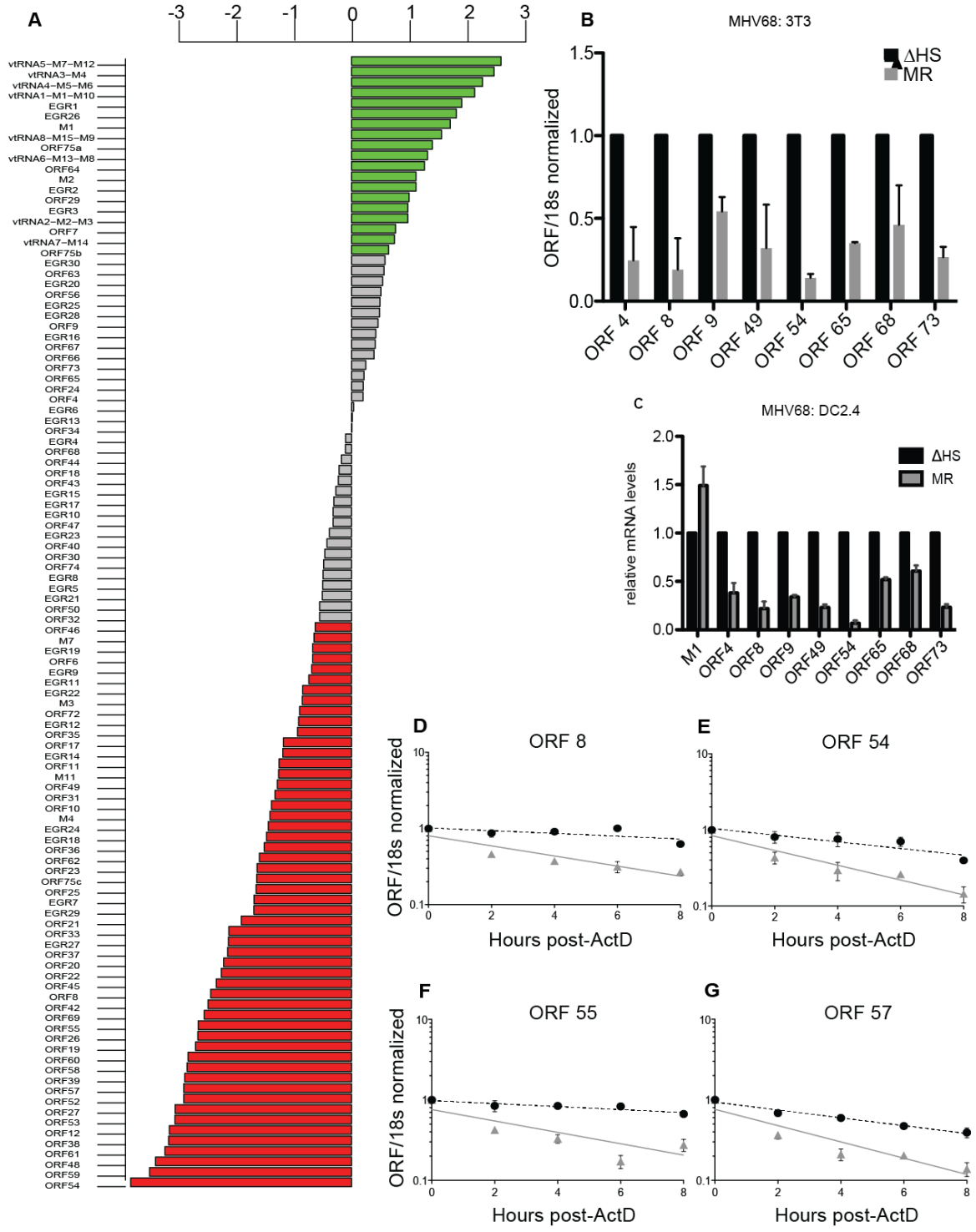

Figure 1. Expression of the majority of viral mRNAs is dampened during host shutoff. (A) For viral genes, the $\log_2$ fold change in expression upon infection with WT compared to ΔHS MHV68 expression was plotted and data points were colored to indicate the adjusted P values, with green points indicating positive $\log_2$ fold change with

P value <0.05 and red indicating negative $\log_2$ fold change with P value <0.05. (B) RT-qPCR was used to validate selective viral transcripts. RNA was isolated at 24 hpi from NIH 3T3 cells infected with MR or ΔHS MHV68 at an MOI of 5. Transcript levels were normalized to 18s and ΔHS levels set to 1. (C) DC2.4 cells were infected as above and RNA isolated and analyzed as above. (D-G) mRNA half-life analyses were conducted by infecting NIH 3T3 cells with MR or ΔHS MHV68 at an MOI of 5. At 18 hpi, 2 ug of Actinomycin D was added to block transcription and RNA was harvested at the indicated times thereafter. RT-qPCR was performed with ORF-specific primers and probes to determine mRNA levels. The black dotted line indicates the best-fit line for the ΔHS virus, and the grey solid line indicates the best-fit line for the MR virus.

Figure 2

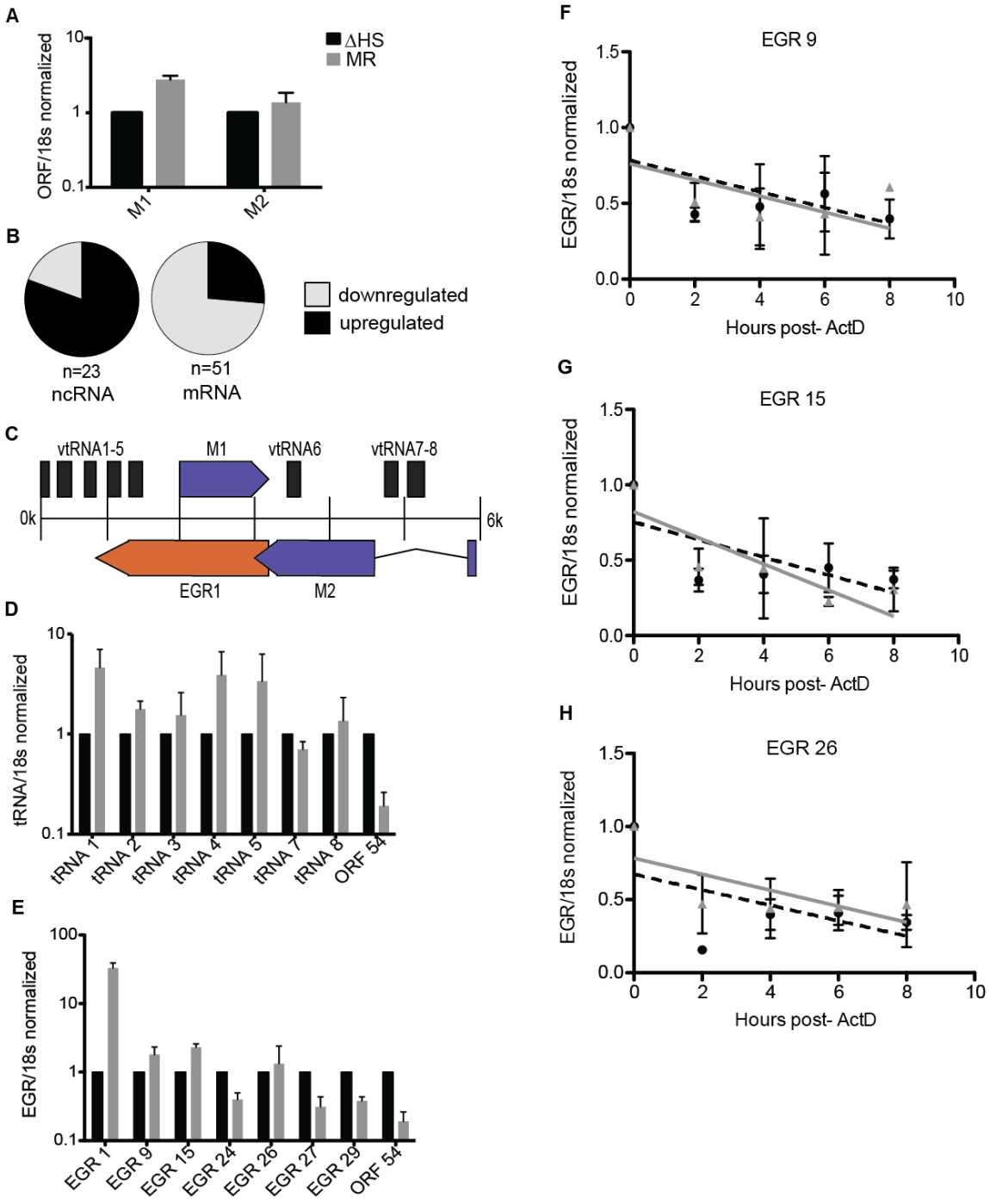

Figure 2. Noncoding RNAs are enriched in the escapee population. (A) RT-qPCR on viral transcripts M1 and M2. RNA was harvested from infected NIH 3T3 cells at 24 hpi. Viral transcripts were normalized to 18s and ΔHS levels set to 1. (B) The array data was used to determine what percentage of viral noncoding RNAs (ncRNAs) are upregulated during a MR infection (70%), and what percentage of viral mRNAs are downregulated (83.3%). (C) Schematic of the left end of the MHV68 genome, including the 8 viral

tRNAs, Expressed Genomic Region (EGR 1), and ORFs M1 and M2. (D and E) RT-qPCR on viral ncRNA was done by harvesting RNA from infected NIH 3T3 cells at 24 hpi. cDNA was made using transcript specific reverse primers and each transcript was normalized to 18s and ΔHS levels set to 1. ORF54 was used as a control to show downregulation. 3-5 independent RT-qPCRs were done for each transcript. (F-H) EGR half-life analyses were conducted by infecting NIH 3T3 cells with MR or ΔHS MHV68 at an MOI of 5. At 18 hpi, 2 ug of Actinomycin D was added to block transcription and RNA was harvested at the indicated times thereafter. RT-qPCR was performed with EGR-specific primers to determine transcript levels. The black dotted line indicates the best-fit line for the ΔHS virus, and the grey solid line indicates the best-fit line for the MR virus.

Figure 3

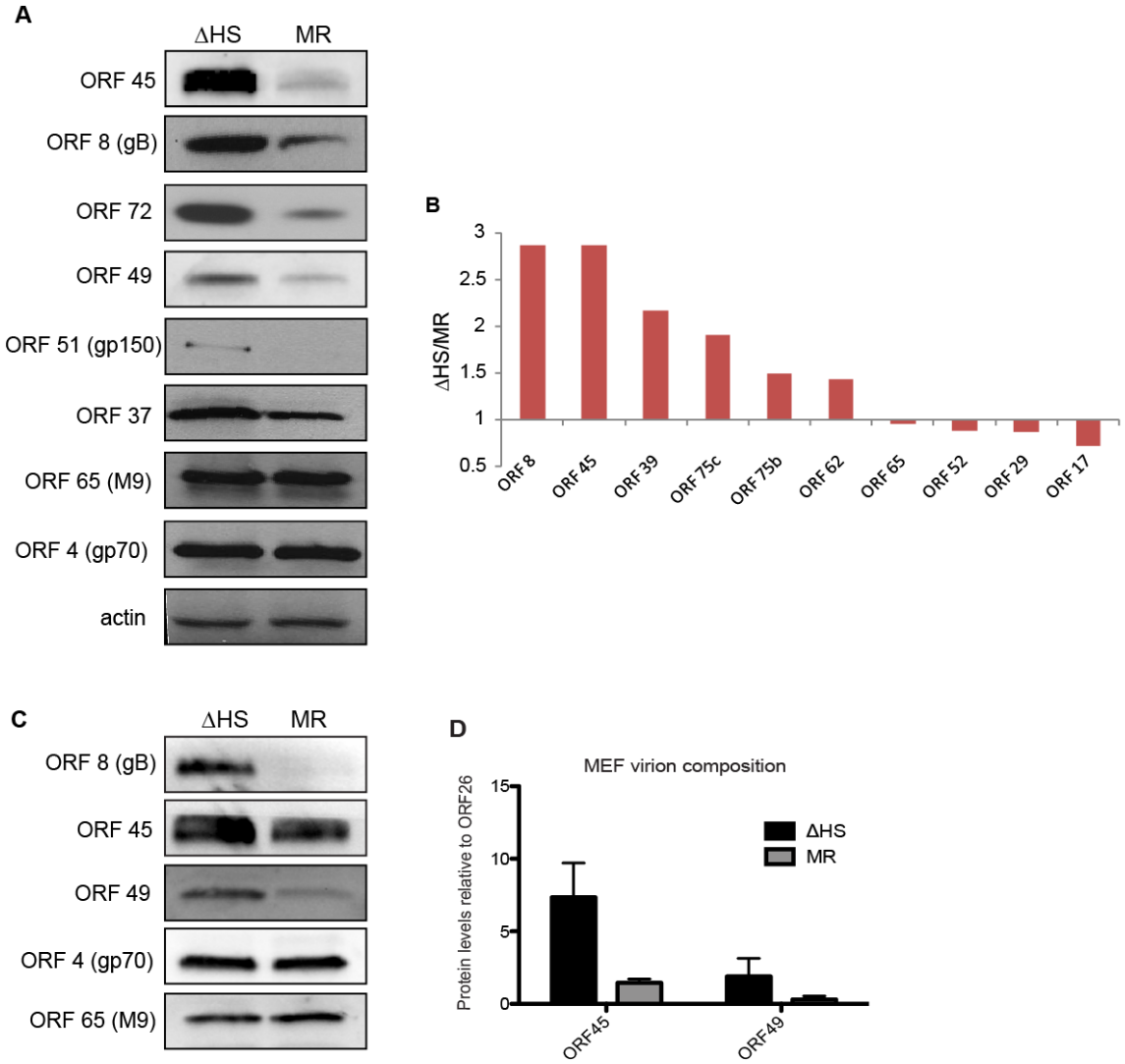

Figure 3. RNA degradation alters intracellular viral protein levels and virion composition. (A) To compare the accumulation of viral proteins during infection with ΔHS and MR MHV68, NIH 3T3 cells were infected at MOI of 5 and cell lysates collected at 24 hpi. Viral proteins were detected using antibodies against ORF 45, 8, 72, 49, 51, 37, 65, and 4. Actin was used as a loading control. (B) Relative abundance of some virion proteins comparing ΔHS levels over MR based on mass spectrometry (MS) peptide counts. Virions were isolated by sucrose gradient centrifugation and run through MS. Peptide numbers were normalized to major capsid ORF 25 and genome number as determined by qPCR. Graph includes data from two independent MS runs. (C) Virions were isolated by sucrose gradient centrifugation and abundance of the virion proteins ORF 8, 45, 49, 4, and 65 were determined by Western blot. (D) Virions were isolated from infected MEFs by sucrose gradient centrifugation and abundance of the virion tegument proteins ORF45 and ORF49, and the capsid protein ORF26 were determined by

Western blot. Protein abundance was quantified and graphed relative to the ORF26 capsid protein. At least 2 independent replicates of each Western blot were analyzed.

Table 1

	MR			ΔHS		
			Genome #			Genome #
ORF		ORF/capsid	[a]42100000		ORF/capsid	[a]21100000
capsid 25	1.22E-06	-	-	6.31E-07	-	-
ORF75c	7.52E-07	0.618955524	1.47E-08	3.72E-07	0.589510263	2.79E-08
ORF75b	5.57E-07	0.457868722	1.09E-08	2.17E-07	0.343556856	1.63E-08
gB	1.85E-07	0.151811516	3.61E-09	1.38E-07	0.218056541	1.03E-08
gM	2.96E-07	0.243808397	5.79E-09	1.68E-07	0.265301148	1.26E-08
ORF29	2.25E-07	0.185355195	4.40E-09	5.09E-08	0.080678019	3.82E-09
ORF59	8.43E-08	0.069367842	1.65E-09	1.40E-07	0.221416547	1.05E-08
			[b]9220000			[b]5880000
capsid 25	1.57E-06			1.33E-06		
ORF62	7.81E-07	0.496152539	5.38E-08	6.02E-07	0.45300884	7.70E-08
ORF52	2.51E-06	1.595994443	1.73E-07	1.19E-06	0.896746041	1.53E-07
ORF65	1.30E-06	0.823241982	8.93E-08	6.65E-07	0.501103815	8.52E-08
ORF59	2.05E-07	0.130477608	1.42E-08	7.38E-07	0.555948069	9.45E-08
ORF17	3.73E-07	0.236822723	2.57E-08	1.44E-07	0.108114721	1.84E-08
ORF45	2.56E-07	0.162445417	1.76E-08	3.94E-07	0.296639457	5.04E-08

Table 1. Top portion of the table are proteins identified in both ΔHS and MR samples for the first mass spectrometry (MS) run. Lower portion of the table is from the second MS run. The peptide count was normalized to major capsid protein ORF 25, and subsequently normalized to genome number, as determined by qPCR. [a]Genome number for first MS run. [b]Genome number for second MS run.

Figure 4

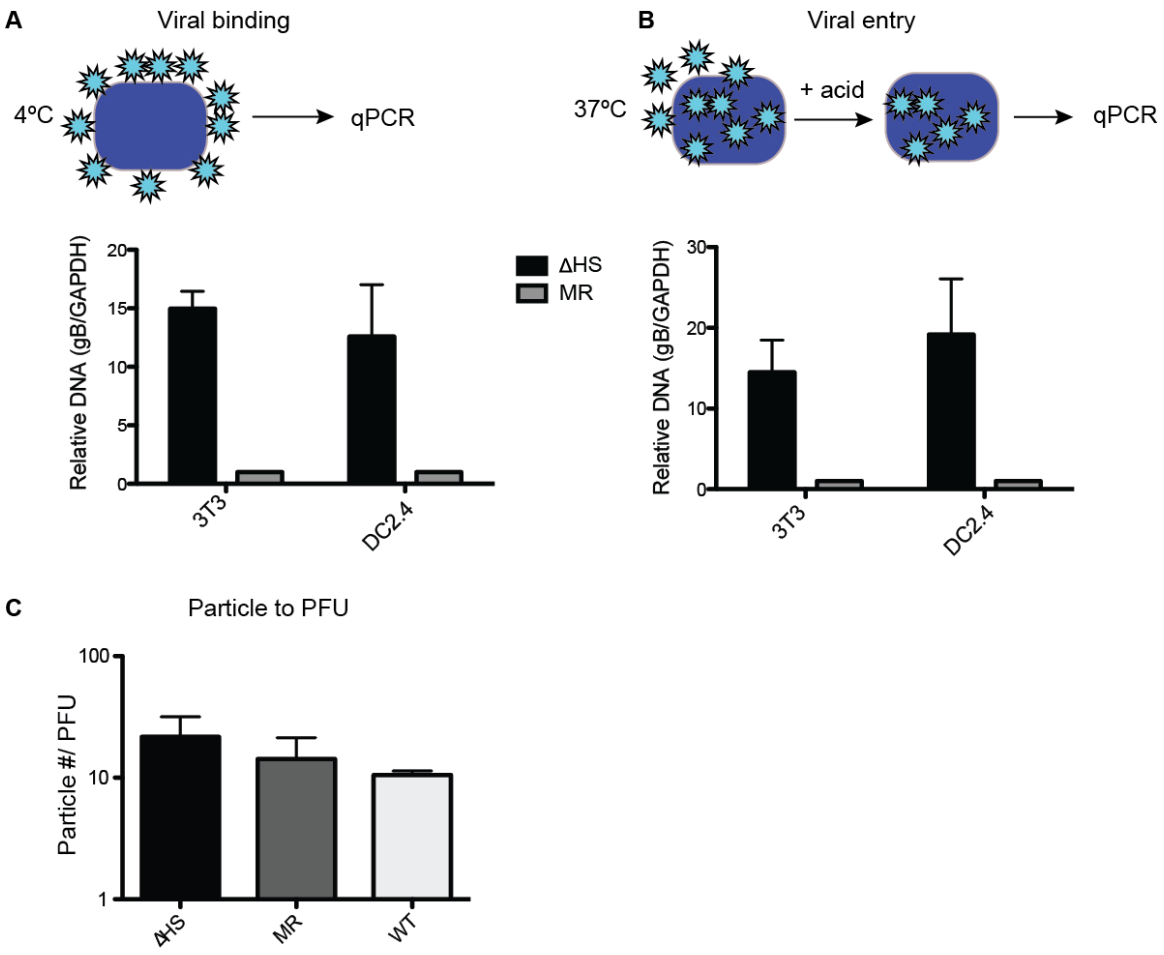

Figure 4. Altered virion composition leads to enhanced cell surface binding and entry. (A) Schematic showing cells were infected at an MOI of 5 at 4°C to allow viral binding, but prevent uptake. Both NIH 3T3 cells and DC2.4 cells were infected with MR or ΔHS MHV68. Cells were washed 4X with PBS at 90 min post infection, DNA was isolated, and qPCR used to quantify relative DNA levels by normalizing gB to GAPDH levels and setting MR levels to 1. (B) Cells were infected at an MOI of 5 at 37°C to allow uptake of virions. At 90 min post infection, the viral particles not internalized were stripped from the surface by the addition of 40 mM citric acid for 5 minutes and washed 4X with PBS. DNA was isolated and qPCR used to quantify relative DNA levels of internalized virus. Each graph represents 3 independent experiments. (C) Particle number was determined by isolating DNA from viral stocks and performing qPCR using gB primers. PFU was determined by plaque assay. At least 5 viral stocks from ΔHS and MR, and 3 from WT were assessed for both particle number and PFU. Differences are not statistically significant.

Figure 5

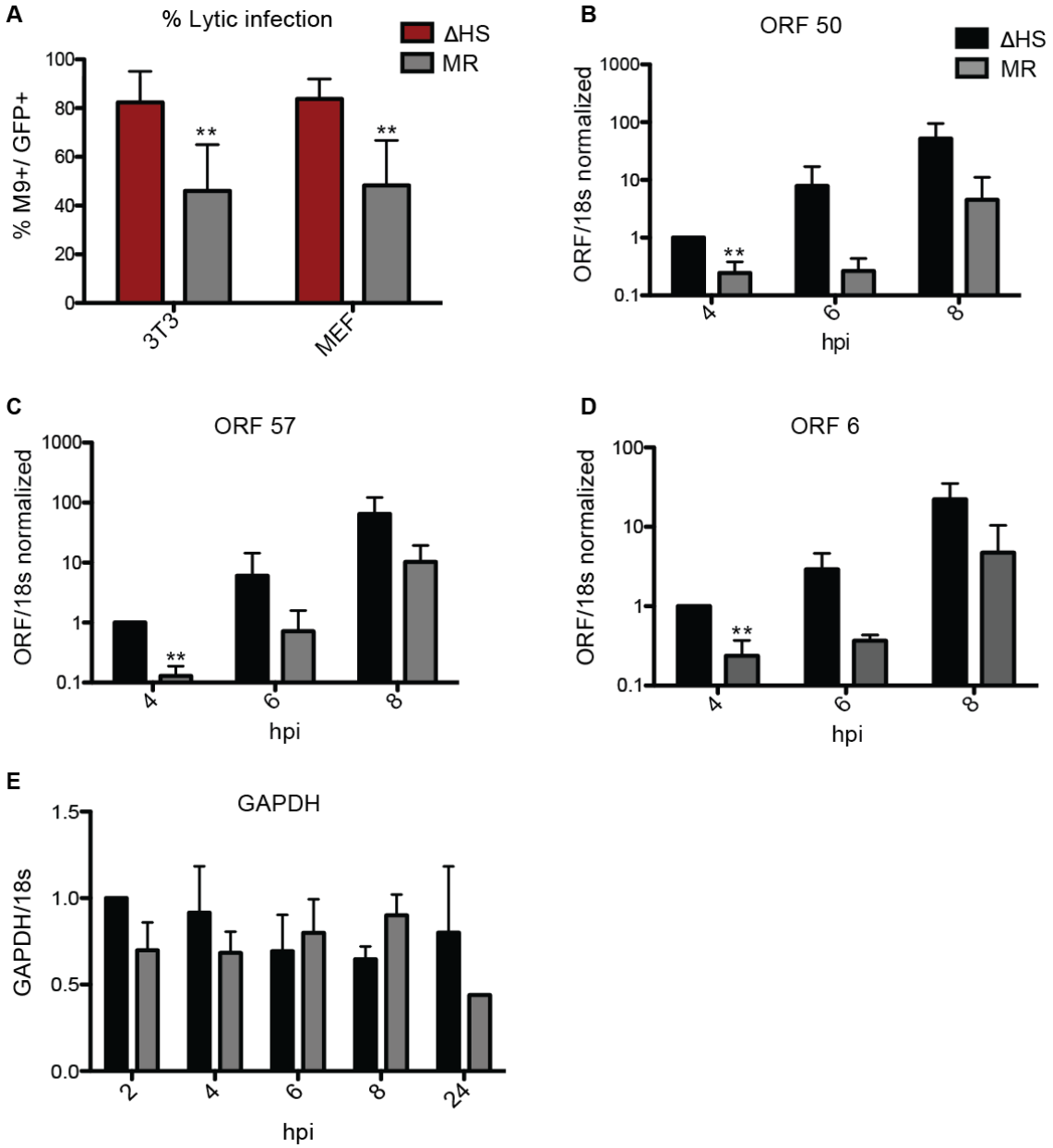

Figure 5. Failure to degrade viral mRNAs leads to enhanced lytic cycle entry. (A) Shown is the percent of lytic-expressing infected NIH 3T3 or MEF cells. Cells were infected at an MOI of 5 with GFP-BAC MHV68 MR or ΔHS and were analyzed at 18 hpi for GFP and M9 expression by immunofluorescence using anti-M9 antibodies. 5 fields of view from three independent experiments were counted and the percentage of GFP+M9+ cells calculated. ** Indicates p-value <0.01, determined by student t-test. (B-D) To measure levels of RTA-responsive transcripts after infection with MR or ΔHS MHV68, NIH 3T3 cells were infected at an MOI of 5 and RNA harvested at indicated times post infection. RT-qPCR was used to quantify relative levels of ORF 50 (B), ORF 57 (C), and ORF 6 (D). (E) GAPDH levels were measured to show that host shutoff had not yet initiated at the 8 hpi time point.

Figure 6

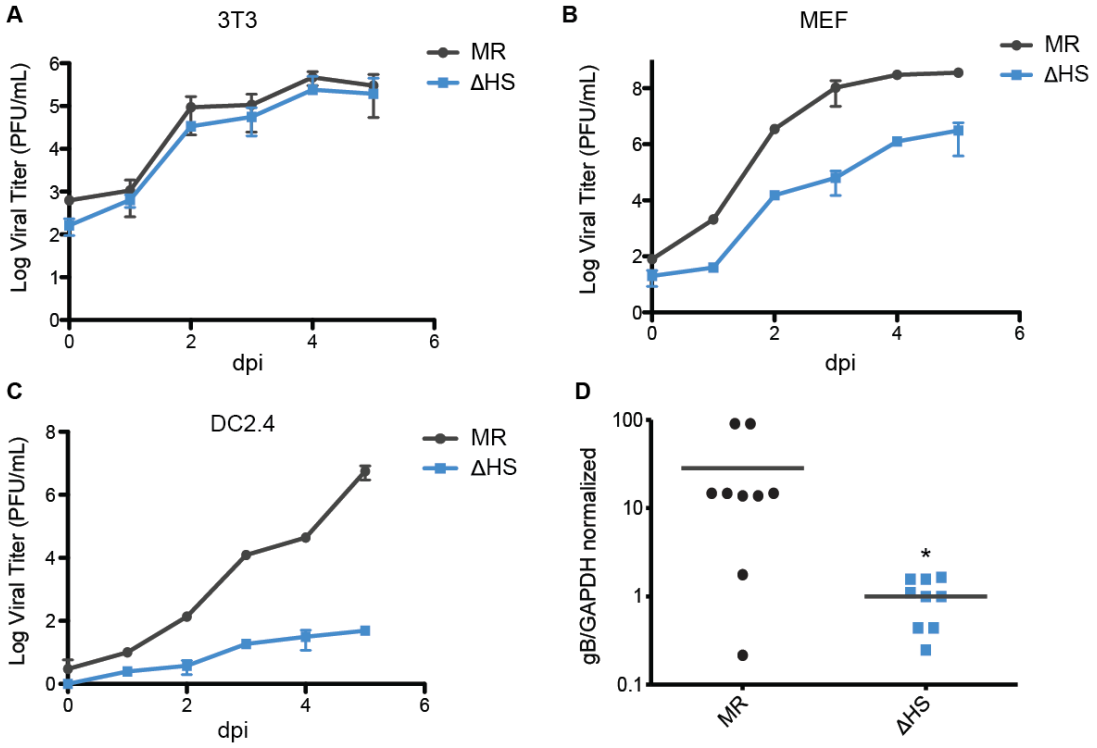

Figure 6. muSOX-induced mRNA degradation is important for viral amplification in a cell type specific manner in vitro and in vivo. (A-C) Multi-step growth curves were done in (A) NIH 3T3 cells, (B) murine embryonic fibroblasts, or (C) DC2.4 cells. Cells were infected at an MOI of 0.05 with MR or ΔHS MHV68, cells and supernatant collected at the indicated times post infection, and the titer was determined by plaque assay. At least three independent experiments were performed for each cell type. (D) C57BL/6 mice were infected by the intraperitoneal route with 1 x 10^3 pfu of MR or ΔHS MHV68. At 10 dpi spleens were harvested, homogenized, DNA extracted, and qPCR used to quantify viral particles. Each dot represents the relative value from a single spleen, and the bar indicates the mean value for each virus. * Indicates p-value <0.05.

Chapter 3: Viral nucleases reveal an mRNA degradation-transcription feedback loop in mammalian cells

Introduction

Viruses are extensively integrated into the cellular gene expression network, having evolved strategies to alter or co-opt machinery involved in the stages of transcription and RNA fate through translation and protein turnover. As such, they have served as valuable tools to dissect the pathways that govern cellular gene expression. Though gene expression is often considered in terms of a unidirectional flow of discrete events, there are an increasing number of examples of how these basic stages are interconnected (Braun and Young, 2014; Huch and Nissan, 2014). Such feedback mechanisms may enable cells to maintain homeostasis or mount appropriate responses during periods of perturbation. Viral infections represent a significant stress for the cell, and thus are likely to alter or stimulate crosstalk between components of the gene expression cascade.

Recent work has revealed that a feedback loop exists between messenger RNA (mRNA) synthesis and degradation in *S. cerevisiae*, thereby linking these two processes (Haimovich et al., 2013a; Lei et al., 2013). Deleting components of the cellular mRNA decay machinery to reduce rates of cytoplasmic mRNA degradation results in a decrease in RNA polymerase II (RNAPII) transcription, suggesting that cells can buffer against broad changes in mRNA stability by inducing compensatory alterations in mRNA synthesis (Haimovich et al., 2013b; Sun et al., 2012). One of the key proteins involved in linking mRNA decay to transcription is the 5'-3' mRNA exonuclease Xrn1, which is the primary exonuclease involved in cytoplasmic mRNA degradation in Drosophila, yeast and mammals (Nagarajan et al., 2013). However, although the data are consistent that Xrn1 deletion impacts mRNA synthesis in yeast, reports differ both as to the specific requirement for Xrn1, as well as whether it serves as a direct or indirect transcriptional regulator (Haimovich et al., 2013b; Sun et al., 2013). In the direct regulation model, Xrn1 shuttles into the nucleus and binds upstream promoter elements to impact transcription (Haimovich et al., 2013b). In the indirect regulation model, the absence of Xrn1 leads to accumulation of transcriptional repressors such as Nrg1 through mRNA stabilization, and it is these repressors that subsequently dampen transcription (Sun et al., 2013).

Whether similar cytoplasmic mRNA decay-transcription feedback mechanisms are operational in higher eukaryotes such as mammals remains unknown. Furthermore, how enhanced mRNA degradation might signal through such a feedback loop is an open question and one that is difficult to address through mutant studies. In this regard, several mammalian viruses rapidly accelerate cytoplasmic mRNA degradation through the combined activity of virally encoded mRNA-targeting endonucleases and mammalian Xrn1, and thus could provide insight into these questions (Gaglia et al., 2012).

Normally, mRNAs are protected from decay by a 5' cap and 3' poly(A) tail, and their degradation progresses through a regulated series of events. Decay begins with shortening of the poly(A) tail (deadenylation), and is followed by decapping and subsequent rapid degradation of the unprotected RNA body by exonucleases such as Xrn1. Members of the alpha- and gamma-herpesvirus subfamilies, as well as influenza A virus (IAV) and SARS coronavirus (SCoV) all encode viral proteins that target mRNAs for endonucleolytic cleavage (Glaunsinger and Ganem, 2004; Jagger et al., 2012;

Kamitani et al., 2009; Kwong and Frenkel, 1987; Rowe et al., 2007). Though the viral proteins are not homologous, in all examined cases they bypass the rate-limiting deadenylation and decapping events by inducing internal cleavages in cytoplasmic mRNA, and then rely on the cellular mRNA decay machinery to degrade the cleaved mRNA fragments. For the alpha- and gamma-herpesviruses and SCoV, clearance of cleaved mRNAs requires Xrn1 (Covarrubias et al., 2011; Gaglia et al., 2012).

Here, by comparing the effects of gamma-herpesviruses that contain wild type or inactivated mRNA-targeting nucleases, we reveal a direct connection between accelerated cytoplasmic mRNA decay and altered RNAPII transcription in mammalian cells. However, contrary to what might be predicted based on observations in *S. cerevisiae*, we find that enhancing mRNA degradation leads predominantly to a decrease in RNAPII activity on cellular genes, although a subset of genes are transcriptionally upregulated. We show a central role for cellular exonucleases including Xrn1 in this repression, indicating that Xrn1-linked transcriptional regulation is a feature conserved between *S. cerevisiae* and mammals. Furthermore, our findings support the conclusion that it is the act of mRNA degradation by Xrn1 that is sensed and triggers transcriptional alterations, rather than secondary effects from stabilization of mRNAs encoding transcriptional regulators. Interestingly, viral transcription, which is also mediated by RNAPII, largely escapes transcriptional repression and this escape requires Xrn1. Thus, viral mRNA transcription may benefit from mRNA degradation.

Results

Enhanced mRNA turnover in the cytoplasm suppresses RNAP II transcription

Infection with murine gamma-herpesvirus 68 (MHV68) leads to widespread acceleration of mRNA decay in the cytoplasm that is initiated by mRNA cleavage by the viral endoribonuclease muSOX, and completed by degradation of the cleaved fragments by the cellular 5'-3' exoribonuclease Xrn1 (Covarrubias et al., 2009; Gaglia et al., 2012). A point mutation in the muSOX gene at position R443 (R443I; ΔHS) renders it defective for cleaving cytoplasmic RNAs, and thus infection with the ΔHS virus does not broadly increase mRNA decay (Richner et al., 2011). We therefore queried how infection of NIH 3T3 cells with WT MHV68 versus the ΔHS mutant impacted rates of cellular mRNA transcription as measured by 4-thiouradine (4sU) pulse labeling. Just prior to harvesting, cells were incubated for 30 min with 4sU, which gets incorporated into actively transcribing mRNAs and can be subsequently coupled to HPDP-biotin and purified over magnetic streptavidin beads. Quantification by RT-qPCR of the housekeeping genes Gapdh, Rpl37, and ActB from purified 4sU-labeled RNA showed a significant transcriptional reduction during MHV68 infection compared to mock infected cells (Figure 1A). No reduction in transcription was detected in cells infected with the ΔHS point mutant virus, suggesting that the transcriptional suppression observed during WT MHV68 infection was specifically linked to enhanced cytoplasmic mRNA decay (Figure 1A). We detected robust transcriptional activation during both MHV68 WT and ΔHS infection of the interferon-stimulated gene IFIH1, in agreement with previous findings (Liu et al., 2012), indicating the 4sU assay accurately portrays transcription changes. We also confirmed that the abundance of 4sU-containing mRNA reflected nascent transcription rather than decay rates in the cytoplasm by showing that 4sU-labeled mRNA remained largely confined to the nucleus at the time of harvest (Figure 1B).

To test directly whether the transcriptional alterations that occurred during MHV68 infection were due to accelerated mRNA decay, we examined whether this phenotype could be recapitulated upon expression of the viral endonuclease alone. HEK 293T cells were transfected with plasmids expressing WT muSOX, the catalytically dead muSOX point mutant D219A, or the viral endonuclease vhs from herpes simplex virus (HSV-1). Although not homologous to muSOX, HSV-1 vhs is also a broad-acting, cytoplasmic, mRNA-specific endonuclease that engages Xrn1 to degrade the cleaved RNA fragments (Gaglia et al., 2012; Read, 2013). Similar to our results in infected cells, 4sU labeling showed a reduction of transcription of the housekeeping genes Gapdh, ActB, GusB, and eEF-1a in cells expressing muSOX or vhs, but not in cells expressing the muSOX D219A mutant (Figure 1C). We also measured RNAPII occupancy at cellular promoters by chromatin immunoprecipitation (ChIP) assays and, in agreement with our 4sU labeling, observed a reduction in RNAPII occupancy in cells expressing vhs or muSOX but not muSOX D219A (Figure 1D). The fact that muSOX and vhs displayed similar phenotypes further implicates mRNA degradation as the event driving transcriptional changes in the nucleus.

Finally, to determine whether this mRNA degradation-transcription feedback mechanism was similarly operational during infection with a human virus, we performed a similar set of experiments with the gamma-herpesvirus Kaposi's sarcoma-associated herpesvirus (KSHV). KSHV encodes a SOX gene that functions in a manner analogous to MHV68 muSOX (Covarrubias et al., 2009; Glaunsinger and Ganem, 2004). To recapitulate our MHV68 ΔHS mutant control in KSHV, we engineered a P176S point mutation in the KSHV SOX gene, which similarly confers a specific mRNA degradation defect (Glaunsinger et al., 2005). We monitored mRNA degradation-induced transcriptional changes during the lytic KSHV replication cycle using iSLK renal carcinoma cells, which harbor a doxycycline (dox)-inducible version of the major lytic cycle transactivator RTA. Efficient reactivation of the KSHV lytic cycle can be induced in iSLK cells containing a latent version of the viral genome upon treatment with dox and sodium butyrate (Myoung and Ganem, 2011). Similar to our results with MHV68, measurement of transcription rates 48h post lytic reactivation by 4sU labeling showed a specific transcriptional repression of the housekeeping genes Gapdh, ActB, GusB, and eEF-1a in cells containing WT KSHV but not the P176S mutant (Figure 1E). Collectively, these data suggest that virus-induced cytoplasmic mRNA degradation induces RNAPII transcriptional repression.

Xrn1 is required for the mRNA decay-transcription feedback mechanism

We next sought to determine what cellular factor(s) were required to activate the mRNA decay-induced transcriptional feedback mechanism. In *S. cerevisiae*, Xrn1 has been shown to be required for transcriptional alterations in cells lacking cytoplasmic decay factors (Haimovich et al., 2013b; Sun et al., 2013). Given that Xrn1 degrades the mRNA fragments cleaved by the viral endonucleases, we reasoned that Xrn1 activity might be involved in the transcriptional response to mRNA degradation in mammalian cells. We generated HEK 293T cells stably expressing dox-inducible Xrn1-targeting shRNAs. After Xrn1 depletion by dox treatment for 4 days, the cells were transfected with plasmids expressing either WT or D219A muSOX and RNAPII promoter occupancy was measured by ChIP. In control cells not treated with dox, we observed the expected

reduced RNAPII occupancy at the Gapdh promoter in the presence of WT muSOX but not the D219A catalytic mutant (Figure 2A). However, Xrn1 knock down restored RNAPII occupancy at the Gapdh promoter in cells expressing muSOX to levels observed in cells expressing D219A. Importantly, in these experiments mRNAs are cleaved by muSOX regardless of Xrn1 levels, as Xrn1 only contributes to degradation of the cleaved fragments. Thus, it can be concluded that differences in transcription result from a mechanism to sense accelerated mRNA degradation, rather than secondary effects stemming from altered stability of mRNAs encoding transcriptional regulators. These data also indicate that Xrn1 is required for repression of cellular RNAPII transcription in response to accelerated mRNA decay.

To determine if this effect was specific to Xrn1, we also created cell lines containing dox-inducible shRNAs directed against two other mammalian factors involved in basal mRNA decay, the 3'-5' exonuclease Dis3L2 and the deadenylase Ccr4 (Figure 2B, 2C). It was previously shown that mRNAs targeted by SOX do not undergo prior deadenylation (Covarrubias et al., 2011), suggesting that Ccr4 activity was unlikely to be enhanced in muSOX-expressing cells. However, it was possible that Dis3L2 participates in degradation of the 5' fragments resulting from muSOX cleavage. Indeed, similar to the results with Xrn1, depletion of Dis3L2 restored RNAPII occupancy in muSOX-expressing cells to those of control cells (Figure 2B). However, depletion of Ccr4 did not impact the reduction of RNAPII during muSOX expression (Figure 2C). These data suggest the exonucleases Xrn1 and Dis3L2 contribute to transcriptional feedback in mammalian cells.

Xrn1 catalytic activity is required for reduced RNAPII transcription

We next applied a complementation assay to determine if Xrn1 catalytic activity was required for repression of cellular transcription in muSOX-expressing cells. Dox-treated cells depleted of endogenous Xrn1were transfected with plasmids expressing either WT Xrn1 or the catalytically dead mutant D208A (Jinek et al., 2011). After subsequent transfection with WT or the D219A mutant of muSOX, RNAPII ChIP was used to evaluate the transcriptional response (Figure 3A). Introduction of WT Xrn1 restored the degradation-induced transcriptional repression of the Gapdh promoter in WT muSOX-expressing cells. However, in the presence of Xrn1 D208A, muSOX was unable to induce transcriptional repression (Figure 3B). This suggests that catalytic activity is required to induce repression of RNAPII transcription, and is in agreement with findings in *S. cerevisiae* (Haimovich et al., 2013b).

We next explored the possibility that Xrn1 might be directly acting to influence transcription, as has been suggested in yeast (Haimovich et al., 2013b). To determine whether Xrn1 translocates to the nucleus in cells undergoing accelerated mRNA decay, we monitored Xrn1 localization during MHV68 infection by immunofluorescence assay (IFA). Although transiently expressed Xrn1 appears to be exclusively cytoplasmic (unpublished observations), we observed endogenous Xrn1 in both the nucleus and cytoplasm in 3T3 cells (Figure 3C). The IFA signal was specific for Xrn1, as pre-treatment of the cells with Xrn1-targeting siRNAs significantly decreased the staining in both the nucleus and the cytoplasm (Figure 3C). However, the nuclear-cytoplasmic distribution of Xrn1 was not altered during infection with WT MHV68 or the ΔHS mutant (Figure 3D). We were also unable to detect enrichment of Xrn1 at

transcriptionally impacted cellular promoters in ChIP assays (data not shown). These data suggest that it is the sensing of Xrn1 activity in the cytoplasm that leads to transcriptional alterations, rather than a cis-acting effect of Xrn1 on cellular promoters.

RNAPII is recruited to promoters in an unphosphorylated state, but is progressively phosphorylated in its carboxyl-terminal domain (CTD) repeat region during promoter escape and elongation. To determine whether mRNA decay impacted RNAPII initiation or elongation, we performed ChIP with antibodies recognizing either total RNAPII or serine-2 phosphorylated RNAPII, as serine-2 phosphorylation is a marker of elongating polymerase (Phatnani and Greenleaf, 2006). Although WT MHV68 infection decreased total RNAPII promoter occupancy, the ratio of total to serine-2 phosphorylated RNAPII was unchanged in response to infection of NIH 3T3 cells (Figure 3E, 3F). As expected, no alterations in RNAPII occupancy were observed in cells infected with the ΔHS MHV68 (Figure 3E). Therefore, the transcriptional repression induced by WT MHV68 infection is most likely due to reduced RNAPII recruitment rather than reduced rates of elongation.

Cellular transcriptional changes occur throughout the mRNA transcriptome

To determine the extent of transcriptional alterations that occur in response to accelerated cytoplasmic degradation, we sequenced libraries of 4sU-labeled RNA from mock, WT, or ΔHS MHV68-infected NIH 3T3 cells on the Illumina platform (Figure 4A). Relative to uninfected samples, WT MHV68 infection resulted in a ≥1.5-fold transcriptional decrease of 9.25% of genes based on log2 fold change (Figure 4B). Independent validations of 4sU-labeled mRNA levels by RT-qPCR confirmed the sequencing results for 12 out of 19 genes tested (Figure 4E, F). The 7 genes in which the 2 assays were not in agreement showed transcriptional repression by RT-qPCR but not by 4sU-seq, perhaps suggesting that the 4sU-seq represents a conservative estimation of the breadth of degradation-induced transcriptional alterations. Significantly fewer genes (3.18%) were decreased during ΔHS MHV68 infection, indicating that the majority of changes in the WT infected cells were linked to mRNA degradation. Among the set of transcriptionally repressed genes during WT infection, 374 were categorized as statistically significant based on read counts and fold-change. In contrast, only 38 genes were significantly reduced during a ΔHS infection and, among these, 32 overlapped with those in the WT infection samples. Thus, these overlapping genes are likely downregulated as a result of viral infection and are not specific to mRNA degradation (Figure 4C). Gene ontology (GO) term-based analysis of the set of 342 genes that were transcriptionally repressed only during WT MHV68 infection yielded no clear links to specific biological processes, suggesting that mRNA degradation-induced transcriptional repression is not restricted to specific functional classes of genes.

In addition to the set of transcriptionally repressed genes, we also observed a somewhat smaller subset of genes (6.87%) that showed a ≥1.5-fold increase upon WT MHV68 infection (Figure 4B). Unlike during WT infection where transcriptional changes were more frequently repressive, the transcriptional changes that occurred during ΔHS infection were equally split between induced and repressed categories (3.19% versus 3.18%, respectively). Furthermore, a larger fraction of the significantly transcriptionally induced genes during a WT infection overlapped with those induced during ΔHS infection (32.6% compared to 8.6% of reduced genes), suggesting that

upregulation is less likely to be linked to mRNA degradation (Figure 4C). Notably, among the set of 85 genes whose transcriptional induction was common to both WT and ΔHS infection, GO-term analyses returned a clear enrichment for genes involved in antiviral defense mechanisms and in nucleotide binding (Figure 4D). Although the significance of the latter remains to be determined, the induction of antiviral response factors would be a predicted transcriptional response to infection, independent of mRNA degradation.

Viral mRNAs escape degradation-induced transcriptional repression

Herpesviral mRNAs are transcribed in the nucleus using the host machinery, and thus in theory might also be subject to mRNA decay-induced transcriptional suppression. We therefore analyzed the transcriptional changes that occurred at each of the viral genes in response to mRNA degradation during WT MHV68 infection relative to ΔHS infection using the 4sU-seq data set. Interestingly, viral genes largely escaped the transcriptional repression (Figure 5A). Independent validation experiments confirmed that even genes that appeared to undergo modest transcriptional repression during WT infection by 4sU-seq were unchanged or even slightly upregulated as measured by RT-qPCR of 4sU-labeled mRNA (Figure 5B).

In agreement with the 4sU-based transcriptional measurements, we observed no differences in total or serine-2 phosphorylated RNAPII occupancy at the M1 and ORF8 viral genes (Figure 5C, D). Finally, we extended these results to KSHV by comparing viral transcription at 48 h post reactivation of WT or P176S KSHV-containing iSLK cells. Similar to the data for MHV68, each of the KSHV genes examined by RT-qPCR following 4sU labeling exhibited either no transcriptional changes or were modestly transcriptionally induced during WT relative to P176S KSHV lytic infection (Figure 4E). We conclude that viral transcription is not negatively impacted (and in some cases is enhanced) by accelerated cytoplasmic mRNA degradation, and thus the transcriptional impact of mRNA decay may be distinct for the virus versus the host.

Xrn1 positively influences viral transcription during widespread mRNA decay

Although the majority of MHV68 genes are susceptible to muSOX cleavage during infection, several viral transcripts appear to escape muSOX-mediated degradation (Abernathy et al., 2014). Two of these putative 'escapees', the viral ORF M1 (an RNAPII transcript) and the viral tRNA-like gene vtRNA1 (an RNAPIII transcript) exhibit enhanced steady state expression during WT relative to ΔHS infection, perhaps due to increased transcription (Abernathy et al., 2014). To test whether muSOX-induced transcriptional feedback was responsible for their increased abundance during WT infection, we first confirmed that the M1 and vtRNA1 half-lives were not altered during a WT versus ΔHS infection (Figure 6A). We then evaluated whether the transcriptional enhancement of these viral genes during WT MHV68 infection was linked to Xrn1 activity using the HEK 293T cells expressing dox-inducible Xrn1-targeting shRNAs. Upon Xrn1 depletion, M1 expression was significantly reduced during WT but not ΔHS MHV68 infection, and its expression was restored upon introduction of exogenous WT Xrn1 (Figure 6B). The requirement for Xrn1 appeared specific for RNAPII-driven transcription, as its depletion had no significant impact on expression of the RNAPIII-transcribed vtRNA1 (Figure 6C). RNAPII ChIP experiments confirmed that the reduction

in M1 mRNA in the absence of Xrn1 was due to transcriptional repression (Figure 6D). We also observed reduced RNAPII occupancy upon Xrn1 depletion at ORF54, an MHV68 gene that is susceptible to cleavage by muSOX (Abernathy et al., 2014), indicating that the role of Xrn1 in promoting viral transcription is not limited to transcripts that escape degradation (Figure 6D). In each of these experiments, the requirement for Xrn1 was only observed during WT infection and not during infection with the ΔHS virus. We did not detect any binding of Xrn1 to viral promoters by ChIP (data not shown), suggesting that it likely indirectly impacts viral transcription in cells undergoing enhanced mRNA decay. Finally, depletion of the Ccr4 deadenylase did not alter M1 transcription during a WT or ΔHS infection, in agreement with its dispensability for the repression of cellular transcription (Figure 5E). Collectively, these data demonstrate that in contrast to its role in transcriptional repression of many cellular genes, Xrn1 activity during muSOX-induced cytoplasmic mRNA decay is required for robust transcription of viral genes.

Discussion:

Here we used virally encoded mRNA-targeting endonucleases to show that cytoplasmic mRNA degradation and nuclear RNAPII transcription are linked in mammalian cells. Accelerated mRNA degradation generally results in transcriptional repression of cellular genes, although a smaller subset of genes is induced. Our findings therefore suggest that mammalian cells have a mechanism to sense broad alterations in RNA degradation. It is not the initial cleavages by viral endonucleases that are detected, but rather the increased activity of cellular exonucleases involved in degrading the cleaved mRNA fragments that generates a transcriptional response. In particular, the 5'-3' exonucleases Xrn1 and Dis3L2 are central to the transcriptional feedback activated by enhanced mRNA decay. Notably, enhanced Xrn1 activity appears to have opposing consequences for host and viral transcription, suggesting that herpesviruses have evolved to benefit from this intrinsic feedback mechanism.

Our findings have some clear parallels to gene expression feedback pathways recently described in yeast, although the mammalian response to accelerated mRNA decay does not result in the transcriptional "buffering" phenotype observed in *S. cerevisiae.* In yeast, reducing cytoplasmic mRNA decay through the deletion of components of the mRNA degradation machinery results in a compensatory decrease in RNAPII transcription rates (Haimovich et al., 2013b; Sun et al., 2013). Conversely, an RNAPII mutant that exhibits ~3-fold reduced mRNA synthesis rates displays decreased rates of mRNA turnover in the cytoplasm (Sun et al., 2012). Thus, events that broadly alter mRNA levels in yeast are compensated by changes in decay or transcription, presumably to maintain homeostasis. Our data indicate that mammalian cells also possess a mechanism to sense overall mRNA abundance. However, accelerated cytoplasmic mRNA degradation in mammalian cells induces transcriptional alterations that are distinct from this buffering phenotype. Among the genes that were transcriptionally altered during MHV68 infection, the majority of mRNA degradation-induced changes involved repression, which would exacerbate rather than buffer the decrease in mRNA abundance. This could represent a way for the cell to conserve energy during stress. It is also possible this response has evolved as a countermeasure to viral infection, as

widespread mRNA decay is more likely to be linked to pathogenesis. If so, herpesviruses have developed a means to avoid this restriction.

Whether, like yeast, mammalian cells can also buffer against changes in mRNA abundance that may occur in response to non-pathogenic environmental cues remains unknown. We did not detect substantial or reproducible alterations in transcription as measured by RNAPII ChIP in response to decay factor depletion in the absence of viral nuclease expression. However, this was only examined for select genes and thus it is possible that transcriptional compensation occurs at other loci. Additionally, other signals may be necessary to activate an mRNA degradation-transcription buffering mechanism in uninfected cells.

Our observations linking Xrn1 activity in the cytoplasm to transcriptional alterations complements recent reports in yeast that document a role for Xrn1 in the degradation-transcription feedback loop. Although there is a consensus that Xrn1 is involved in transcription, whether it operates directly via promoter binding, or indirectly by impacting the abundance of mRNAs encoding transcriptional regulators (or by another mechanism) remains to be resolved. Two studies demonstrate that yeast Xrn1 can shuttle into the nucleus and bind cellular promoters to enhance transcription initiation and elongation (Haimovich et al., 2013b; Medina et al., 2014). These same studies show that several other cellular decay factors also shuttle into the nucleus and rely on Xrn1 catalytic activity for nuclear import (Haimovich et al., 2013b). Another report instead suggests that Xrn1 impacts transcription indirectly in yeast through degradation of mRNAs encoding transcriptional regulators (Sun et al., 2013), although how protein levels would increase upon Xrn1 depletion given that Xrn1 targets deadenylated and decapped messages is unclear. We did not observe a significant increase in the nuclear population of Xrn1 in cells expressing muSOX, nor were we able to detect Xrn1 associated with cellular or viral promoters via ChIP. However, a significant proportion of endogenous Xrn1 resides in the nucleus regardless of viral nuclease expression, hinting that Xrn1 may have nuclear functions in mammalian cells in addition to its well-characterized role in cytoplasmic mRNA decay.

The seemingly opposing roles for Xrn1 in the host and viral transcriptional response may indicate that gamma-herpesviruses benefit from reduced levels of RNAPII occupancy at cellular promoters. One possibility is that degradation-induced cellular transcriptional repression enables the virus to more efficiently recruit polymerases to viral promoters. Indeed, RNAPII is concentrated in herpesviral replication factories in the nucleus (Rice et al., 1994; Sugimoto et al., 2013). However, we did not observe a reduction in virally sequestered RNAPII in cells infected with ΔHS relative to WT MHV68 (unpublished observations), suggesting this cannot fully explain cellular transcriptional repression or viral escape. Alternatively, Xrn1 may more directly impact the transcription of viral promoters in an mRNA decay-dependent manner.

We previously showed that SOX-cleaved mRNAs are not first deadenylated and, in agreement with this observation, we did not detect a role for the Ccr4 deadenylase in the transcriptional response. However, Xrn1 is not the sole factor whose activity modulates transcription in cells expressing viral endonucleases, as depletion of the Dis3L2 3'-5' exonuclease similarly disrupts this feedback mechanism. A role for Dis3L2 is not unexpected, as we hypothesize that it may be responsible for degrading the 5' mRNA fragments generated by muSOX, in which case its activity would similarly be

increased during gamma-herpesvirus infection. The observation that deleting either Xrn1 or Dis3L2 prevents the transcriptional repression suggests that both factors are required for feedback. Whether this is linked to a physical interaction between these proteins, or perhaps a failure to reach a necessary threshold of degradation to trigger a transcriptional response in the absence of one of the exonucleases remains to be determined.

The fact that both exonucleases are linked to transcriptional repression is consistent with the idea that the act of mRNA degradation is sensed. Depletion of Xrn1 and Dis3L2 in cells expressing the viral nucleases should not impact the overall pool of translationally competent mRNAs, as the mRNAs will still be translationally inactivated by viral endonucleolytic cleavage. However, the cleaved fragments will not be efficiently degraded. Thus, transcriptional changes we observed in mammalian cells should not be due to altered levels of transcriptional regulators. Instead, we hypothesize that feedback between RNA decay and synthesis may instead be regulated by altered nuclear-cytoplasmic distribution of nucleic acid binding proteins in response to mRNA degradation. For example, yeast polymerase subunits Rpb4/7 shuttle between the nucleus where they function in transcription, and the cytoplasm where they are involved in mRNA decay and translation initiation (Harel-Sharvit et al., 2010; Lotan et al., 2007). It may be that factors classically linked to transcription, mRNA decay, and translation function to coordinate and integrate several cellular processes in response to pathogenic or environmental cues (Harel-Sharvit et al., 2010). We propose that this systemic interconnectedness is present in mammalian cells, and that viral infections introduce perturbations to mRNA stability whose downstream consequences impact multiple cellular processes.

Materials and Methods:

Cells, transfections, and transductions

NIH 3T3 and HEK 293T cells were maintained in Dulbecco's modified Eagle medium (DMEM; Invitrogen) supplemented with 10% fetal bovine serum (FBS; Invitrogen). Cells were transfected at 75-90% confluence with polyethylenimine (PEI) for 24 h. Plasmids pCDNA3-muSOX, pCDNA3-muSOX.D219A, and pCDNA3-vhs have been described previously (Covarrubias et al., 2009; Glaunsinger and Ganem, 2004). Plasmid pFN21-Halo-Xrn1 was kindly provided by Carol Wilusz, and subcloned into the pFN21 vector with a FLAG tag. The Xrn1 D208A mutation was introduced by site directed mutagenesis to generate FLAG-Xrn1.D208A.

HEK 293T cells were transduced with TRIPZ inducible lentiviral shRNA constructs (Thermo scientific) against Xrn1 (clone ID: V2THS_89028), Dis3L2 (clone ID: V3THS_391760), or CNOT6 (clone ID: V2THS_262587). Cells were transfected with shRNA, psPAX2 (lentiviral packaging), and pMD2.G (lentiviral envelope) (Addgene) for 48 h, whereupon the supernatant was passed through 0.45 um filters, mixed with 8 mg/ml of polybrene, and spun onto a monolayer of HEK 293T cells at 1500 rpm for 1.5 h. Fresh media was then added and the cells were incubated for 5-7 days in selection media containing 1mg/ml of puromycin. Cell lines were induced with 1 mg/ml of doxycycline for 4-5 days and knock down efficiency determined by Western blot and RT-qPCR.

Viruses and infections

The MHV68 bacterial artificial chromosome (BAC) has been described elsewhere (Adler et al., 2000), and the construction of the R443I muSOX mutant (ΔHS) was previously described (Richner et al., 2011). MHV68 was produced by transfecting NIH 3T3 cells with BAC DNA using SuperFect (Qiagen). Virus was amplified in NIH 3T12 cells and titered by plaque assay. Cells were infected with MHV68 at an MOI of 5 for 24 h unless otherwise noted.

KSHV BAC mutagenesis has been described elsewhere (Brulois et al., 2012). Briefly, the P176S mutation was built into 60-mer homologous arms of flanking sequence in the SOX gene and used to amplify the region by PCR. The P176S-containing PCR fragment of SOX was then electroporated into iSLK cells containing the KSHV BAC16. Two rounds of recombination replaced the WT SOX gene with the insert containing the P176S mutation. Isolated BAC DNA was transfected into iSLK-puro cells with PolyJet (SignaGen labs) and cells selected with 500 mg/ml of hygromycin (Omega Scientific) for 1-2 weeks. BAC-containing colonies (GFP+) were individually isolated and maintained in hygromycin-containing media. Each clone was sequenced to confirm the P176S mutation, once after cell line construction and once after 2 weeks of cell maintenance. KSHV was reactivated by adding 1 mg/ml of doxycycline and 1 mg/ml of sodium butyrate for 48 h. Reactivation efficiency was determined by qPCR on isolated DNA and found to be equivalent between WT and P176S.

4-thiouridine labeling

Cells were labeled with DMEM containing 500 mM of 4-thiouridine (4sU; Sigma) for 30 min prior to isolating RNA with Trizol, followed by isopropanol precipitation. Total RNA (100 mg) was incubated in biotinylation buffer (10 mM Tris pH 7.4, 1 mM EDTA) and 200 mg of HPDP-biotin (EZ-link HPDP-biotin; Thermo scientific) with constant rotation at room temperature for 1.5 h. RNA was then phenol-chloroform extracted and precipitated with isopropanol. The pellet was resuspended in DEPC-treated water and mixed with 50 ml of Dynabeads MyOne streptavidin C1 (Invitrogen) that had been pre-washed twice with 1X wash buffer (100 mM Tris pH 7.5, 10 mM EDTA, 1 M NaCl, 0.1% Tween20). Samples were rotated for 15 minutes at RT, then washed 3x with 65 °C wash buffer and 3x with RT wash buffer. Samples were eluted with 100 mM DTT and the RNA precipitated with ethanol prior to RT-qPCR. All qPCR results were normalized to 18S levels and WT or vector control set to 1.

For fractionated 4sU assays, cells were labeled with 4sU for 30 min and washed with ice-cold PBS. Cells were scraped and spun in an eppendorf tube for 10 sec at 4°C at max speed. Supernatant was removed and pellet was resuspended in 380 µl ice-cold hypotonic lysis buffer (HLB; 10 mM Tris pH 7.5, 10 mM NaCl, 3 mM $MgCl_2$, 0.3% NP-40, 10% glycerol). Cells were incubated on ice for 10 min, then vortexed and spun again. The supernatant was collected as the cytoplasmic fraction and the pellet resuspended in HLB. The cells were washed with HLB 3x and the pellet (nuclear fraction) resuspended in 1 ml of Trizol and phenol-chloroform extracted. The cytoplasmic fraction was phenol-chloroform extracted and the 4sU protocol continued as described above.

Chromatin immunoprecipitation (ChIP)

Cells in 10-cm plates were washed 2X with ice-cold PBS at 24 h post infection/transfection and fixed in 1% formaldehyde at RT for 10 minutes. To stop cross-

linking, 2.5 M glycine was added for 5 min. Cells were scraped, collected, and washed 2X with ice-cold PBS. Pellets were resuspended in 1 ml of ChIP lysis buffer (0.5% SDS, 10 mM EDTA, 50 mM Tris pH 8) and rotated at 4 °C for 10 min. Chromatin was sheared using a Covaris sonicator for 30 rounds of 30-second pulses with 210 volts. Chromatin (100 ml) was diluted in 400 ml of ChIP dilution buffer (1.1% Triton-X-100, 1.2 mM EDTA, 16.7 mM Tris pH 8, 167 mM NaCl) containing 10 mg of RNAPII antibody (N20-X, Santa Cruz), RNAPII CTD repeat YSPTSPS (phosphor S2; Abcam), or Xrn1 (Sigma) and rotated overnight at 4 °C. Pre-washed Protein G Dynabeads (20 ml) (Life technologies) were then added to each sample and rotated at 4 °C for 2 h. Beads were washed rotating at 4 °C for 5 min each with low salt immune complex (0.1% SDS, 1% Tritox-X-100, 2mM EDTA, 20 mM Tris pH 8, 150 mM NaCl), high salt immune complex (0.1% SDS, 1% Triton-X-100, 2 mM EDTA, 20 mM Tris pH 8, 500 mM NaCl), LiCl immune complex (0.25 M LiCl, 1% NP-40, 1% deoxycholi acid, 1 mM EDTA, 10 mM Tris pH 8), and TE buffer (10 mM Tris pH 8, 1 mM EDTA). ChIPs were eluted in 100 ml of ChIP elution buffer (1% SDS, 150 mM NaCl, 50 ug/ml Proteinase K). Proteinase K was activated at 55 °C for 2 h and cross-links were reversed at 65 °C overnight. DNA was isolated using Qiagen PCR clean up kit prior to qPCR. Each sample was normalized to input.

RT-qPCR

RNA was treated with Turbo DNase (Ambion) and reverse transcribed using AMV RT (Promega) with random 9-mer primers. cDNA was quantified using iTaq Universal SYBR master mix (Bio-Rad) and transcript specific primers. For RNA half-life analyses, 5 mg/ml of actinomycin D (Sigma) was added to infected NIH 3T3 cells and RNA isolated at the indicated time points for quantification by RT-qPCR. All qPCR results were normalized to 18S levels. All primers used in this study are in Table S3.

4sU RNA sequencing

4sU labeled RNA was enriched, precipitated and ribosome depleted (Ribo-Zero). The resulting RNA was used to construct a whole RNA Illumina TruSeq library. Following library prep, 100 bp paired end sequencing was performed on Illumina HiSeq 2500. Raw reads from the instrument were subjected to adapter and read quality trimming (Trim Galore, Babraham Institute). Following this, the reads were aligned to the mouse genome (mm10) or to the murine viral genome using Tophat (Trapnell et al., 2009). Gene count tables for known mouse and viral genes were constructed from tophat2 alignments using htseq-count (Anders et al., 2015). DESeq2 (Love et al., 2014) was then used to estimate pairwise differentially expressed genes. False discovery rate of 10% and log2 ratio of +/-1 were used to filter differentially expressed genes.

GO-term analysis was performed for the induced and reduced gene sets found in both WT and ΔHS infected cells (85 and 32 genes, respectively), as well as the genes reduced only during a WT infection (342 genes), and genes only induced during a WT infection (176 genes), using DAVID bioinformatics resources (v. 6.7). A functional annotation chart was generated and sorted by Benjamini false discovery rate ≤ 0.05.

Western blots

Dox-inducible cell lines were treated with 1 mg/ml of dox for 5 days and cell lysates were prepared with lysis buffer (50 mM Tris pH 7.6, 150 mM NaCl, 3 mM MgCl, 10% glycerol, 0.5% NP-40) and quantified by Bradford assay. Equivalent amounts of each sample were resolved by SDS-PAGE and Western blotted with antibodies against Xrn1 (Bethyl; diluted 1:200), Dis3L2 (kindly provided by Torben Jensen; diluted 1:500), and actin (diluted 1:200). Primary antibodies were followed by HRP-conjugated goat anti- rabbit secondary antibodies (Southern Biotechnology, 1:5000).

Immunofluorescence (IFA)

NIH 3T3 cells were plated on coverslips, infected for 24 hours, and then fixed in 4% formaldehyde. Cells were permeabilized with ice-cold methanol at -80 °C for 10 min and incubated with anti-Xrn1 antibody (Sigma) at 1:200 in 5% BSA overnight at 4 °C. AlexaFluor546 secondary antibody was added (1:1000) for 1 hour at 37 °C. Coverslips were mounted in DAPI-containing Vectashield (VectorLabs). Nuclear and cytoplasmic intensity of Xrn1 staining was quantified using ImageJ software and the ratio calculated by measuring corrected total cell fluorescence (CTCF) of individual cells (Burgess et al., 2010).

DsiRNA duplexes targeting Xrn1 (GGAAAUUUCAGUAGACAUAGUGCAC; IDT) were transfected into NIH 3T3 cells using INTERFERin (Polyplus) for 36 h. Cells were fixed and stained as described above.

Figure 1

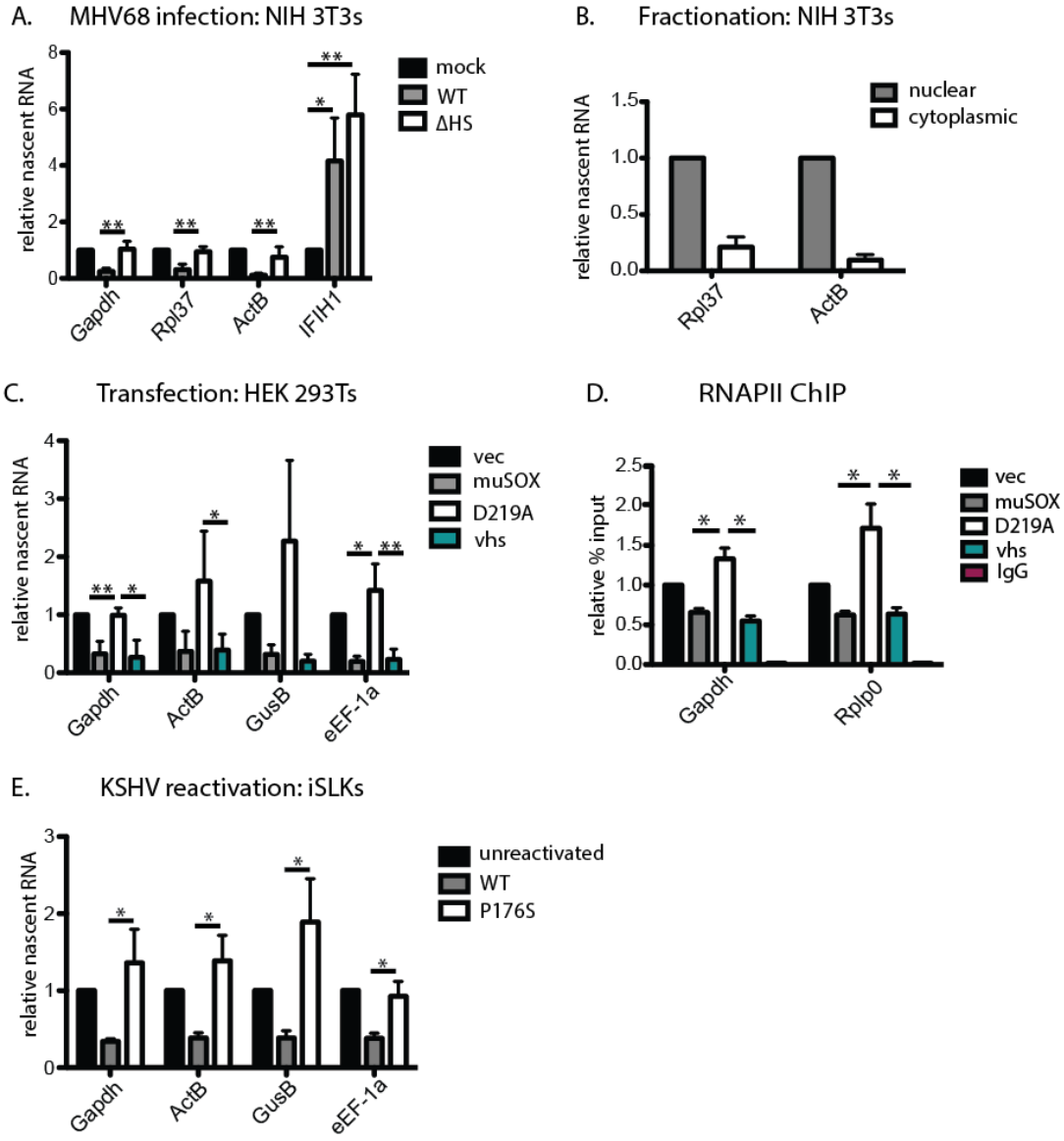

Figure 1: Enhanced mRNA turnover in the cytoplasm suppresses RNAP II transcription. (A) NIH 3T3 cells were infected with WT or ΔHS MHV68 for 24 h, whereupon 500uM of 4sU was added for 30 min and labeled RNA was isolated by biotin-streptavidin pull down. Levels of newly transcribed RNA were measured by RT-qPCR. All samples were normalized to 18S and the levels of RNA from mock-infected cells were set to 1. (B) 4sU was added to NIH 3T3 cells for 30 min, followed by fractionation into nuclear and cytoplasmic fractions. Purified 4sU-labeled RNA quantified by RT-qPCR for the indicated genes. (C) HEK 293T cells were transfected with the indicated plasmids for 24 h, then labeled with 4sU for 30 min prior to RNA purification and quantification by RT-qPCR. (D) HEK 293T cells were transfected as above for 24 h and cells crosslinked prior to analysis of RNAPII occupancy at the indicated promoters by

ChIP followed by qPCR. IgG served as a negative control. (E) iSLK cells latently infected with WT or P176S KSHV were reactivated for 48 h with dox and sodium butyrate. 4sU was added for 30 m and labeled RNA isolated and quantified by RT-qPCR.

Figure 2

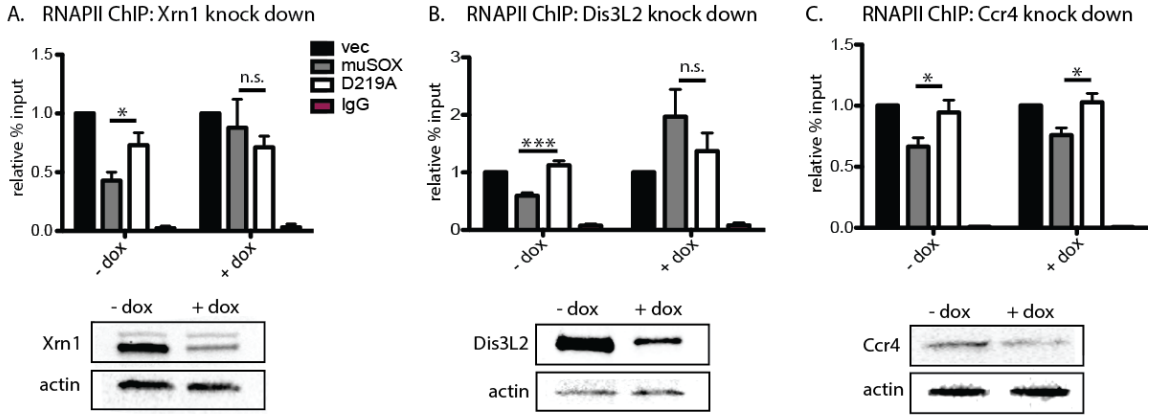

Figure 2: Xrn1 is required for the mRNA decay-transcription feedback mechanism. (A-C) HEK 293T cells with dox-inducible Xrn1, Dis3L2, or Ccr4 shRNAs were mock or dox-treated for 4 days, then transfected with the indicated plasmid for 24 h. Levels of RNAPII at the Gapdh promoter were measured by ChIP followed by qPCR (*upper panels*). The level of protein knockdown was assessed by Western blotting with the indicated antibodies (*lower panels*), with actin serving as a loading control.

Figure 3

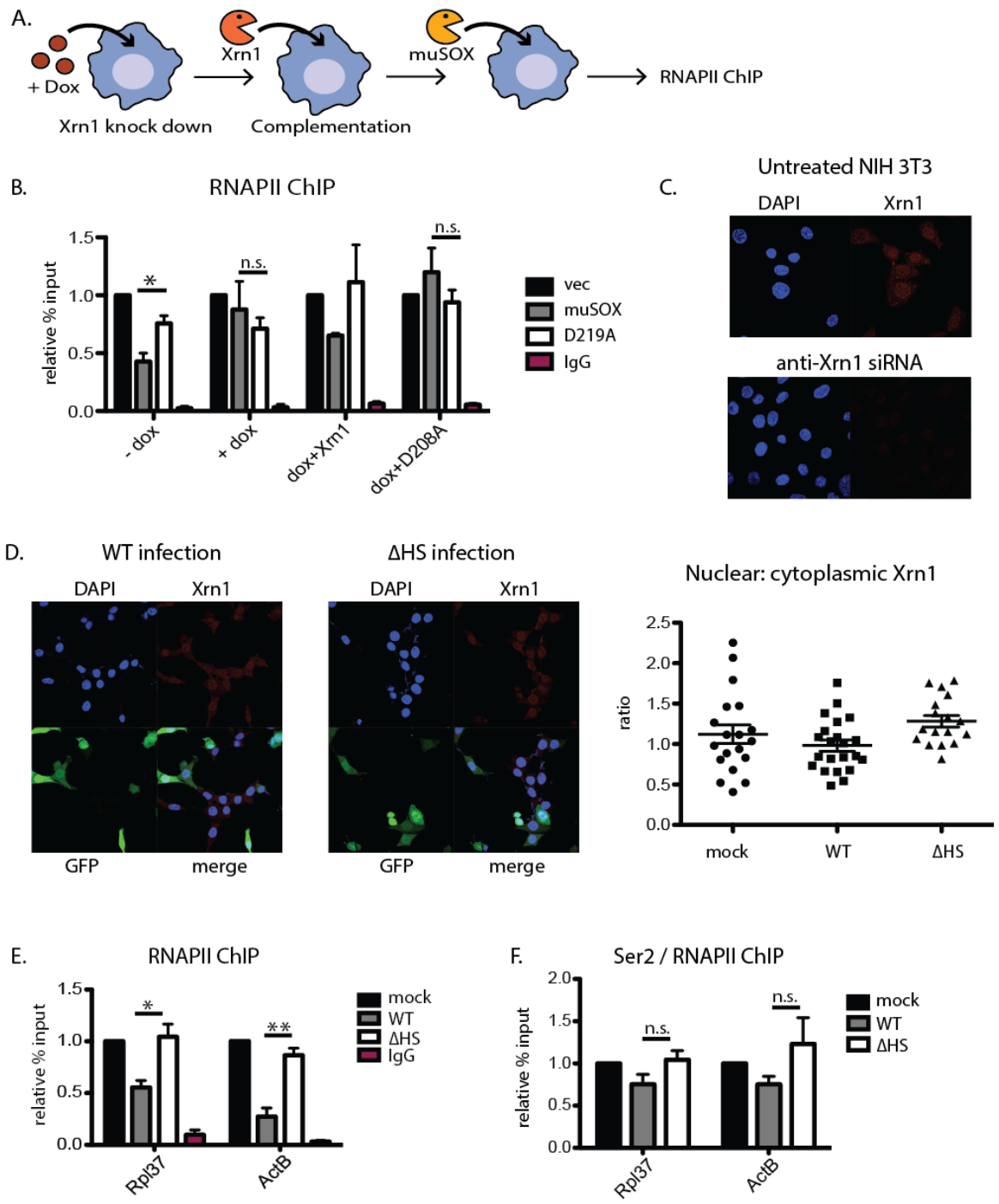

Figure 3: Xrn1 catalytic activity is required for reduced RNAPII transcription. (A) Diagram showing the complementation assay procedure. HEK 293T cells with dox-inducible Xrn1 were mock or dox-treated for 4 days, whereupon cells were transfected with plasmids expressing WT or the catalytically dead D208A Xrn1 mutant, and subsequently with muSOX or muSOX D219A. (B) Following the procedure in (A), ChIP and qPCR were performed to measure RNAPII recruitment to the human Gapdh

promoter. (C) NIH 3T3 cells were transfected with control scramble siRNAs or siRNAs targeting Xrn1. Cells were fixed and stained using an anti-Xrn1 antibody. DAPI was used to visualize nuclei. (D) NIH 3T3 cells were infected with GFP-expressing WT or ΔHS MHV68 for 24 h and fixed and stained with an anti-Xrn1 antibody. Infected cells express GFP. The nuclear to cytoplasmic ratio of Xrn1 was quantified by calculating the corrected total cell fluorescence using ImageJ for mock, WT, and ΔHS-infected cells. Each data point represents a cell. (E) NIH 3T3 cells were infected with WT or ΔHS MHV68 for 24 h. RNAPII recruitment to the Rpl37 and ActB promoters was measured by ChIP followed by qPCR. (F) ChIP was performed with antibodies recognizing serine-2-phosphorylated or total RNAPII, and the % input values at the indicated promoters were compared.

Figure 4

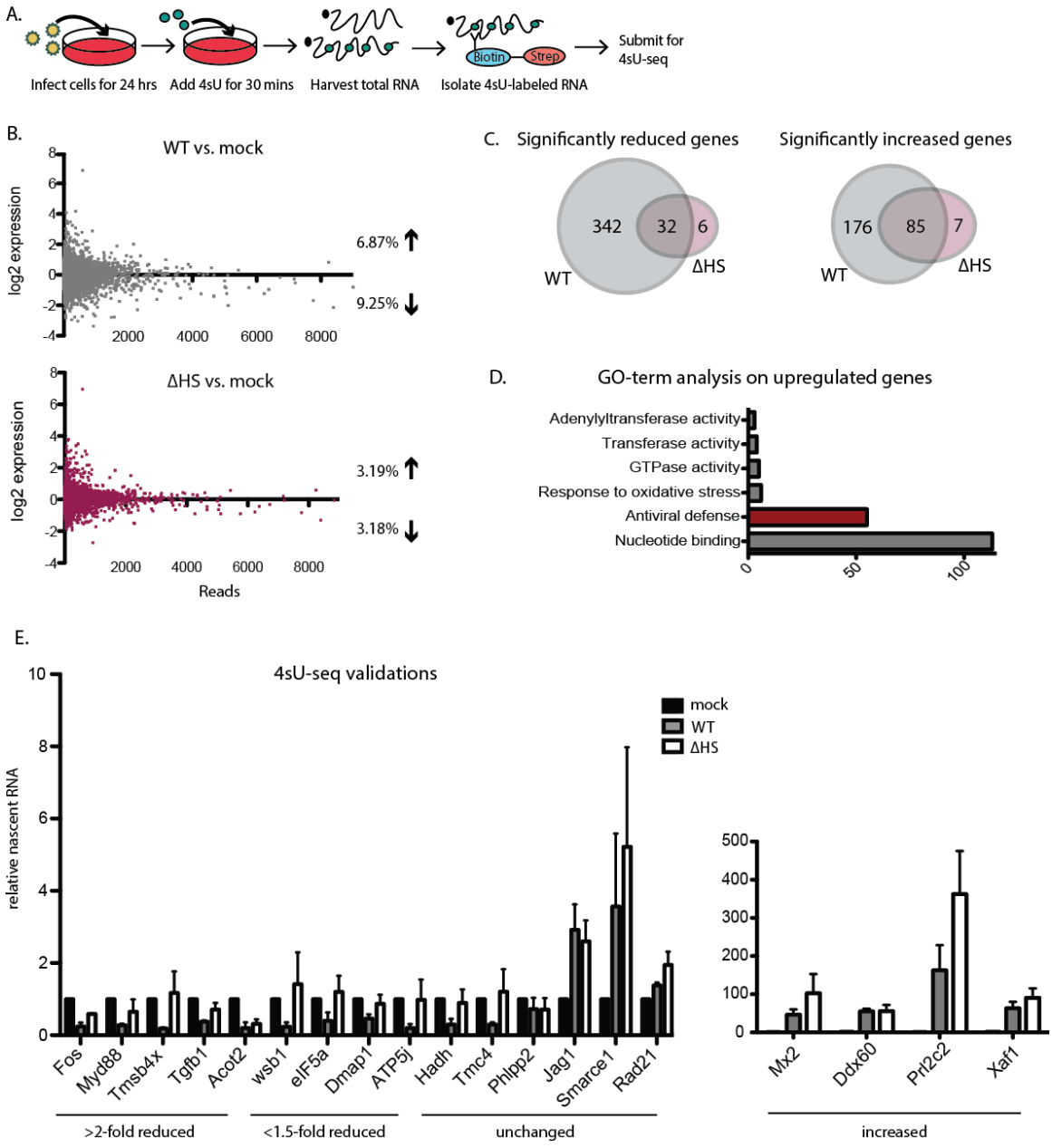

Figure 4: Cellular transcriptional changes occur throughout the mRNA transcriptome. (A) Libraries were generated from purified 4sU-labled RNA isolated from NIH 3T3 cells infected with WT or ΔHS MHV68 for 24 h, and sequenced on an Illumina platform. (B) All genes that aligned to the mouse genome (13,516 genes) were graphed with differential log2 expression values on the y-axis and read counts on the x-axis. The percentages of genes showing >1.5-fold increased or decreased expression during infection relative to uninfected cells are indicated. (C) Venn diagram showing genes that scored as significantly changed during a WT or ΔHS infection, with the overlap region depicting the number of genes significantly reduced or increased in both

infections. (D) Results from a GO-term analysis using DAVID bioinformatics software on the genes found to be increased upon both WT and ΔHS infection. (E) 15 cellular genes were randomly selected from the 4sU-seq data set for validation by RT-qPCR from purified 4sU-labeled RNA. From the 4sU-seq data set 6 genes appeared reduced during WT infection (>2-fold change), 4 appeared very modestly reduced during a WT infection (<1.5-fold change), and 6 appeared unchanged during a WT infection. Four cellular genes were selected from the 4sU-seq data set that showed increased transcription upon WT and ΔHS infection for validation by RT-qPCR from purified 4sU-labeled RNA.

Figure 5

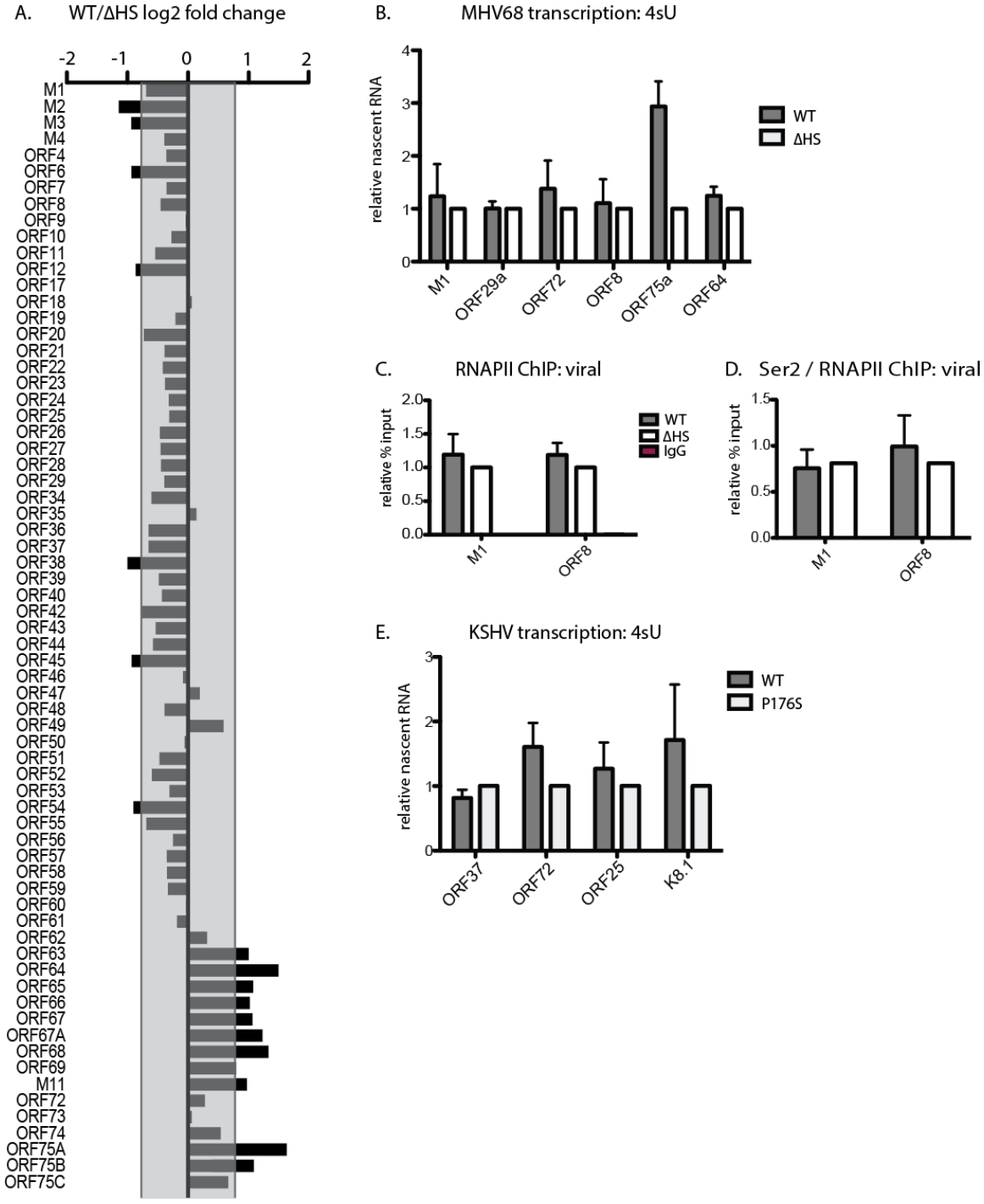

Figure 5: Viral mRNAs escape degradation-induced transcriptional repression. (A) 4sU-seq data were used to determine the differential expression of all viral genes between WT and ΔHS infection. Log2 expression changes of WT/ΔHS are shown on the x-axis and ORFs are listed in genome order on the y-axis. Values outside the shaded box indicate a significant fold change. (B) Validations of 4sU-seq data by RT-qPCR of

purified 4sU-labeled RNA isolated from cells infected with the WT or ΔHS MHV68. Results are normalized to 18S and ΔHS values set to 1. (C) ChIP for total RNAPII was performed on NIH 3T3 cells infected with WT or ΔHS MHV68, and the % input values of the viral M1 and ORF8 promoters was compared. (D) ChIP was performed with antibodies recognizing serine-2-phosphorylated or total RNAPII, and the % input values at the M1 and gB promoters were compared. (E) iSLK cells latently infected with WT or P176S KSHV were reactivated for 48 h with dox and sodium butyrate, then labeled with 4sU for 30 min prior to RNA isolation and purification. RNA levels were compared by RT-qPCR for the indicated viral genes.

Figure 6

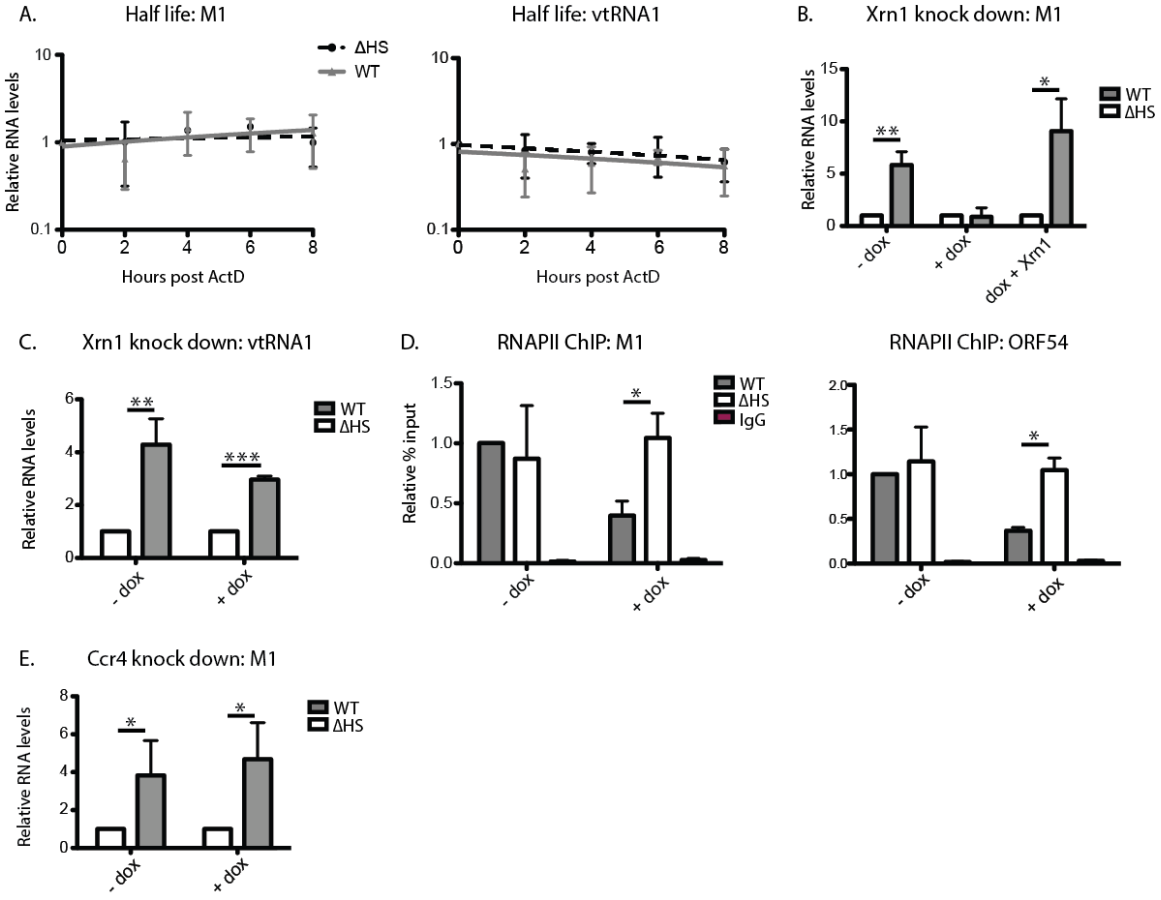

Figure 6: Xrn1 positively influences viral transcription during widespread mRNA decay. (A) NIH 3T3 cells were infected with WT or ΔHS MHV68 for 25 h, whereupon actinomycin D (ActD) was added to halt transcription, and RNA was harvested at 0, 2, 4, 6, 8 h post addition. RT-qPCR was used to measure the abundance of the viral M1 and vtRNA1 transcripts and values were normalized to 18S. (B-C) Complementation assays were performed as described in Figure 3A, except following 4 d of dox treatment cells were infected with WT or ΔHS MHV68 for 24 h. For complementation, exogenous Xrn1 was transfected into the cells prior to MHV68 infection. RT-qPCR was performed for M1 or vtRNA1 on steady state levels and all samples were normalized to 18S and ΔHS levels set to 1 for each condition. (D) RNAPII ChIP was performed on infected HEK 293T cells with or without Xrn1 knock down. Viral genes M1 and ORF54 were analyzed. (E) 293T cells containing dox-inducible shRNAs against Ccr4 were mock or dox treated for 4 days, whereupon levels of the viral M1 mRNA were measured by RT-qPCR.

Chapter 4: Discussion and Conclusions

Viral manipulation of host gene expression occurs on every level, including transcription, splicing, nuclear export, translation, and RNA decay. We are also beginning to understand how all layers of gene expression are mechanistically connected to each other, allowing a high level of control as well as rapid responses to perturbations in any one pathway. The ability of different viruses to tap into cellular processes in order to promote their own transcription, translation, and replication is a valuable tool for understanding not only how to stop these potential pathogens from causing diseases but also how basic cellular processes function and interact within the cellular environment.

Interconnected cellular processes

Here we have uncovered an underlying RNA feedback loop, linking cytoplasmic RNA decay to nuclear RNA transcription. This is the first connection between these two processes identified in mammalian cells. Many such connections have been found by studying the yeast strain *Saccharomyces cerevisiae,* where many tools exist to tease apart how different cellular processes affect others. A connection between transcription as well as multiple mRNA metabolic processes and splicing was revealed by deleting intronic sequences of several yeast genes and observing a decrease in transcript levels (Juneau et al., 2006). Whether this is due to a direct effect of introns on transcription rates or a simple derailing of the RNA processing route remains unclear. Yeast devoid of introns showed lower levels of RNA and exhibited a growth defect, suggesting the introns themselves or the process of splicing contributes to growth fitness (Juneau et al., 2006).

The spliceosome is closely coupled to proteins involved in transcription, capping and polyadenylation, RNA export, and RNA decay (Maniatis and Reed, 2002). Several viruses have been shown to inhibit splicing, including HSV-1. ICP27 blocks splicing, but only after most of the HSV-1 genes containing introns are spliced and exported, allowing for blocks to host gene expression that the virus circumvents (Hardwicke and Sandri-Goldin, 1994). Most viral proteins that inhibit splicing have been looked at in relation to how this facilitates viral replication and fitness, but many downstream host RNA processes are likely affected by the virus targeting one arm. From the virus's perspective this is a highly efficient strategy for dampening host gene expression, as a single viral protein can block multiple layers of gene expression.

Similar connections have been found between translation and RNA decay in yeast (Huch and Nissan, 2014). If translation is inhibited in a transcript-intrinsic way, such as an NMD-targeted transcript, RNA decay is accelerated in that transcript. However, if translation is inhibited in a global way, such as in response to a cellular stress or drug, RNA decay is generally inhibited and not directed to a specific transcript. Thus, global blocks to cellular processes are thought to trigger cellular stress responses for the purpose of maintaining cellular integrity during times of extrinsic stresses. Viral infection is considered a cellular stress that is known to trigger an enormous cascade of varying events within the cell in an attempt to stop viral propagation and spread. However, viruses have evolved many ways around these stress responses and in some cases have even evolved ways to use them to their advantage.

Inhibiting translation can also contribute to formation of stress granules (SGs), structures within cells that contain mRNA and various translation initiation proteins. These are in contrast to P-bodies (PBs), which contain mRNA and RNA decay proteins (Decker and Parker, 2012). The number and size of PBs is proportional to the amount of nontranslating mRNAs, and therefore increase during times of translational arrest. It is hypothesized that cytoplasmic mRNAs are cycling through polysomes, PBs, and SGs, suggesting there is a tight relationship between these structures, translation and mRNA decay. We have observed that PB composition is altered during infection with MHV68 or even transfection of muSOX (data not shown). Xrn1 appears to leave PBs, possibly because the number of Xrn1 substrates, or 5' monophosphate mRNAs, dramatically increases in the presence of muSOX, drawing Xrn1 specifically away from PBs. Alternatively, PB structure could be compromised due to the excess of nontranslating mRNAs. Many more experiments looking at PB structure during infection are needed to draw conclusions about how accelerating mRNA decay affects cytoplasmic RNA structures.

Many viruses aim to dampen host gene expression by inhibiting translation. For example, poliovirus induces the cleavage of eIF4B by a viral protease, effectively inhibiting host translation, but allowing viral translation as viral transcripts do not contain a 5' cap and instead utilize an internal ribosome entry site (IRES), bypassing the need for eIF4B in promoting translation initiation (Rose et al., 1978). However, how other cellular processes are affected by blocking translation during poliovirus infection has not been teased apart.

The work presented here addresses how accelerating mRNA decay leads to subsequent changes in transcription, specifically suppressing a subset of host genes. The conclusions from these data point to an underlying stress response whereby the cell senses global mRNA and relays that information back to the nucleus to enact changes there that might benefit the cell under conditions of stress. This differs from the way most connections between cellular processes are studied, which is mainly by inhibiting pathways. Indeed, the yeast data exploring a feedback loop between transcription and degradation does so by blocking either transcription with a point mutation in RNAPII (Sun et al., 2012), or by blocking RNA decay by knocking out decay factors (Haimovich et al., 2013b; Sun et al., 2013). Their findings indicate there is an underlying connectivity between these two systems that allows a buffering of RNA levels in order to maintain homeostasis in response to perturbations. However, this is not necessarily in disagreement with the finding presented here, considering the directionality of the arms of the feedback loop. Slowing down decay may not be "sensed" in the same way as accelerating decay; indeed, accelerating decay may be sensed as pathogenic, while slowing down decay may instead be sensed as simply unbalanced homeostasis.

Multi-level gene expression block

The viral strategy of targeting RNA decay has evolved independently multiple times. This points to the success of such a strategy. With a single viral protein capable of broadly targeting the majority of cytoplasmic mRNAs that would normally be translated by the cell, the virus can cripple the cell's gene expression cascade, as well as affect multiple downstream processes. Viruses, which have limited coding capacity, can

therefore enact enormous changes that harm the host while benefiting the virus with a single protein. Of course, the dangers of this from the viral perspective is that inactivation of that one viral protein would have serious consequences for the virus's ability to overcome host defenses. This is probably why so many viruses have evolved redundant ways to target host gene expression, each target likely having ripple effects throughout the gene expression cascade, amplifying any small effect that targeting might have.

So far, two additional blocks to host gene expression have been discovered as linked to viral-mediated mRNA degradation during MHV68 infection. The first process is linked to PABPC relocalization upon bulk cytoplasmic mRNA decay (Kumar and Glaunsinger, 2010). One cellular downstream effect of RNA decay is the liberation of PABPC molecules normally bound tightly to mRNA poly(A) tails. This liberation leads to hidden NLS motifs binding importin machinery and moving into the nucleus. Nuclear localized PABPC promotes hyperadenylation and export block of nascent transcripts (Kumar et al., 2011). If newly made mRNAs are not able to escape the nucleus, they cannot repopulate the cytoplasm with more transcripts to buffer the effect of accelerated RNA decay. This export block is thought to be a cellular stress response, as PABPC also relocalizes to the nucleus during heat shock. Nuclear PABPC could be a signal to the cell that something is wrong. The second downstream consequence to viral-mediated mRNA decay is described above—the transcriptional repression. This makes sense from the cell's perspective, as blocking export of RNAs would negate any nascent transcription from getting expressed as protein.

An interesting observation about these three blocks to gene expression that result from a single viral protein is that the virus may be able to circumvent some of the blocks. For example, we see that viral transcription, while utilizing the host RNA transcription machinery, is not suppressed even though viral transcripts are subjected to cleavage and degradation in the cytoplasm. Although it has not been directly assessed, it seems likely that viral mRNAs can escape the PABPC-mediated export block as well. ORF57 is known to play multiple roles in mRNA processing and export (Schumann et al., 2013) and could facilitate nuclear export of viral mRNAs. Additionally, PABPC is excluded from replication sites within the nucleus, suggesting it cannot promote hyperadenylation of viral transcripts. This leaves the intriguing possibility that viral mRNAs are degraded in the cytoplasm during host shutoff, but they are able to repopulate by high rates of transcription and alleviation of a host-induced export block. This pathway may allow expression of viral genes that is tempered by RNA decay, but not totally blocked by cellular stress responses, allowing adequate gene expression for virion production.

Future directions

There are many mechanistic details that remain to be worked out, such as how accelerated decay is sensed by cells and relayed into changes in transcription. We are actively pursuing two possible routes of sensing and transcriptional changes. One possibility is that an increase in free 5' monophosphate nucleotides is triggering a stress response via a nucleotide binding protein. During host shutoff, viral endonuclease cleavage leads to an excess of Xrn1 substrates, which means that a cell undergoing host shutoff should have substantially higher levels of nucleotides released during Xrn1 decay. A preliminary experiment adding excess nucleosides to cells did not result in any

transcriptional changes, as measured by RNAPII ChIP or 4sU-labeling. However, nucleosides were added to ensure they could get into cells, but these molecules lack a phosphate group and thus are not identical to the molecules released by Xrn1 degradation. Therefore, this study is currently being repeated with 5' monophosphate nucleotides that more closely mimic the molecules assumed to be in excess during host shutoff.

Transcriptional changes on a global level are often accomplished by changes to the chromatin structure or epigenetic marks. We are therefore focusing on exploring the chromatin states of those genes transcriptionally repressed during host shutoff compared to those that remain unchanged. The data procured from the 4sU-seq experiment gives us a group of seemingly unrelated genes that we can use to deduce a common mechanism for their repression. A closed chromatin state is associated with transcriptional repression and is accomplished by tightly packing nucleosomes together, physically blocking transcription machinery from accessing the gene. Preliminary experiments looking at histone occupancy for the transcriptionally repressed genes suggests that no gross changes in chromatin structure are occurring at these locations, although these experiments were somewhat inconclusive. We further explored the possibility of histone modifications at these genes. Histone 3 (H3) acetylation is typically a marker for open chromatin, or regions of active transcription, while H3 methylation typically marks closed chromatin, or regions of silenced transcription (Kouzarides, 2007). ChIP experiments comparing H3-acetylation levels for repressed genes during a WT infection or muSOX transfection actually showed a higher level of H3 acetylation. It remains to be determined if these regions also show higher H3 methylation, which might indicate a "poised" state of transcription, sometimes associated with stress responses (Kouzarides, 2007).

While the mechanism of RNA decay sensing and transcriptional repression remains elusive, how the virus escapes the repression could also shed light on the mechanism. How the virus utilizes the host chromatin and transcription machinery might have profound effects on the rate of viral transcription. We are therefore currently comparing how cellular and viral promoters might effect transcription of a reporter gene with and without muSOX-mediated host shutoff. Preliminary results indicate that when either MHV68 or KSHV promoters are driving the expression of luciferase, muSOX expression leads to higher transcription of luciferase as measured by 4sU. This is in contrast to two cellular promoters, EF1-a and Ap1, which show lower levels of transcription of the luciferase construct with muSOX expression. These data indicate there could be something fundamentally different about how viral and cellular promoters interact with transcription machinery.

Uncovering the feedback loop that exists in mammalian cells between RNA decay and transcription opens up the possibility that many other cellular processes are linked in mammalian cells, as has been shown for yeast. Using viral infection to tease apart the existence of this connection allows us to compare how cellular and viral transcription and decay differ, considering viral transcripts escape transcriptional repression but are subjected to RNA decay. It is also interesting to consider how viral-mediated host shutoff contributes to immune evasion during an MHV68 infection. As discussed above, many other host shutoff factors from diverse viruses are thought to contribute to immune evasion by dampening expression of host proteins involved with sensing viral infection.

It would be interesting to tease out the role this potentially plays during MHV68 infection, as well as how degradation of viral transcripts could contribute to immune evasion by resulting in less viral RNA and proteins to trigger an immune response. Overall, the findings presented here suggest that viral-mediated RNA decay has many diverse downstream consequences that affect both the viral lifecycle as well as host cellular processes.

References

Abernathy, E., Clyde, K., Yeasmin, R., Krug, L.T., Burlingame, A., Coscoy, L., Glaunsinger, B., 2014. Gammaherpesviral gene expression and virion composition are broadly controlled by accelerated mRNA degradation. PLoS pathogens 10, e1003882.

Adler, H., Messerle, M., Wagner, M., Koszinowski, U.H., 2000. Cloning and mutagenesis of the murine gammaherpesvirus 68 genome as an infectious bacterial artificial chromosome. Journal of virology 74, 6964-6974.

Almeida, M.S., Johnson, M.A., Herrmann, T., Geralt, M., Wuthrich, K., 2007. Novel beta-barrel fold in the nuclear magnetic resonance structure of the replicase nonstructural protein 1 from the severe acute respiratory syndrome coronavirus. Journal of virology 81, 3151-3161.

Anders, S., Pyl, P.T., Huber, W., 2015. HTSeq-a Python framework to work with high-throughput sequencing data. Bioinformatics 31, 166-169.

Arias, C., Walsh, D., Harbell, J., Wilson, A.C., Mohr, I., 2009. Activation of host translational control pathways by a viral developmental switch. PLoS pathogens 5, e1000334.

Bagneris, C., Briggs, L.C., Savva, R., Ebrahimi, B., Barrett, T.E., 2011. Crystal structure of a KSHV-SOX-DNA complex: insights into the molecular mechanisms underlying DNase activity and host shutoff. Nucleic acids research 39, 5744-5756.

Barton, E., Mandal, P., Speck, S.H., 2011. Pathogenesis and host control of gammaherpesviruses: lessons from the mouse. Annual review of immunology 29, 351-397.

Bechtel, J., Grundhoff, A., Ganem, D., 2005a. RNAs in the virion of Kaposi's sarcoma-associated herpesvirus. Journal of virology 79, 10138-10146.

Bechtel, J.T., Winant, R.C., Ganem, D., 2005b. Host and viral proteins in the virion of Kaposi's sarcoma-associated herpesvirus. Journal of virology 79, 4952-4964.

Bhutani, M., Polizzotto, M.N., Uldrick, T.S., Yarchoan, R., 2015. Kaposi Sarcoma-Associated Herpesvirus-Associated Malignancies: Epidemiology, Pathogenesis, and Advances in Treatment. Seminars in oncology 42, 223-246.

Blaskovic, D., Stancekova, M., Svobodova, J., Mistrikova, J., 1980. Isolation of five strains of herpesviruses from two species of free living small rodents. Acta virologica 24, 468.

Bohannon, K.P., Jun, Y., Gross, S.P., Smith, G.A., 2013. Differential protein partitioning within the herpesvirus tegument and envelope underlies a complex and variable virion architecture. Proceedings of the National Academy of Sciences of the United States of America 110, E1613-1620.

Bortz, E., Whitelegge, J.P., Jia, Q., Zhou, Z.H., Stewart, J.P., Wu, T.T., Sun, R., 2003. Identification of proteins associated with murine gammaherpesvirus 68 virions. Journal of virology 77, 13425-13432.

Bowden, R.J., Simas, J.P., Davis, A.J., Efstathiou, S., 1997. Murine gammaherpesvirus 68 encodes tRNA-like sequences which are expressed during latency. The Journal of general virology 78 (Pt 7), 1675-1687.

Braun, K.A., Young, E.T., 2014. Coupling mRNA Synthesis and Decay. Molecular and cellular biology 34, 4078-4087.

Bresnahan, W.A., Shenk, T.E., 2000. UL82 virion protein activates expression of immediate early viral genes in human cytomegalovirus-infected cells. Proceedings of the National Academy of Sciences of the United States of America 97, 14506-14511.
Brulois, K.F., Chang, H., Lee, A.S., Ensser, A., Wong, L.Y., Toth, Z., Lee, S.H., Lee, H.R., Myoung, J., Ganem, D., Oh, T.K., Kim, J.F., Gao, S.J., Jung, J.U., 2012. Construction and manipulation of a new Kaposi's sarcoma-associated herpesvirus bacterial artificial chromosome clone. Journal of virology 86, 9708-9720.
Buisson, M., Geoui, T., Flot, D., Tarbouriech, N., Ressing, M.E., Wiertz, E.J., Burmeister, W.P., 2009. A bridge crosses the active-site canyon of the Epstein-Barr virus nuclease with DNase and RNase activities. Journal of molecular biology 391, 717-728.
Burgess, A., Vigneron, S., Brioudes, E., Labbe, J.C., Lorca, T., Castro, A., 2010. Loss of human Greatwall results in G2 arrest and multiple mitotic defects due to deregulation of the cyclin B-Cdc2/PP2A balance. Proceedings of the National Academy of Sciences of the United States of America 107, 12564-12569.
Canny, S.P., Reese, T.A., Johnson, L.S., Zhang, X., Kambal, A., Duan, E., Liu, C.Y., Virgin, H.W., 2014. Pervasive transcription of a herpesvirus genome generates functionally important RNAs. mBio 5, e01033-01013.
Chen, I.H., Sciabica, K.S., Sandri-Goldin, R.M., 2002. ICP27 interacts with the RNA export factor Aly/REF to direct herpes simplex virus type 1 intronless mRNAs to the TAP export pathway. Journal of virology 76, 12877-12889.
Cheng, B.Y., Zhi, J., Santana, A., Khan, S., Salinas, E., Forrest, J.C., Zheng, Y., Jaggi, S., Leatherwood, J., Krug, L.T., 2012. Tiled microarray identification of novel viral transcript structures and distinct transcriptional profiles during two modes of productive murine gammaherpesvirus 68 infection. Journal of virology 86, 4340-4357.
Clyde, K., Glaunsinger, B.A., 2011. Deep sequencing reveals direct targets of gammaherpesvirus-induced mRNA decay and suggests that multiple mechanisms govern cellular transcript escape. PloS one 6, e19655.
Collins, C.M., Boss, J.M., Speck, S.H., 2009. Identification of infected B-cell populations by using a recombinant murine gammaherpesvirus 68 expressing a fluorescent protein. Journal of virology 83, 6484-6493.
Connolly, S.A., Jackson, J.O., Jardetzky, T.S., Longnecker, R., 2011. Fusing structure and function: a structural view of the herpesvirus entry machinery. Nature reviews. Microbiology 9, 369-381.
Covarrubias, S., Gaglia, M.M., Kumar, G.R., Wong, W., Jackson, A.O., Glaunsinger, B.A., 2011. Coordinated destruction of cellular messages in translation complexes by the gammaherpesvirus host shutoff factor and the mammalian exonuclease Xrn1. PLoS pathogens 7, e1002339.
Covarrubias, S., Richner, J.M., Clyde, K., Lee, Y.J., Glaunsinger, B.A., 2009. Host shutoff is a conserved phenotype of gammaherpesvirus infection and is orchestrated exclusively from the cytoplasm. Journal of virology 83, 9554-9566.
Dauber, B., Saffran, H.A., Smiley, J.R., 2014. The herpes simplex virus 1 virion host shutoff protein enhances translation of viral late mRNAs by preventing mRNA overload. Journal of virology 88, 9624-9632.

Decker, C.J., Parker, R., 2012. P-bodies and stress granules: possible roles in the control of translation and mRNA degradation. Cold Spring Harbor perspectives in biology 4, a012286.
del Rio, T., DeCoste, C.J., Enquist, L.W., 2005. Actin is a component of the compensation mechanism in pseudorabies virus virions lacking the major tegument protein VP22. Journal of virology 79, 8614-8619.
Desmet, E.A., Bussey, K.A., Stone, R., Takimoto, T., 2013. Identification of the N-terminal domain of the influenza virus PA responsible for the suppression of host protein synthesis. Journal of virology 87, 3108-3118.
Diebel, K.W., Oko, L.M., Medina, E.M., Niemeyer, B.F., Warren, C.J., Claypool, D.J., Tibbetts, S.A., Cool, C.D., Clambey, E.T., van Dyk, L.F., 2015. Gammaherpesvirus small noncoding RNAs are bifunctional elements that regulate infection and contribute to virulence in vivo. mBio 6, e01670-01614.
Ebrahimi, B., Dutia, B.M., Roberts, K.L., Garcia-Ramirez, J.J., Dickinson, P., Stewart, J.P., Ghazal, P., Roy, D.J., Nash, A.A., 2003. Transcriptome profile of murine gammaherpesvirus-68 lytic infection. The Journal of general virology 84, 99-109.
Eckmann, C.R., Rammelt, C., Wahle, E., 2011. Control of poly(A) tail length. Wiley interdisciplinary reviews. RNA 2, 348-361.
Feederle, R., Bannert, H., Lips, H., Muller-Lantzsch, N., Delecluse, H.J., 2009. The Epstein-Barr virus alkaline exonuclease BGLF5 serves pleiotropic functions in virus replication. Journal of virology 83, 4952-4962.
Feldman, E.R., Kara, M., Coleman, C.B., Grau, K.R., Oko, L.M., Krueger, B.J., Renne, R., van Dyk, L.F., Tibbetts, S.A., 2014. Virus-encoded microRNAs facilitate gammaherpesvirus latency and pathogenesis in vivo. mBio 5, e00981-00914.
Feng, P., Everly, D.N., Jr., Read, G.S., 2005. mRNA decay during herpes simplex virus (HSV) infections: protein-protein interactions involving the HSV virion host shutoff protein and translation factors eIF4H and eIF4A. Journal of virology 79, 9651-9664.
Finnen, R.L., Hay, T.J., Dauber, B., Smiley, J.R., Banfield, B.W., 2014. The herpes simplex virus 2 virion-associated ribonuclease vhs interferes with stress granule formation. Journal of virology 88, 12727-12739.
Flano, E., Husain, S.M., Sample, J.T., Woodland, D.L., Blackman, M.A., 2000. Latent murine gamma-herpesvirus infection is established in activated B cells, dendritic cells, and macrophages. J Immunol 165, 1074-1081.
Gaglia, M.M., Covarrubias, S., Wong, W., Glaunsinger, B.A., 2012. A common strategy for host RNA degradation by divergent viruses. Journal of virology 86, 9527-9530.
Gallouzi, I.E., Wilusz, J., 2013. A DIStinctively novel exoribonuclease that really likes U. The EMBO journal 32, 1799-1801.
Gaspar, M., May, J.S., Sukla, S., Frederico, B., Gill, M.B., Smith, C.M., Belz, G.T., Stevenson, P.G., 2011. Murid herpesvirus-4 exploits dendritic cells to infect B cells. PLoS pathogens 7, e1002346.
Glaunsinger, B., Chavez, L., Ganem, D., 2005. The exonuclease and host shutoff functions of the SOX protein of Kaposi's sarcoma-associated herpesvirus are genetically separable. Journal of virology 79, 7396-7401.
Glaunsinger, B., Ganem, D., 2004. Lytic KSHV infection inhibits host gene expression by accelerating global mRNA turnover. Molecular cell 13, 713-723.

Goodwin, M.M., Molleston, J.M., Canny, S., Abou El Hassan, M., Willert, E.K., Bremner, R., Virgin, H.W., 2010. Histone deacetylases and the nuclear receptor corepressor regulate lytic-latent switch gene 50 in murine gammaherpesvirus 68-infected macrophages. Journal of virology 84, 12039-12047.
Gunther, T., Grundhoff, A., 2010. The epigenetic landscape of latent Kaposi sarcoma-associated herpesvirus genomes. PLoS pathogens 6, e1000935.
Guo, H., Wang, L., Peng, L., Zhou, Z.H., Deng, H., 2009. Open reading frame 33 of a gammaherpesvirus encodes a tegument protein essential for virion morphogenesis and egress. Journal of virology 83, 10582-10595.
Gwack, Y., Nakamura, H., Lee, S.H., Souvlis, J., Yustein, J.T., Gygi, S., Kung, H.J., Jung, J.U., 2003. Poly(ADP-ribose) polymerase 1 and Ste20-like kinase hKFC act as transcriptional repressors for gamma-2 herpesvirus lytic replication. Molecular and cellular biology 23, 8282-8294.
Haimovich, G., Choder, M., Singer, R.H., Trcek, T., 2013a. The fate of the messenger is pre-determined: a new model for regulation of gene expression. Biochimica et biophysica acta 1829, 643-653.
Haimovich, G., Medina, D.A., Causse, S.Z., Garber, M., Millan-Zambrano, G., Barkai, O., Chavez, S., Perez-Ortin, J.E., Darzacq, X., Choder, M., 2013b. Gene expression is circular: factors for mRNA degradation also foster mRNA synthesis. Cell 153, 1000-1011.
Hair, J.R., Lyons, P.A., Smith, K.G., Efstathiou, S., 2007. Control of Rta expression critically determines transcription of viral and cellular genes following gammaherpesvirus infection. The Journal of general virology 88, 1689-1697.
Hardwicke, M.A., Sandri-Goldin, R.M., 1994. The herpes simplex virus regulatory protein ICP27 contributes to the decrease in cellular mRNA levels during infection. Journal of virology 68, 4797-4810.
Harel-Sharvit, L., Eldad, N., Haimovich, G., Barkai, O., Duek, L., Choder, M., 2010. RNA polymerase II subunits link transcription and mRNA decay to translation. Cell 143, 552-563.
Harigaya, Y., Parker, R., 2010. No-go decay: a quality control mechanism for RNA in translation. Wiley interdisciplinary reviews. RNA 1, 132-141.
Horst, D., Burmeister, W.P., Boer, I.G., van Leeuwen, D., Buisson, M., Gorbalenya, A.E., Wiertz, E.J., Ressing, M.E., 2012. The "Bridge" in the Epstein-Barr virus alkaline exonuclease protein BGLF5 contributes to shutoff activity during productive infection. Journal of virology 86, 9175-9187.
Huang, C., Lokugamage, K.G., Rozovics, J.M., Narayanan, K., Semler, B.L., Makino, S., 2011. SARS coronavirus nsp1 protein induces template-dependent endonucleolytic cleavage of mRNAs: viral mRNAs are resistant to nsp1-induced RNA cleavage. PLoS pathogens 7, e1002433.
Huch, S., Nissan, T., 2014. Interrelations between translation and general mRNA degradation in yeast. Wiley interdisciplinary reviews. RNA 5, 747-763.
Hutin, S., Lee, Y., Glaunsinger, B.A., 2013. An RNA element in human interleukin 6 confers escape from degradation by the gammaherpesvirus SOX protein. Journal of virology 87, 4672-4682.
Hwang, S., Kim, K.S., Flano, E., Wu, T.T., Tong, L.M., Park, A.N., Song, M.J., Sanchez, D.J., O'Connell, R.M., Cheng, G., Sun, R., 2009. Conserved herpesviral kinase promotes

viral persistence by inhibiting the IRF-3-mediated type I interferon response. Cell host & microbe 5, 166-178.
Hwang, S., Wu, T.T., Tong, L.M., Kim, K.S., Martinez-Guzman, D., Colantonio, A.D., Uittenbogaart, C.H., Sun, R., 2008. Persistent gammaherpesvirus replication and dynamic interaction with the host in vivo. Journal of virology 82, 12498-12509.
Inada, T., 2013. Quality control systems for aberrant mRNAs induced by aberrant translation elongation and termination. Biochimica et biophysica acta 1829, 634-642.
Jagger, B.W., Wise, H.M., Kash, J.C., Walters, K.A., Wills, N.M., Xiao, Y.L., Dunfee, R.L., Schwartzman, L.M., Ozinsky, A., Bell, G.L., Dalton, R.M., Lo, A., Efstathiou, S., Atkins, J.F., Firth, A.E., Taubenberger, J.K., Digard, P., 2012. An overlapping protein-coding region in influenza A virus segment 3 modulates the host response. Science 337, 199-204.
Jauregui, A.R., Savalia, D., Lowry, V.K., Farrell, C.M., Wathelet, M.G., 2013. Identification of residues of SARS-CoV nsp1 that differentially affect inhibition of gene expression and antiviral signaling. PloS one 8, e62416.
Jinek, M., Coyle, S.M., Doudna, J.A., 2011. Coupled 5' nucleotide recognition and processivity in Xrn1-mediated mRNA decay. Molecular cell 41, 600-608.
Johnson, L.S., Willert, E.K., Virgin, H.W., 2010. Redefining the genetics of murine gammaherpesvirus 68 via transcriptome-based annotation. Cell host & microbe 7, 516-526.
Juneau, K., Miranda, M., Hillenmeyer, M.E., Nislow, C., Davis, R.W., 2006. Introns regulate RNA and protein abundance in yeast. Genetics 174, 511-518.
Kamitani, W., Huang, C., Narayanan, K., Lokugamage, K.G., Makino, S., 2009. A two-pronged strategy to suppress host protein synthesis by SARS coronavirus Nsp1 protein. Nature structural & molecular biology 16, 1134-1140.
Karr, B.M., Read, G.S., 1999. The virion host shutoff function of herpes simplex virus degrades the 5' end of a target mRNA before the 3' end. Virology 264, 195-204.
Kelly, B.J., Fraefel, C., Cunningham, A.L., Diefenbach, R.J., 2009. Functional roles of the tegument proteins of herpes simplex virus type 1. Virus research 145, 173-186.
Khaperskyy, D.A., Emara, M.M., Johnston, B.P., Anderson, P., Hatchette, T.F., McCormick, C., 2014. Influenza a virus host shutoff disables antiviral stress-induced translation arrest. PLoS pathogens 10, e1004217.
Knipe, D.M., Cliffe, A., 2008. Chromatin control of herpes simplex virus lytic and latent infection. Nature reviews. Microbiology 6, 211-221.
Koffa, M.D., Clements, J.B., Izaurralde, E., Wadd, S., Wilson, S.A., Mattaj, I.W., Kuersten, S., 2001. Herpes simplex virus ICP27 protein provides viral mRNAs with access to the cellular mRNA export pathway. The EMBO journal 20, 5769-5778.
Kouzarides, T., 2007. Chromatin modifications and their function. Cell 128, 693-705.
Krausslich, H.G., Nicklin, M.J., Toyoda, H., Etchison, D., Wimmer, E., 1987. Poliovirus proteinase 2A induces cleavage of eucaryotic initiation factor 4F polypeptide p220. Journal of virology 61, 2711-2718.
Krishnan, H.H., Naranatt, P.P., Smith, M.S., Zeng, L., Bloomer, C., Chandran, B., 2004. Concurrent expression of latent and a limited number of lytic genes with immune modulation and antiapoptotic function by Kaposi's sarcoma-associated herpesvirus

early during infection of primary endothelial and fibroblast cells and subsequent decline of lytic gene expression. Journal of virology 78, 3601-3620.
Kumar, G.R., Glaunsinger, B.A., 2010. Nuclear import of cytoplasmic poly(A) binding protein restricts gene expression via hyperadenylation and nuclear retention of mRNA. Molecular and cellular biology 30, 4996-5008.
Kumar, G.R., Shum, L., Glaunsinger, B.A., 2011. Importin alpha-mediated nuclear import of cytoplasmic poly(A) binding protein occurs as a direct consequence of cytoplasmic mRNA depletion. Molecular and cellular biology 31, 3113-3125.
Kuyumcu-Martinez, N.M., Van Eden, M.E., Younan, P., Lloyd, R.E., 2004. Cleavage of poly(A)-binding protein by poliovirus 3C protease inhibits host cell translation: a novel mechanism for host translation shutoff. Molecular and cellular biology 24, 1779-1790.
Kwong, A.D., Frenkel, N., 1987. Herpes simplex virus-infected cells contain a function(s) that destabilizes both host and viral mRNAs. Proceedings of the National Academy of Sciences of the United States of America 84, 1926-1930.
Kwong, A.D., Frenkel, N., 1989. The herpes simplex virus virion host shutoff function. Journal of virology 63, 4834-4839.
Kwong, A.D., Kruper, J.A., Frenkel, N., 1988. Herpes simplex virus virion host shutoff function. Journal of virology 62, 912-921.
Lam, Q., Smibert, C.A., Koop, K.E., Lavery, C., Capone, J.P., Weinheimer, S.P., Smiley, J.R., 1996. Herpes simplex virus VP16 rescues viral mRNA from destruction by the virion host shutoff function. The EMBO journal 15, 2575-2581.
Lee, S., Cho, H.J., Park, J.J., Kim, Y.S., Hwang, S., Sun, R., Song, M.J., 2007. The ORF49 protein of murine gammaherpesvirus 68 cooperates with RTA in regulating virus replication. Journal of virology 81, 9870-9877.
Lee, Y.J., Glaunsinger, B.A., 2009. Aberrant herpesvirus-induced polyadenylation correlates with cellular messenger RNA destruction. PLoS biology 7, e1000107.
Lei, L., Ying, S., Baojun, L., Yi, Y., Xiang, H., Wenli, S., Zounan, S., Deyin, G., Qingyu, Z., Jingmei, L., Guohui, C., 2013. Attenuation of mouse hepatitis virus by deletion of the LLRKxGxKG region of Nsp1. PloS one 8, e61166.
Leib, D.A., Harrison, T.E., Laslo, K.M., Machalek, M.A., Moorman, N.J., Virgin, H.W., 1999. Interferons regulate the phenotype of wild-type and mutant herpes simplex viruses in vivo. The Journal of experimental medicine 189, 663-672.
Ling, P.D., Tan, J., Sewatanon, J., Peng, R., 2008. Murine gammaherpesvirus 68 open reading frame 75c tegument protein induces the degradation of PML and is essential for production of infectious virus. Journal of virology 82, 8000-8012.
Liu, S., Pavlova, I.V., Virgin, H.W.t., Speck, S.H., 2000. Characterization of gammaherpesvirus 68 gene 50 transcription. Journal of virology 74, 2029-2037.
Liu, S.W., Wyatt, L.S., Orandle, M.S., Minai, M., Moss, B., 2014. The D10 decapping enzyme of vaccinia virus contributes to decay of cellular and viral mRNAs and to virulence in mice. Journal of virology 88, 202-211.
Liu, S.Y., Sanchez, D.J., Aliyari, R., Lu, S., Cheng, G., 2012. Systematic identification of type I and type II interferon-induced antiviral factors. Proceedings of the National Academy of Sciences of the United States of America 109, 4239-4244.
Lokugamage, K.G., Narayanan, K., Huang, C., Makino, S., 2012. Severe acute respiratory syndrome coronavirus protein nsp1 is a novel eukaryotic translation

inhibitor that represses multiple steps of translation initiation. Journal of virology 86, 13598-13608.
Lotan, R., Goler-Baron, V., Duek, L., Haimovich, G., Choder, M., 2007. The Rpb7p subunit of yeast RNA polymerase II plays roles in the two major cytoplasmic mRNA decay mechanisms. The Journal of cell biology 178, 1133-1143.
Love, M.I., Huber, W., Anders, S., 2014. Moderated estimation of fold change and dispersion for RNA-seq data with DESeq2. Genome biology 15, 550.
Lykke-Andersen, S., Chen, Y., Ardal, B.R., Lilje, B., Waage, J., Sandelin, A., Jensen, T.H., 2014. Human nonsense-mediated RNA decay initiates widely by endonucleolysis and targets snoRNA host genes. Genes & development 28, 2498-2517.
Maniatis, T., Reed, R., 2002. An extensive network of coupling among gene expression machines. Nature 416, 499-506.
May, J.S., Coleman, H.M., Smillie, B., Efstathiou, S., Stevenson, P.G., 2004. Forced lytic replication impairs host colonization by a latency-deficient mutant of murine gammaherpesvirus-68. The Journal of general virology 85, 137-146.
Medina, D.A., Jordan-Pla, A., Millan-Zambrano, G., Chavez, S., Choder, M., Perez-Ortin, J.E., 2014. Cytoplasmic 5'-3' exonuclease Xrn1p is also a genome-wide transcription factor in yeast. Frontiers in genetics 5, 1.
Mettenleiter, T.C., 2004. Budding events in herpesvirus morphogenesis. Virus research 106, 167-180.
Michael, K., Klupp, B.G., Mettenleiter, T.C., Karger, A., 2006. Composition of pseudorabies virus particles lacking tegument protein US3, UL47, or UL49 or envelope glycoprotein E. Journal of virology 80, 1332-1339.
Milho, R., Smith, C.M., Marques, S., Alenquer, M., May, J.S., Gillet, L., Gaspar, M., Efstathiou, S., Simas, J.P., Stevenson, P.G., 2009. In vivo imaging of murid herpesvirus-4 infection. The Journal of general virology 90, 21-32.
Moon, S.L., Wilusz, J., 2013. Cytoplasmic viruses: rage against the (cellular RNA decay) machine. PLoS pathogens 9, e1003762.
Mounce, B.C., Tsan, F.C., Kohler, S., Cirillo, L.A., Tarakanova, V.L., 2011. Dynamic association of gammaherpesvirus DNA with core histone during de novo lytic infection of primary cells. Virology 421, 167-172.
Myoung, J., Ganem, D., 2011. Infection of lymphoblastoid cell lines by Kaposi's sarcoma-associated herpesvirus: critical role of cell-associated virus. Journal of virology 85, 9767-9777.
Nagarajan, V.K., Jones, C.I., Newbury, S.F., Green, P.J., 2013. XRN 5'-->3' exoribonucleases: structure, mechanisms and functions. Biochimica et biophysica acta 1829, 590-603.
Narayanan, K., Makino, S., 2013. Interplay between viruses and host mRNA degradation. Biochimica et biophysica acta 1829, 732-741.
Nekorchuk, M., Han, Z., Hsieh, T.T., Swaminathan, S., 2007. Kaposi's sarcoma-associated herpesvirus ORF57 protein enhances mRNA accumulation independently of effects on nuclear RNA export. Journal of virology 81, 9990-9998.
Noh, C.W., Cho, H.J., Kang, H.R., Jin, H.Y., Lee, S., Deng, H., Wu, T.T., Arumugaswami, V., Sun, R., Song, M.J., 2012. The virion-associated open reading frame 49 of murine gammaherpesvirus 68 promotes viral replication both in vitro and in vivo as a derepressor of RTA. Journal of virology 86, 1109-1118.

Oroskar, A.A., Read, G.S., 1987. A mutant of herpes simplex virus type 1 exhibits increased stability of immediate-early (alpha) mRNAs. Journal of virology 61, 604-606.
Oroskar, A.A., Read, G.S., 1989. Control of mRNA stability by the virion host shutoff function of herpes simplex virus. Journal of virology 63, 1897-1906.
Page, H.G., Read, G.S., 2010. The virion host shutoff endonuclease (UL41) of herpes simplex virus interacts with the cellular cap-binding complex eIF4F. Journal of virology 84, 6886-6890.
Park, R., El-Guindy, A., Heston, L., Lin, S.F., Yu, K.P., Nagy, M., Borah, S., Delecluse, H.J., Steitz, J., Miller, G., 2014. Nuclear translocation and regulation of intranuclear distribution of cytoplasmic poly(A)-binding protein are distinct processes mediated by two Epstein Barr virus proteins. PloS one 9, e92593.
Parrish, S., Hurchalla, M., Liu, S.W., Moss, B., 2009. The African swine fever virus g5R protein possesses mRNA decapping activity. Virology 393, 177-182.
Parrish, S., Moss, B., 2006. Characterization of a vaccinia virus mutant with a deletion of the D10R gene encoding a putative negative regulator of gene expression. Journal of virology 80, 553-561.
Parrish, S., Moss, B., 2007. Characterization of a second vaccinia virus mRNA-decapping enzyme conserved in poxviruses. Journal of virology 81, 12973-12978.
Peng, L., Ryazantsev, S., Sun, R., Zhou, Z.H., 2010. Three-dimensional visualization of gammaherpesvirus life cycle in host cells by electron tomography. Structure 18, 47-58.
Penkert, R.R., Kalejta, R.F., 2011. Tegument protein control of latent herpesvirus establishment and animation. Herpesviridae 2, 3.
Phatnani, H.P., Greenleaf, A.L., 2006. Phosphorylation and functions of the RNA polymerase II CTD. Genes & development 20, 2922-2936.
Popp, M.W., Maquat, L.E., 2013. Organizing principles of mammalian nonsense-mediated mRNA decay. Annual review of genetics 47, 139-165.
Quinn, L.L., Zuo, J., Abbott, R.J., Shannon-Lowe, C., Tierney, R.J., Hislop, A.D., Rowe, M., 2014. Cooperation between Epstein-Barr virus immune evasion proteins spreads protection from CD8+ T cell recognition across all three phases of the lytic cycle. PLoS pathogens 10, e1004322.
Read, G.S., 2013. Virus-encoded endonucleases: expected and novel functions. Wiley interdisciplinary reviews. RNA 4, 693-708.
Reese, T.A., Xia, J., Johnson, L.S., Zhou, X., Zhang, W., Virgin, H.W., 2010. Identification of novel microRNA-like molecules generated from herpesvirus and host tRNA transcripts. Journal of virology 84, 10344-10353.
Rice, S.A., Long, M.C., Lam, V., Spencer, C.A., 1994. RNA polymerase II is aberrantly phosphorylated and localized to viral replication compartments following herpes simplex virus infection. Journal of virology 68, 988-1001.
Richner, J.M., Clyde, K., Pezda, A.C., Cheng, B.Y., Wang, T., Kumar, G.R., Covarrubias, S., Coscoy, L., Glaunsinger, B., 2011. Global mRNA degradation during lytic gammaherpesvirus infection contributes to establishment of viral latency. PLoS pathogens 7, e1002150.

Rickabaugh, T.M., Brown, H.J., Martinez-Guzman, D., Wu, T.T., Tong, L., Yu, F., Cole, S., Sun, R., 2004. Generation of a latency-deficient gammaherpesvirus that is protective against secondary infection. Journal of virology 78, 9215-9223.
Rochford, R., Lutzke, M.L., Alfinito, R.S., Clavo, A., Cardin, R.D., 2001. Kinetics of murine gammaherpesvirus 68 gene expression following infection of murine cells in culture and in mice. Journal of virology 75, 4955-4963.
Rose, J.K., Trachsel, H., Leong, K., Baltimore, D., 1978. Inhibition of translation by poliovirus: inactivation of a specific initiation factor. Proceedings of the National Academy of Sciences of the United States of America 75, 2732-2736.
Rowe, M., Glaunsinger, B., van Leeuwen, D., Zuo, J., Sweetman, D., Ganem, D., Middeldorp, J., Wiertz, E.J., Ressing, M.E., 2007. Host shutoff during productive Epstein-Barr virus infection is mediated by BGLF5 and may contribute to immune evasion. Proceedings of the National Academy of Sciences of the United States of America 104, 3366-3371.
Sahin, B.B., Patel, D., Conrad, N.K., 2010. Kaposi's sarcoma-associated herpesvirus ORF57 protein binds and protects a nuclear noncoding RNA from cellular RNA decay pathways. PLoS pathogens 6, e1000799.
Sarma, N., Agarwal, D., Shiflett, L.A., Read, G.S., 2008. Small interfering RNAs that deplete the cellular translation factor eIF4H impede mRNA degradation by the virion host shutoff protein of herpes simplex virus. Journal of virology 82, 6600-6609.
Sathish, N., Wang, X., Yuan, Y., 2012. Tegument Proteins of Kaposi's Sarcoma-Associated Herpesvirus and Related Gamma-Herpesviruses. Frontiers in microbiology 3, 98.
Schoenberg, D.R., Maquat, L.E., 2009. Re-capping the message. Trends in biochemical sciences 34, 435-442.
Schumann, S., Jackson, B.R., Baquero-Perez, B., Whitehouse, A., 2013. Kaposi's sarcoma-associated herpesvirus ORF57 protein: exploiting all stages of viral mRNA processing. Viruses 5, 1901-1923.
Schweingruber, C., Rufener, S.C., Zund, D., Yamashita, A., Muhlemann, O., 2013. Nonsense-mediated mRNA decay - mechanisms of substrate mRNA recognition and degradation in mammalian cells. Biochimica et biophysica acta 1829, 612-623.
Sciabica, K.S., Dai, Q.J., Sandri-Goldin, R.M., 2003. ICP27 interacts with SRPK1 to mediate HSV splicing inhibition by altering SR protein phosphorylation. The EMBO journal 22, 1608-1619.
Sewatanon, J., Ling, P.D., 2013. Murine gammaherpesvirus 68 ORF75c contains ubiquitin E3 ligase activity and requires PML SUMOylation but not other known cellular PML regulators, CK2 and E6AP, to mediate PML degradation. Virology 440, 140-149.
Shen, G., Wang, K., Wang, S., Cai, M., Li, M.L., Zheng, C., 2014. Herpes simplex virus 1 counteracts viperin via its virion host shutoff protein UL41. Journal of virology 88, 12163-12166.
Shiflett, L.A., Read, G.S., 2013. mRNA decay during herpes simplex virus (HSV) infections: mutations that affect translation of an mRNA influence the sites at which it is cleaved by the HSV virion host shutoff (Vhs) protein. Journal of virology 87, 94-109.

Shors, T., Keck, J.G., Moss, B., 1999. Down regulation of gene expression by the vaccinia virus D10 protein. Journal of virology 73, 791-796.
Shu, M., Taddeo, B., Roizman, B., 2013a. The nuclear-cytoplasmic shuttling of virion host shutoff RNase is enabled by pUL47 and an embedded nuclear export signal and defines the sites of degradation of AU-rich and stable cellular mRNAs. Journal of virology 87, 13569-13578.
Shu, M., Taddeo, B., Zhang, W., Roizman, B., 2013b. Selective degradation of mRNAs by the HSV host shutoff RNase is regulated by the UL47 tegument protein. Proceedings of the National Academy of Sciences of the United States of America 110, E1669-1675.
Simas, J.P., Swann, D., Bowden, R., Efstathiou, S., 1999. Analysis of murine gammaherpesvirus-68 transcription during lytic and latent infection. The Journal of general virology 80 (Pt 1), 75-82.
Sivan, G., Martin, S.E., Myers, T.G., Buehler, E., Szymczyk, K.H., Ormanoglu, P., Moss, B., 2013. Human genome-wide RNAi screen reveals a role for nuclear pore proteins in poxvirus morphogenesis. Proceedings of the National Academy of Sciences of the United States of America 110, 3519-3524.
Smibert, C.A., Popova, B., Xiao, P., Capone, J.P., Smiley, J.R., 1994. Herpes simplex virus VP16 forms a complex with the virion host shutoff protein vhs. Journal of virology 68, 2339-2346.
Smiley, J.R., 2004. Herpes simplex virus virion host shutoff protein: immune evasion mediated by a viral RNase? Journal of virology 78, 1063-1068.
Smyth, G.K., 2004. Linear models and empirical bayes methods for assessing differential expression in microarray experiments. Statistical applications in genetics and molecular biology 3, Article3.
Souliere, M.F., Perreault, J.P., Bisaillon, M., 2009. Characterization of the vaccinia virus D10 decapping enzyme provides evidence for a two-metal-ion mechanism. The Biochemical journal 420, 27-35.
Souliere, M.F., Perreault, J.P., Bisaillon, M., 2010. Insights into the molecular determinants involved in cap recognition by the vaccinia virus D10 decapping enzyme. Nucleic acids research 38, 7599-7610.
Stevenson, P.G., Efstathiou, S., 2005. Immune mechanisms in murine gammaherpesvirus-68 infection. Viral immunology 18, 445-456.
Strelow, L.I., Leib, D.A., 1995. Role of the virion host shutoff (vhs) of herpes simplex virus type 1 in latency and pathogenesis. Journal of virology 69, 6779-6786.
Sugimoto, A., Sato, Y., Kanda, T., Murata, T., Narita, Y., Kawashima, D., Kimura, H., Tsurumi, T., 2013. Different distributions of Epstein-Barr virus early and late gene transcripts within viral replication compartments. Journal of virology 87, 6693-6699.
Sun, M., Schwalb, B., Pirkl, N., Maier, K.C., Schenk, A., Failmezger, H., Tresch, A., Cramer, P., 2013. Global analysis of eukaryotic mRNA degradation reveals Xrn1-dependent buffering of transcript levels. Molecular cell 52, 52-62.
Sun, M., Schwalb, B., Schulz, D., Pirkl, N., Etzold, S., Lariviere, L., Maier, K.C., Seizl, M., Tresch, A., Cramer, P., 2012. Comparative dynamic transcriptome analysis (cDTA) reveals mutual feedback between mRNA synthesis and degradation. Genome research 22, 1350-1359.

Sunil-Chandra, N.P., Efstathiou, S., Arno, J., Nash, A.A., 1992. Virological and pathological features of mice infected with murine gamma-herpesvirus 68. The Journal of general virology 73 (Pt 9), 2347-2356.
Suzutani, T., Nagamine, M., Shibaki, T., Ogasawara, M., Yoshida, I., Daikoku, T., Nishiyama, Y., Azuma, M., 2000. The role of the UL41 gene of herpes simplex virus type 1 in evasion of non-specific host defence mechanisms during primary infection. The Journal of general virology 81, 1763-1771.
Taddeo, B., Sciortino, M.T., Zhang, W., Roizman, B., 2007. Interaction of herpes simplex virus RNase with VP16 and VP22 is required for the accumulation of the protein but not for accumulation of mRNA. Proceedings of the National Academy of Sciences of the United States of America 104, 12163-12168.
Taddeo, B., Zhang, W., Roizman, B., 2013. The herpes simplex virus host shutoff RNase degrades cellular and viral mRNAs made before infection but not viral mRNA made after infection. Journal of virology 87, 4516-4522.
Tempera, I., Lieberman, P.M., 2010. Chromatin organization of gammaherpesvirus latent genomes. Biochimica et biophysica acta 1799, 236-245.
Terhune, S.S., Schroer, J., Shenk, T., 2004. RNAs are packaged into human cytomegalovirus virions in proportion to their intracellular concentration. Journal of virology 78, 10390-10398.
Trapnell, C., Pachter, L., Salzberg, S.L., 2009. TopHat: discovering splice junctions with RNA-Seq. Bioinformatics 25, 1105-1111.
Trgovcich, J., Johnson, D., Roizman, B., 2002. Cell surface major histocompatibility complex class II proteins are regulated by the products of the gamma(1)34.5 and U(L)41 genes of herpes simplex virus 1. Journal of virology 76, 6974-6986.
Weill, L., Belloc, E., Bava, F.A., Mendez, R., 2012. Translational control by changes in poly(A) tail length: recycling mRNAs. Nature structural & molecular biology 19, 577-585.
Weinberg, J.B., Lutzke, M.L., Alfinito, R., Rochford, R., 2004. Mouse strain differences in the chemokine response to acute lung infection with a murine gammaherpesvirus. Viral immunology 17, 69-77.
Wilkinson, D.E., Weller, S.K., 2003. The role of DNA recombination in herpes simplex virus DNA replication. IUBMB life 55, 451-458.
Zamora, M., Marissen, W.E., Lloyd, R.E., 2002. Multiple eIF4GI-specific protease activities present in uninfected and poliovirus-infected cells. Journal of virology 76, 165-177.
Zenner, H.L., Mauricio, R., Banting, G., Crump, C.M., 2013. Herpes simplex virus 1 counteracts tetherin restriction via its virion host shutoff activity. Journal of virology 87, 13115-13123.
Zhu, F.X., Chong, J.M., Wu, L., Yuan, Y., 2005. Virion proteins of Kaposi's sarcoma-associated herpesvirus. Journal of virology 79, 800-811.
Zuo, J., Thomas, W., van Leeuwen, D., Middeldorp, J.M., Wiertz, E.J., Ressing, M.E., Rowe, M., 2008. The DNase of gammaherpesviruses impairs recognition by virus-specific CD8+ T cells through an additional host shutoff function. Journal of virology 82, 2385-2393.

Zust, R., Cervantes-Barragan, L., Kuri, T., Blakqori, G., Weber, F., Ludewig, B., Thiel, V., 2007. Coronavirus non-structural protein 1 is a major pathogenicity factor: implications for the rational design of coronavirus vaccines. PLoS pathogens 3, e109.